

**University of Alberta**

*Sinosaurus* from southwestern China

by

Lida Xing

A thesis submitted to the Faculty of Graduate Studies and Research  
in partial fulfillment of the requirements for the degree of

Master of Science  
in  
Systematics and Evolution

Department of Biological Sciences

©Lida Xing  
Fall 2012  
Edmonton, Alberta

Permission is hereby granted to the University of Alberta Libraries to reproduce single copies of this thesis and to lend or sell such copies for private, scholarly or scientific research purposes only. Where the thesis is converted to, or otherwise made available in digital form, the University of Alberta will advise potential users of the thesis of these terms.

The author reserves all other publication and other rights in association with the copyright in the thesis and, except as herein before provided, neither the thesis nor any substantial portion thereof may be printed or otherwise reproduced in any material form whatsoever without the author's prior written permission.

## ABSTRACT

Early Jurassic *Sinosaurus triassicus* (=“*Dilophosaurus sinensis*”) is the earliest large dinosaur predator from China; however, all the specimens of this species have remained poorly known. The Hewanzi specimen described in this thesis is the only well prepared one. Morphology of the crest and braincase of the Hewanzi specimen indicates that it possesses advanced characteristics that are more developed than in *Dilophosaurus*. A phylogenetic analysis shows *Sinosaurus* and *Cryolophosaurus* emerge as more derived theropods; they were recovered as more closely related to *Averostra* than to *Coelophysis* and *Dilophosaurus*. These results may suggest the Hewanzi specimen represents another species of *Sinosaurus*. A finite element analysis (FEA) suggests the structural features of the crest in *Dilophosaurus* and *Sinosaurus* cannot play a mechanical role during combat. In addition, a remodeled alveolus in the maxilla of *Sinosaurus* is the first confirmed example of dental pathology in a dinosaur.

## ACKNOWLEDGEMENTS

Since my arrival in Canada in January of 2010, I have been fortunate enough to meet many kind and generous people who are genuinely interested in dinosaurs and paleontology. Without them, my efforts would not have been so near to success.

This research was made possible by the support of the Chinese Academy of Sciences Key Laboratory of Evolutionary Systematics of Vertebrates, the University of Alberta China Institute, and Creativity Funding from Citizen Watches Co.

I would like to thank my supervisor Philip J. Currie (University of Alberta, UA, Canada), and advisor Xing Xu (Institute of Vertebrate Paleontology and Paleoanthropology, Chinese Academy of Sciences, IVPP, China); committee members Alison Murray and Murray Gingras (UA, Canada); Victoria Arbour (UA, Canada), Michael E. Burns (UA, Canada), Tetsuto Miyashita (UA, Canada), Ariana Paulina-Carabajal (Museo Municipal Carmen Funes, Argentina), W. Scott Persons, IV (UA, Canada), Eric Snively (Ohio University, USA), Angelica Torices (Universidad Complutense de Madrid, Spain; UA, Canada), Sekiya Toru (Zigong Dinosaur Museum, China), and Yikun Wang (University of Auckland, New Zealand) for their repeated council and for many fruitful discussions about dilophosaurids.

I am also thankful for those who continue to encourage me in my progress, including Miman Zhang, Zhiming Dong and Zhonghe Zhou, all from the IVPP, China. They are truly the wind beneath my wings. Immense thanks to Robert

Holmes (UA, Canada), for his endless patience and excellent teaching skill in paleontology courses.

I also thank Brandon Strilisky (Royal Tyrrell Museum, Canada), Daqing Li (Geological Museum of Gansu, China), Guangzhao Peng and Yong Ye (Zigong Dinosaur Museum, China), Richard T. McCrea (Peace Region Palaeontology Research Centre, Canada), Laigen Wang and Tao Wang (World Dinosaur Valley Park, China), and Yuan Wang (IVPP, China) for their indispensable assistance when I was checking their collections.

Special thanks are also extended to Clive Coy (University of Alberta, Canada), Kiko (Paleowonders Fossil and Mineral Museum, Taiwan, China) and Yuqing Zhang (Institute of Geology, China) for their preparation of specimens for this project, and to Lisa Buckley (Peace Region Palaeontology Research Centre; UA, Canada), Michael Caldwell (UA, Canada), Julian Divey (UA, Canada), Ruohan Gong (UA, Canada), Paulina Huidobro (UA, Canada), Eva Koppelhus (UA, Canada), Juan Liu (UA, Canada) and her husband Zhijie "Jack" Tseng, Miriam Reichel (UA, Canada), Lara Shychoski (Royal Tyrrell Museum; UA, Canada), and Hailu You (IVPP, China) for their kind consideration and generous favors as my project progressed.

Thanks to Chenyu Liu and Liu Yi, they merit my gratitude for their stunning artistic skills and talents, which were graciously lent to this project; Wei Zhu, Julian Divey, and W. Scott Persons, IV helped to improve the English text.

Finally, I thank my wife Shenna Wang, my son Minghe Xing, my parents, my parents-in-law, and my puppy Eve for their unselfish love and energetic support to my hunting of dinosaurs.

## TABLE OF CONTENTS

**Abstract**

**Acknowledgements**

**List of Tables**

**List of Figures**

**Institutional Abbreviations**

**Introduction.....1**

**Chapter 1 Morphology of a new specimen of *Sinosaurus triassicus*  
(=“*Dilophosaurus sinensis*”) from the Lufeng Formation (Lower Jurassic) of  
Yunnan, China.....8**

**1.1 Introduction.....8**

**1.1.1 Dilophosaurid from China.....8**

**1.1.2 Research History of Chinese "*Dilophosaurus*" .....8**

**1.1.3 Vertebrate fossils of the Lower Jurassic Lufeng Formation.....12**

**1.2 Geological Setting.....13**

**1.3 Systematic paleontology.....18**

**1.3.1 Material.....18**

**1.3.2 Locality and horizon.....18**

**1.3.3 Description and Comparison.....18**

**1.3.3.1 Skull.....18**

**1.3.3.2 Postcranial Skeleton.....37**

**1.3.4 Discussion.....44**

**1.3.5 Conclusions.....49**

<b>Chapter 2 Braincase anatomy of <i>Sinosaurus triassicus</i> from the Lufeng Formation (Lower Jurassic) of Yunnan, China.....</b>	<b>60</b>
<b>2.1 Introduction.....</b>	<b>60</b>
<b>2.2 Methods.....</b>	<b>61</b>
<b>2.3 Anatomical Abbreviations.....</b>	<b>62</b>
<b>2.4 Description and Comparisons.....</b>	<b>66</b>
<b>2.5 Cranial nerves.....</b>	<b>82</b>
<b>2.6 Pneumatic recesses.....</b>	<b>83</b>
<b>2.7 Discussion and Conclusions.....</b>	<b>84</b>
<b>Chapter 3 The Phylogenetic Systematics of the <i>Sinosaurus triassicus</i> from China.....</b>	<b>89</b>
<b>3.1 Introduction.....</b>	<b>89</b>
<b>3.2 Coelophysoids and dilophosaurids.....</b>	<b>90</b>
<b>3.3 New materials of <i>Sinosaurus triassicus</i>.....</b>	<b>92</b>
<b>3.4 Methods.....</b>	<b>93</b>
<b>3.5 Discussion and Conclusions.....</b>	<b>96</b>
<b>3.6 The crest evolution base the phylogenetic analysis.....</b>	<b>102</b>
<b>3.7 Paleobiogeographic Implications.....</b>	<b>104</b>
<b>Chapter 4 Tooth loss and alveolar remodeling in <i>Sinosaurus triassicus</i> from the Early Jurassic in Lufeng Basin, China.....</b>	<b>120</b>
<b>4.1 Introduction.....</b>	<b>120</b>
<b>4.2 Geological Setting.....</b>	<b>121</b>
<b>4.3 Methods.....</b>	<b>122</b>

4.4 Description.....	122
4.5 Discussion and Conclusions.....	127
<b>Chapter 5 Model–based identification of mechanical characters in the crest of <i>Sinosaurus</i> (Dinosauria: Theropoda).....</b>	<b>141</b>
5.1. Introduction.....	141
5.2 Hypotheses of crest function in <i>Dilophosaurus</i> and <i>Sinosaurus</i> ....	141
5.3 Materials.....	143
5.4 Methods.....	145
5.4.1 Modeling approach.....	145
5.4.2 Geometrical Modeling.....	145
5.4.3 Material Modeling.....	148
5.4.3 Computational Experiments.....	148
5.5 Simulations and Results.....	150
5.5.1 Sample Model.....	150
5.5.2 Full Scale Model.....	155
5.6 Discussion.....	160
5.7 Future Research.....	164
<b>CHAPTER 6 The fourth <i>Sinosaurus triassicus</i> from the Lufeng Basin of China, and reflections on the paleoecology of <i>Sinosaurus</i>.....</b>	<b>170</b>
6.1 Introduction.....	170
6.2 Maxilla.....	173
6.3 The crest base.....	180
6.4 Lower jaws.....	182

<b>6.5 Conclusion.....</b>	<b>185</b>
<b>Conclusion.....</b>	<b>198</b>
<b>Appendix 1 .....</b>	<b>201</b>
<b>Appendix 2 .....</b>	<b>247</b>

## **LIST OF TABLES**

### **Chapter 1**

**TABLE 1.1** The distance (in mm) from 6th alveolus and 10th alveolus margin to the ventral rim of the antorbital fossa.

### **Chapter 5**

**TABLE 5.1** JiRui II Technical Data

### **Chapter 6**

**TABLE 6.1** Numbers of recovered specimens of Theropoda (and a carnivorous crocodylomorph) from the Lufeng Formation.

## LIST OF FIGURES

### Chapter 1

**FIGURE 1.1.** Geographic map of the distribution of coelophysoid track sites and localities that produced *Sinosaurus*. 1), Dahuangtian (IVPP V34, V30, V31); 2), Heilongtan (LDM–L10); 3), Konglong Hill (ZLJ0003); 4), Hewanzi (ZLJT01); 5), Qinglongshan (KMV 8701); 6), Zhuqingkou (ZLJ–ZQK1 and ZLJ–ZQK2)

**FIGURE 1.2.** Stratigraphy of the Jurassic strata of Lufeng (adapted from Cheng et al., 2004). Illustration: A. Pelitic siltstone, B. Sandy mudstone, C. Mudstone, D. Sandstone, E. Conglomerate, F. Shale, G. Orthomicrite, H. Orthomicrite containing fossils, I. Arkose.

**FIGURE 1.3.** *Sinosaurus triassicus* (ZLJT01). Fused nasal processes of the premaxillae in right lateral (A), left lateral (B), posterior (C), anterior (D), and proximal (cross section; E) views. 1, right premaxilla–nasal suture; 2, left premaxilla–nasal sutures. Scale bar=10 cm

**FIGURE 1.4.** *Sinosaurus triassicus* (ZLJT01). Right maxilla in ventral (A), dorsal (B), lateral (C), medial (D) and anterior (E) views. Anatomical abbreviations: **aof**, antorbital fenestra; **f**, foramen; **idp**, interdental plates; **nf**, nutrient foramina; **pf**, promaxillary fenestra; **prs**, premaxillary suture of

anteromedial process of the maxilla; **ps**, pterygoid suture on anteromedial process of the maxilla; **voc**, slot for vomer on anteromedial process of the maxilla. Scale bar=10 cm

**FIGURE 1.5.** *Sinosaurus triassicus* (ZLJT01). Left maxilla fragment in medial (A) and lateral (B) views. Scale bar=10 cm

**FIGURE 1.6.** *Sinosaurus triassicus* (ZLJT01). Left lacrimal in lateral (A) and medial (B) views. **Blue line**: lacrimal duct; **Light blue line**: lacrimal openings; **Green line**: nasal suture; **Orange line**: postorbital contact; **Pink line**: edge of the antorbital fenestra; **Purple line**: medial impression; **Red line**: lacrimal pneumatic aperture; **Yellow line**: prefrontal suture. **o**: orbital. Scale bars = 10 cm

**FIGURE 1.7.** *Sinosaurus triassicus* (ZLJT01). Left dentary in lateral (A), medial (B) and dorsal (C) views. Anatomical abbreviations: **fb**, foramen for branch of inferior alveolar nerve; **idp**, interdental plate; **lsd**, lateral sulcus of the dentary; **mg**, Meckelian groove; **mf**, mental foramen; **mkf**, Meckelian foramen; **ms**, medial symphysis. Scale bars = 10 cm

**FIGURE 1.8.** *Sinosaurus triassicus* (ZLJT01). The first left dentary tooth (A), fifth right maxillary tooth (B), and fourth left maxillary tooth (C). Scale bars = 1 mm

**FIGURE 1.9.** *Sinosaurus triassicus* (ZLJT01). Atlantal intercentrum in dorsal (A), ventral (B), anterior (C), and posterior (D) views. 1, suture for neurapophysis; 2, axial articulation on atlas; 3, odontoid concavity; 4, articular surface on atlantal intercentrum for occipital condyle. Scale bars = 5 cm.

**FIGURE 1.10.** *Sinosaurus triassicus* (ZLJT01). Caudal vertebra in posterior view. Anatomical abbreviations: **ns**, neural spine; **pf**, pneumatic foramina; **pog**, postspinal groove; **pot**, postspinal trough; **poz**, postzygopophysis; **tr**, transverse process. Scale bars = 10 cm

**FIGURE 1.11.** *Sinosaurus triassicus* (ZLJT01). Ribs in anteroventral (A and C) and posterodorsal (B and D) views. Anatomical abbreviations: **cap**, capitulum; **sh**, shaft; **tub**, tuberculum. Scale bars = 10 cm

**FIGURE 1.12.** *Sinosaurus triassicus* (LDM–L10). A transverse section in the middle of the left crest. Scale bars = 5 mm

## Chapter 2

**FIGURE 2.1.** *Sinosaurus triassicus* (ZLJT01). Right frontal in dorsal (A) and ventral (B) views. Scale bars = 10 cm

**FIGURE 2.2.** Right frontal of *Sinosaurus triassicus* (ZLJT01) in dorsal (A) and ventral (B) views. Scale bars = 10 cm

**FIGURE 2.3.** Braincase of *Sinosaurus triassicus* (ZLJT01). in occipital (A), left lateral (B), right lateral (C), dorsal (D), and ventral (E) views. Scale bar = 10 cm.

**FIGURE 2.4.** Illustration of a *Sinosaurus triassicus* (ZLJT01) braincase in posterior (A), posteroventral (B), left lateral (C), right lateral (D), and ventral (E) views. Scale bar = 10 cm.

### **Chapter 3**

**FIGURE 3.1.** Strict consensus tree (Smith et al., 2007a)

**FIGURE 3.2.** Strict consensus of 1968 MPTs. All trees have length of 383 steps, CI 0.446, RI 0.728. Several theropod clades are indicated in bold.

**FIGURE 3.3.** Early Jurassic theropod paleogeographic reconstruction. Labeled faunas: (1) *Sinosaurus*, Lufeng Formation, China; *Cryolophosaurus*, Hanson Formation, Antarctica; (3) *Piatnitzkysaurus*, Canadon Asfalto Formation, Argentina. Paleogeographic map from Blakey (2006: <http://jan.ucc.nau.edu/>).

### **Chapter 4**

**FIGURE 4.1.** Palaeopathological characters of ZLJT01 (*Sinosaurus triassicus*), a right maxilla in A, medial; B, lateral; C, dorsal; D, E, ventral views. Position of the abnormal alveolus mx6 is indicated by an arrowhead. F, G, incomplete, normal left maxilla of ZLJT01 in F, medial and G, ventral aspects showing non-pathologic alveolus mx6. Numerals in E and G refer to alveoli. Scale bar = 10 cm.

**FIGURE 4.2.** X-ray scan of ZLJT01 (*Sinosaurus triassicus*), a pathological right maxilla in lateral aspect. Anterior is right. Arrowhead indicates pathologic alveolus mx6. Pyrite growths (P) show up as white discs. Note the near absence of pyrite in mx6. Scale bar = 5 cm.

**FIGURE 4.3.** CT scan of the pathological right maxilla (ZLJT01) in lateral aspect. Anterior is right. Arrowheads indicate the positions of the alveoli for mx3, mx5 and mx6. The white discs are pyrite.

**FIGURE 4.4.** Life reconstruction of *Sinosaurus triassicus* with dental abnormality based on ZLJT01. Illustration by Mr. Chenyu Liu.

## **Chapter 5**

**FIGURE 5.1.** *Sinosaurus triassicus* (LDM-L10) skull, and *Sinosaurus triassicus* (ZLJT01) lacrimal crest in lateral views. Scale bar=10 cm

**FIGURE 5.2.** A, B, C, D show overall views of the FE crest model. C is anterior and B and D are left lateral and right lateral views, respectively. A indicates the loading areas coloured as red; the blue area in E, F and G represents the spatially fixed boundary. Red, green and blue arrows represent x, y and z directions.

**FIGURE 5.3.** Deformations of the crest model corresponding to 1000N (A), 2000N (B), 3000N (C) and 4000N (D) loading.

**FIGURE 5.4.** Subfigures A and B show the conceptual full scale crest model of the *Sinosaurus* crests; C and D demonstrate a solid body model used for comparisons. The x axis is in the anterior–posterior direction, where + x is anterior. Subfigures A and C therefore show the lateral direction of two full crest models. Red, green and blue arrows represent x, y and z directions.

**FIGURE 5.5.** A, B and C depict the front, middle and back loading areas on the full crest model with cavities; the middle and third columns depict the effective stress distribution corresponding to the loading magnitude of 0.009115 GPa and 0.01823 GPa.

**FIGURE 5.6.** Case study of different loading areas on the counterexample model without crest cavities. The second and third columns shows the stress distribution under the loads with magnitudes of 0.006415 GPa and 0.01283 GPa.

## Chapter 6

**FIGURE 6.1.** *Sinosaurus triassicus* (ZLJ0003) skull display in the World Dinosaur Valley Park, Yunnan Province, China. Scale bar = 10 cm.

**FIGURE 6.2.** Composite skull of *Sinosaurus triassicus* (ZLJ0003). Left maxilla (A) and right maxilla (B) in medial views; left (C) and right (D) dentaries in lateral views. Scale bar = 10 cm.

**FIGURE 6.3.** *Sinosaurus triassicus* (ZLJ0003) Right maxilla in lateral (A) and medial (B) views. Scale bar = 10 cm.

**FIGURE 6.4.** *Sinosaurus triassicus* (ZLJ0003). Left maxilla in medial view, plus portion of the base of the nasal-lacrimal crest. Scale bar = 10 cm.

**FIGURE 6.5.** Right maxilla of *Sinosaurus triassicus* (ZLJ0003) shown overlapping one of the skulls of *Sinosaurus triassicus* (LDM-L10). Scale bar = 10 cm.

**FIGURE 6.6.** *Sinosaurus triassicus* (ZLJ0003). Left maxilla in dorsal view (A). The red circles indicate alveoli (B). Scale bar = 10 cm.

**FIGURE 6.7.** Naso-lacrima crests of *Sinosaurus triassicus* (ZLJ0003) in dorsal view (A). The region between the yellow lines is formed by the resin reconstruction done by the local museum (B). Scale bar = 10 cm.

**FIGURE 6.8.** *Sinosaurus triassicus* (ZLJ0003). Left dentary in lateral (A) and medial (B) views. Scale bar = 10 cm.

**FIGURE 6.9.** *Sinosaurus triassicus* (ZLJ0003). Right dentary in lateral (A) and medial (B) views. Scale bar = 10 cm.

**FIGURE 6.10.** *Sinosaurus triassicus* (KMV 8701) and *Yunnanosaurus* found in the same quarry.

**FIGURE 6.11.** Braincase of *Sinosaurus triassicus* (LDM-L10) in occipital view (A); close-up of cross-section of tooth (B) and outline drawing (C).

## **Institutional Abbreviations**

**CM**, Carnegie Museum of Natural History, Pittsburgh, Pennsylvania, USA;

**CMNH**, Cleveland Museum of Natural History, Cleveland, Ohio, USA;

**FMNH CUP**, Field Museum of Natural History (Catholic University of Peking collection), Chicago, Illinois, USA;

**IVPP**, Institute of Vertebrate Paleontology and Paleoanthropology, Beijing, China;

**KMV**, Kunming City Museum, Kunming, Yunnan, China;

**LDM**, Lufeng Dinosaurian Museum, Lufeng, Yunnan, China;

**MNA**, Museum of Northern Arizona, Flagstaff, Arizona, USA;

**MWC**, Museum of Western Colorado, Fruita, Colorado, USA;

**PULR**, Paleontología, Universidad de La Rioja, Argentina;

**QG**, originally catalogued at the Queen Victoria Museum, Department of Paleontology, Harare (formerly Salisbury), now curated at the National Museum of Natural History, Bulawayo, Zimbabwe;

**UCMP**, University of California Museum of Paleontology, Berkeley, California, USA.

**ZLJ**, Lufeng World Dinosaur Valley Park, Yunnan, China

## Introduction

Theropoda, a taxon that includes mostly carnivorous dinosaurs, survived more than 160 million years of the Mesozoic Era. When birds are taken into consideration, the theropod lineage has been dominant for 230 million years and is still prominent in the modern world (Currie, 1999).

The earliest and most primitive of the theropod dinosaurs included the carnivorous *Eodromaeus* and herrerasaurids of the Upper Triassic of Argentina (Martinez et al., 2011). These oldest dinosaurs and giant predators such as the tyrannosaurids (Currie, 2003) have also received a lot of recent research attention. Another hotspot of theropod research surrounds the feathered dinosaurs, such as the compsognathid *Sinosauropteryx* (Ji and Ji, 1996; Currie and Chen, 2001), the therizinosauroid *Beipiaosaurus* (Xu et al., 1999), the dromaeosaurid *Microraptor* (Xu et al., 2000) and the tyrannosauroid *Yutyrannus* (Xu et al., 2012).

However, in the global scope, large theropod dinosaurs from the Early Jurassic have not been the focus of sufficient research. A major reason is certainly the lack of sufficient fossil materials. These dinosaurs are known from Africa, Antarctica, China and North America, and most are assigned to Dilophosauridae (Madsen and Welles, 2000). With other Coelophysoidea and Neoceratosauria, they represent the first widespread and diverse radiation of theropod dinosaurs. The remains of these predators are the most common theropod fossils recovered from Upper Triassic and Lower Jurassic deposits worldwide.

Initially, Dilophosauridae included only the type species, *Dilophosaurus wetherilli* (Welles, 1984). Other genera, such as *Dracovenator regenti* (Yates,

2005), *Syntarsus kayentakatae* (Rowe, 1989), and *Zupaysaurus rougieri* (Arcucci and Coria, 2003), have been assigned to this family, although the group has never been given phylogenetic definition and is not currently considered as a well-defined clade. Tykoski and Rowe (2004) referred *Dilophosaurus* to the superfamily Coelophysoidea. Some analyses, including Smith et al. (2007), suggest that dilophosaurids may have been more closely related to the Tetanurae (the more advanced carnosaurs and coelurosaurs), and referred *Cryolophosaurus*, *Dilophosaurus*, *Dracovenator* and *Sinosaurus* to this branch.

Dilophosaurids are well-known for their distinctive head crests, which are widely assumed to be probable display structures (Welles, 1984), to attract mates or intimidate rivals. Sexual dimorphism has been suggested (Gay, 2005) but is controversial. Another distinctive cranial feature is the presence of a notch or diastema behind the premaxillary teeth, which gives a dilophosaurid an almost crocodile-like appearance, similar to the putatively piscivorous spinosaurid dinosaurs. This makes some suspect that the front teeth were too weak to bring down and hold large prey, and that dilophosaurids scavenged dead carcasses (Norman, 1985). Some tracks seem to indicate that dilophosaurids might swim and feed on fish, of which the most famous fossil evidence is the St. George Dinosaur Discovery Site, Utah, U.S.A. (Milner et al., 2006).

In 1993, Hu described a dilophosaurid fossil from the Lufeng Basin. The fossil was considered to be *Dilophosaurus* by Hu (1993), but differed from *Dilophosaurus wetherilli*. The fossil was named *Dilophosaurus sinensis*, but still lacks sufficient preparation and description. However, the research of Hu opened

the gates for research on dilophosaurids of China. Currently at least five dilophosaurid fossils have been discovered in the Lower Jurassic Lufeng Basin. Dong (2003) considered “*Dilophosaurus sinensis*” to be similar to *Sinosaurus triassicus*, but did not publish details. Currie et al. (in progress) compared the two specimens, and concluded they should be referred to *Sinosaurus triassicus*. However, all of the specimens up to now have been incompletely prepared. This thesis attempts to better understand *Sinosaurus triassicus* based on an incomplete but well-prepared specimen.

This thesis is a compilation of work from a three year master’s research project that consists of six chapters. Skeleton morphology, phylogenetic systematics, paleopathology and engineering are involved. CT scans and 3D reconstructions of *Sinosaurus triassicus* helped improved my understanding. Five chapters will be submitted to peer-reviewed scientific journals, including;

- (1) a paper based on the morphologic and phylogenetic analysis to establish a new species of *Sinosaurus*;
- (2) morphological and anatomical details of the braincase of *Sinosaurus*;
- (3) a rare pathology involving tooth loss and alveolar remodeling in *Sinosaurus*;
- (4) computer model–based identification of mechanical characteristics of the crest of *Sinosaurus*, and
- (5) the diet and paleoecology of *Sinosaurus* (a possibly piscivorous theropod), potentially may have included cannibalism.

In conjunction with the research and study of Currie et al. (in progress) on

previous specimens, we will soon witness a tremendous increase in knowledge about *Sinosaurus*.

Future work needs to include the preparation of previously discovered specimens, further excavation of the Hewanzi bonebed, and use of aerodynamic principles to understand the aerodynamic characteristics of the head of *Sinosaurus* to determine the influence of the crest on the animal's running speed.

### **Bibliography**

Arcucci AB, Coria RA. 2003. A new Triassic carnivorous dinosaur from Argentina. *Ameghiniana* 40: 217–228.

Currie PJ, Chen PJ. 2001. Anatomy of *Sinosauropteryx prima* from Liaoning, northeastern China. *Canadian Journal of Earth Sciences* 38 (1): 705–727.

Currie PJ. 2003. Cranial anatomy of tyrannosaurid dinosaurs from the Late Cretaceous of Alberta, Canada. *Acta Palaeontologica Polonica* 48 (2): 191–226.

Currie PJ, Xing LD, Wu XC, Dong ZM. In progress. Anatomy and relationships of *Sinosaurus triassicus* (“*Dilophosaurus sinensis*”) from the Lufeng Formation (Lower Jurassic) of Yunnan, China.

Gay R. 2005. Sexual dimorphism in the early Jurassic theropod dinosaur

- Dilophosaurus* and a comparison with other related forms. In: Carpenter K, editor. The carnivorous dinosaurs. Indiana University Press, Bloomington. 277–28.
- Hu SJ. 1993. A short report on the occurrence of *Dilophosaurus* from Jinning County, Yunnan Province. *Vertebrata Palasiatica* 31: 65–69.
- Ji Q, Ji S. 1996. On discovery of the earliest bird fossil in China and the origin of birds. *Chinese Geology* 10 (233): 30–33.
- Madsen JH, Welles SP. 2000. *Ceratosaurus* (Dinosauria, Therapoda), a revised osteology. Miscellaneous Publication. Utah Geological Survey 1–80.
- Martinez RN, Sereno PC, Alcober OA, Colombi CE, Renne PR, Montañez IP, Currie BS. 2011. A basal dinosaur from the dawn of the Dinosaur Era in Southwestern Pangaea. *Science* 331 (6014): 206–210.
- Milner ARC, Lockley MG, Kirkland JI. 2006. A large collection of well-preserved theropod dinosaur swim tracks from the Lower Jurassic Moenave Formation, St. George. In: Harris JD, Lucas SG, Spielmann JA et al. (eds.), The Triassic-Jurassic Terrestrial Transition. *Bulletin of the New Mexico Museum of Natural History and Science* 37: 315–328.

- Rowe T. 1989. A new species of the theropod *Syntarsus* from the Early Jurassic Kayenta Formation of Arizona. *Journal of Vertebrate Paleontology* 9: 125–136.
- Smith ND, Makovicky PJ, Hammer WR, Currie PJ. 2007. Osteology of *Cryolophosaurus ellioti* (Dinosauria: Theropoda) from the Early Jurassic of Antarctica and implications for early theropod evolution. *Zoological Journal of the Linnean Society* 151 (2): 377–421.
- Tykoski RS, Rowe T. 2004. Ceratosauria. In: Weishampel DB, Dodson P, Osmolska H. (eds.), *The Dinosauria* (2nd edition). University of California Press, Berkeley. 47–70.
- Welles SP. 1984. *Dilophosaurus wetherilli* (Dinosauria, Theropoda): Osteology and comparisons. *Palaeontographica Abteilung A*. 185, 85–180.
- Xu X, Tang ZL, Wang XL. 1999. A therizinosauroid dinosaur with integumentary structures from China. *Nature* 399(6734): 350–354.
- Xu X, Zhou Z, Wang X. 2000. The smallest known non-avian theropod dinosaur. *Nature* 408: 705–708.
- Xu X, Wang K, Zhang K, Ma Q, Xing LD, Sullivan C, Hu D, Cheng S. 2012. A

gigantic feathered dinosaur from the Lower Cretaceous of China. *Nature* 484:  
92–95.

Yates AM. 2005. A new theropod dinosaur from the Early Jurassic of South  
Africa and its implications for the early evolution of theropods.  
*Palaeontologia Africana*. 41, 105–122.

## CHAPTER 1

### **Morphology of a new specimen of *Sinosaurus triassicus* (=“*Dilophosaurus sinensis*”) from the Lufeng Formation (Lower Jurassic) of Yunnan, China**

#### **1.1 Introduction**

##### **1.1.1 Dilophosaurid from China**

Dilophosaurid fossils are known from Upper Triassic and Lower Jurassic deposits worldwide, including Africa, Antarctica, China, and North America (Tykoski and Rowe, 2004). The first recognized Chinese form was named “*Dilophosaurus*” *sinensis* by Shaojin Hu in 1993. Due to poor preparation and protectionism on the part of the collecting institution, external researchers were not permitted to observe the specimen. As a result, the Chinese dilophosaurid did not draw much attention until 2000, when Currie et al. (in progress) recognized “*Dilophosaurus*” *sinensis* as being the same as *Sinosaurus triassicus* – a coelophysoid described in 1948 by C.C. Young. Recently, several new dilophosaurid specimens have been discovered in China that provide critical information about the morphology of the Chinese dilophosaurids.

##### **1.1.2 Research History of the Chinese “*Dilophosaurus*”**

In 1948, the first Chinese dinosaur paleontologist, C.C. Young, described *Sinosaurus triassicus* from the Lufeng Formation of Dahuangtian Village, Dawa Village Committees, Jinshan Township, Lufeng County (Figure 1). This is one of

the first theropods described from China. The holotype (IVPP V34) is a partial maxilla (three fragments with several teeth in position) and three associated isolated teeth. In addition, two dorsal vertebrae (IVPP V30, V31) are attributed to *Sinosaurus triassicus*. It is worth mentioning that a pelvic girdle (IVPP V21), which was later attributed to *Yunnanosaurus* (Dong Z.M., pers. comm.), was discovered along with *Sinosaurus triassicus*. *Sinosaurus triassicus* was first attributed to Carnosauria (Young, 1948), but Rauhut (2000) suggests it was related to *Cryolophosaurus* and “*Dilophosaurus*” *sinensis*.

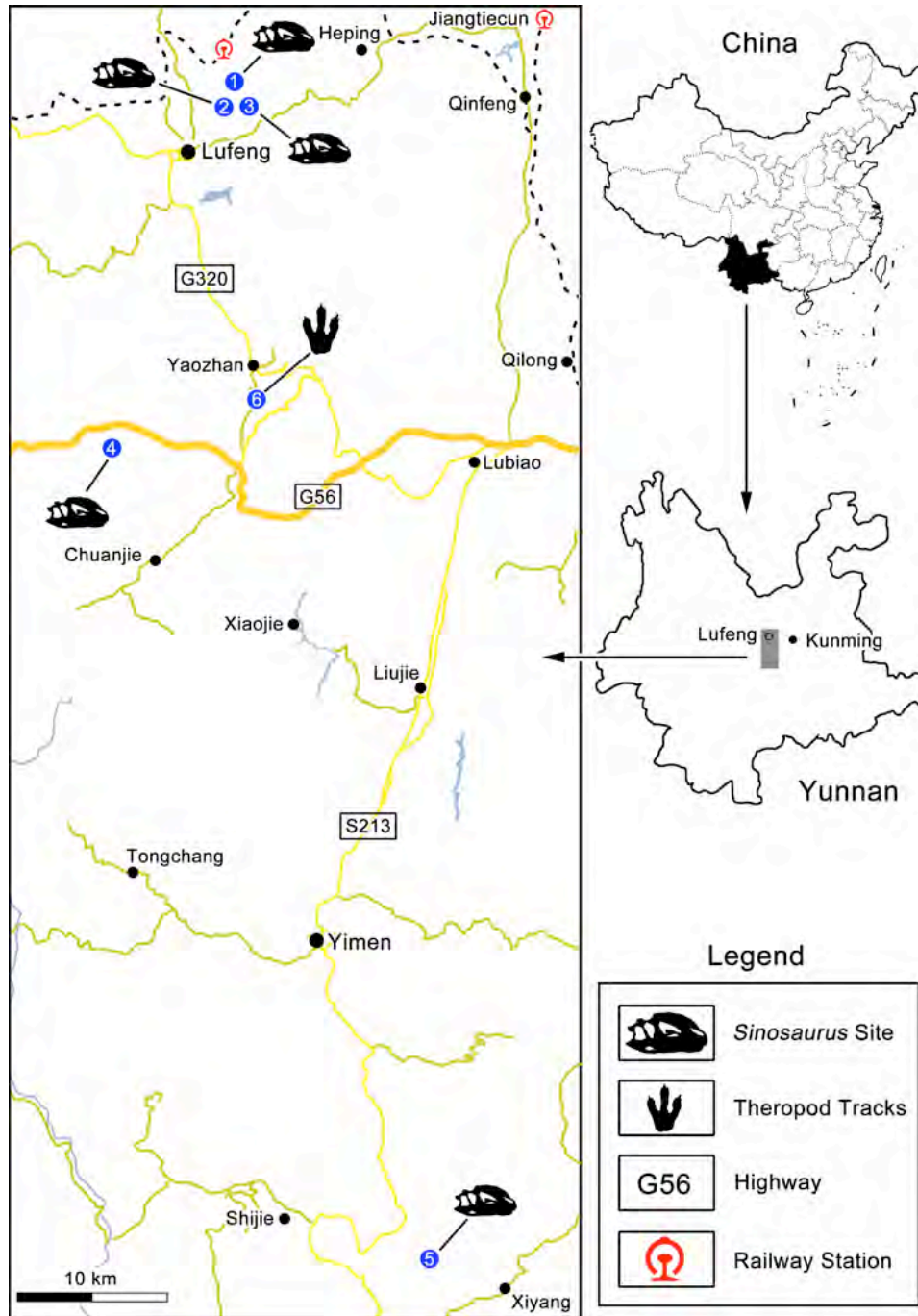


**FIGURE 1.1.** Geographic map of the distribution of coelophysoid track sites and localities that produced *Sinosaurus*. 1), Dahuangtian (IVPP V34, V30, V31); 2), Heilongtan (LDM–L10); 3), Konglong Hill (ZLJ0003); 4), Hewanzi (ZLJT01); 5), Qinglongshan (KMV 8701); 6), Zhuqingkou (ZLJ–ZQK1 and ZLJ–ZQK2)

In August of 1987, two dinosaur specimens were discovered by the Kunming City Museum in the Lufeng Formation of Qinglongshan Mountain, Muchulang Village, Xiyang Yi Township, Jinning County, Yunnan, China (Fig. 1.1). One specimen is a nearly complete theropod (KMV 8701) that is 5.6m long, whereas the other one is the prosauropod *Yunnanosaurus*. The skull of KMV 8701 is that described as the holotype of *Dilophosaurus sinensis* by Hu (1993).

In 1994, a nearly complete theropod skeleton (LDM-L10) was collected by the Lufeng Dinosaurian Museum from the Lufeng Formation of Heilongtan Village, Songjiapo Village Committees, Jinshan Township, Lufeng County, Yunnan, China (Fig. 1.1). The skull of LDM-L10 is well preserved and has a double crest; the local museum identified it as “*Dilophosaurus*” *sinensis*. Recently, Dong (2003) reviewed the specimen and considered it to be similar to *Sinosaurus triassicus* based the morphology, size, stratigraphic position and geographic proximity. Currie et al. (in progress) supported this view and considered these two specimens (KMV 8701, LDM-L10) to be *Sinosaurus triassicus*, and attributed the differences between these two specimens to strong sexual dimorphism.

In 2006, a Japanese visitor (Dr. Sekiya Toru) discovered the fourth dilophosaurid specimen (ZLJ0003) from the Lufeng Formation of the Konglong Hill, Dawa Village Committees, Jinshan Township, Lufeng County, Yunnan, China (Fig. 1.1). Konglong Hill has also produced a number of *Lufengosaurus* specimens. ZLJ0003 includes the front of a skull and a nearly complete postcranial skeleton. This skull was not prepared but was assembled as part of a composite skull and put on display. The postcranial skeleton was mounted with a

cast of the skull of LDM–L10, and then put on display in the China Science and Technology Museum, Beijing after 2009.

In 2007, the Lufeng Dinosaurian Museum discovered an incomplete “*Dilophosaurus sinensis*” skull, and several postcranial skeleton fragments (ZLJT01) from Hewanzi Village, Ganchong Village Committees, Konglongshan Township, Lufeng County, Yunnan, China (Fig. 1.1). Compared with the four previously discovered specimens, ZLJT01 was better prepared, and the partial skeleton was CT scanned. More skull fragments were discovered during the field expedition in the summer of 2011. This chapter mainly describes ZLJT01, whereas the postcranial skeleton of ZLJ0003 is described more superficially because it is on display.

### **1.1.3 Vertebrate fossils of the Lower Jurassic Lufeng Formation**

Vertebrate fossils from the Lower Jurassic Lufeng Formation of the Lufeng Basin of Yunnan Province, which have been reported since the late 1930s, played an important role in the early career of C.C. Young. The vertebrate fauna from this unit was named the Lufeng Saurischian Fauna (Young, 1951), and its fossils have been recovered from numerous places in Yunnan, including Lufeng, Yimen and Yuanmou.

The dinosaur component of the Lufeng Saurischian Fauna comprises:

(1) the prosauropods (Upchurch et al., 2007) *Anchisaurus sinensis* (Young, 1941 (originally *Gyposaurus*))=*Gyposaurus sinensis*(Young, 1941; Dong, 1992; Galton and Upchurch, 2004); *Lufengosaurus huenei* (Young, 1941),

*Lufengosaurus magnus* (Young, 1947), and *Yunnanosaurus huangi* (Young, 1942).

(2) the basal sauropods *Chinshakiangosaurus chunghoensis* (Dong, 1992; Upchurch et al., 2007), *Jingshanosaurus xinwaensis* (Zhang and Yang, 1995), *Kunmingosaurus wudingensis* (Chao, 1985; nomen nudum), possibly “*Yunnanosaurus*” *robustus* (Young, 1951), and an unnamed taxon (Barrett, 1999);

(3) the theropods “*Dilophosaurus*” *sinensis* (Hu, 1993), possibly *Eshanosaurus deguchiiianus* (Xu, 2001), *Megapnosaurus* sp. (Irmis, 2004), *Lukousaurus yini* (Young, 1948; which is likely a crocodylomorph [Irmis, 2004]), and *Sinosaurus triassicus* (Young, 1948; Currie et al., in progress), and theropod footprints described as *Changpeipus pareschequier* (Xing et al., 2009).

(4) the basal thyreophorans (Norman et al., 2007) *Bienosaurus lufengensis* (Dong, 2001) and *Tatisaurus oehler* (Simmons, 1965). “*Dianchungosaurus lufengensis* (Yang, 1982)” – a supposed ornithopod from the unit – is a chimera, with the holotype representing a crocodylomorph and the paratype an indeterminate prosauropod dinosaur (Barrett and Xu, 2005).

Outside of Yunnan Province, the *Lufengosaurus* Fauna occurs in the Red Beds of Gongxian, Weiyuan of the Sichuan Basin, and in Xizang and Guizhou.

## 1.2 Geological Setting

The exposed Red Beds in the Lufeng Basin are from the Lufeng Series, which is further divided into the upper “Deep Red Beds” and lower “Dark Purple Beds” (Bien, 1941). The age of the Red Beds was originally thought to be Late Triassic based on the evolutionary “grades” of its vertebrate fossils (Young,

1951). Sheng et al. (1962) proposed an Early Jurassic age for the Lower Lufeng Formation, and a Middle Jurassic age for the Upper Lufeng Formation. In 1997, Zhang and Li mapped the position of Lao Changjing (in Chuanjie), and reported the positions of dinosaur fossils in the lower part of Upper Lufeng Formation (Zhang and Li, 1999).

Fang and colleagues (2000) studied the stratigraphic section at Lao Changqing–Da Jianfeng in the Chuanjie Basin and restricted the name “Lufeng Formation” to what was previously known as the Lower Lufeng Formation. They divided their redefined Lufeng Formation into the Shawan and Zhangjia’ao members. Their suggestions are followed in this paper. Strata that had at various times been encompassed in the Upper Lufeng Formation were divided into the Anning, Chuanjie, Laoluocun, and Madishan formations (Fang et al., 2000; Fig. 1.2).

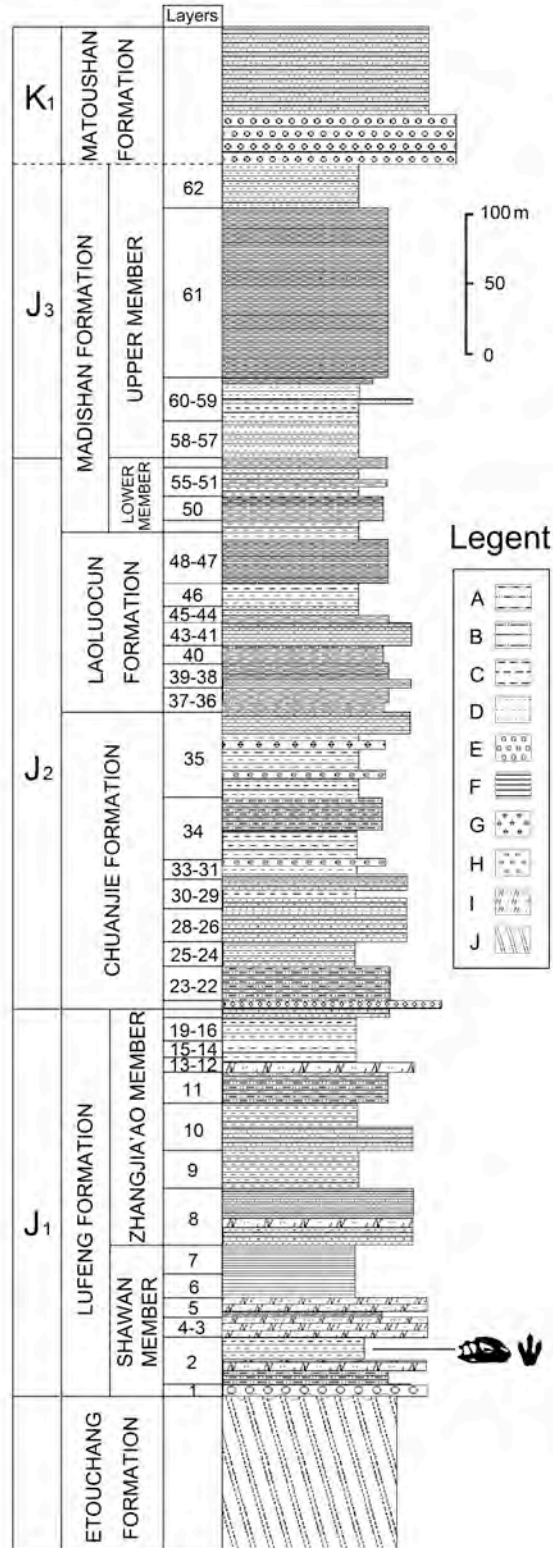


**FIGURE 1.2.** Stratigraphy of the Jurassic strata of Lufeng (adapted from Cheng et al., 2004). Legend: A. Pelitic siltstone, B. Sandy mudstone, C. Mudstone, D. Sandstone, E. Conglomerate, F. Shale, G. Orthomicrite, H. Orthomicrite containing fossils, I. Arkose, J. Slate.

The Zhangjia'ao Member was originally recognized as the “Deep Red Beds” of the Upper Member of the Lower Lufeng Formation. The type section of this unit is between Shawan and Dahuangtian. The Zhangjia'ao Member comprises deep red and tan–red mudstones interbedded with a small amount of thinly laminated siltstones. It is conformable with the underlying Shawan Member but disconformable with the overlying dark yellow sandy conglomerates of the Chuanjie Formation. In the Shawan region of the Lufeng Basin, this unit is 202 m thick (Zhang and Li, 1999; Fang et al., 2000).

The dinosaur fauna in the Zhangjia'ao Member includes *Anchisaurus sinensis*, *Lufengosaurus huenei*, *Lufengosaurus magnus*, *Kunmingosaurus wudingensis*, *Yunnanosaurus huangi*, and *Yunnanosaurus robustus*.

The Shawan Member was originally recognized as the “Dark Purple Beds” of the Lower Member of the Lower Lufeng Formation. The type section of this unit is also in the Shawan to Dahuangtian area. The Shawan Member comprises dark purple–red and dark purple mudstones interbedded with thinly laminated siltstones with well rounded, argillaceous cemented, dark purple or dark tan gravels and conglomerates with 2–3 cm diameter clasts at the base. It is conformable with the overlying Zhangjia'ao Member and is unconformable with the underlying purple phyllites of the Proterozoic Etouchang Formation of the Kunyang Group. In the Lufeng Basin, this unit is 528 m thick, and in the Chuanjie Basin it is over 500 m in thickness (Zhang and Li, 1999; Fang et al., 2000).

The dinosaur fauna in the Shawan Member includes: *Anchisaurus sinensis*, *Jinshanosaurus xinwaensis*, *Lufengosaurus huenei*, *Lufengosaurus magnus*,

*Lukousaurus yini*, *Sinosaurus triassicus*, *Yunnanosaurus huangi*, and  
*Yunnanosaurus robustus*.

### **1.3 Systematic paleontology**

**Dinosauria Owen, 1842**

**Theropoda Marsh, 1881**

**Coelophysoidea Holtz, 1994**

**Dilophosauridae Madsen and Welles, 2000**

***Sinosaurus triassicus* Young, 1948**

#### **1.3.1 Material**

Premaxilla, maxilla, lacrimal, frontal, occiput, dentary, atlantal  
intercentrum, caudal vertebra, and ribs, all catalogued under the number ZLJT01.

#### **1.3.2 Locality and horizon**

Lower Jurassic, Shawan member, Lufeng Formation (Lower Lufeng  
Formation): Hewanzi Village, Ganchong Village Committees, Konglongshan  
Township, Lufeng County, Chuxiong Yi Autonomous Prefecture, Yunnan  
Province, China

#### **1.3.3 Description and Comparison**

##### **1.3.3.1 Skull.**

### **(1) Premaxilla.**

The premaxillae of ZLJT01 are represented only by the paired nasal processes (8.3 cm long), which are fused and form an arch in lateral view (Fig. 1.3). The premaxilla–nasal suture is clearly preserved and the nasal processes of the premaxillae separate the anterior ends of the nasals. The poor preservation of ZLJT01 makes it impossible to determine the extent of the nasal processes. In *Sinosaurus triassicus* (KMV 8701 and LDM–L10), the nasal processes extend between the anterior ends of the nasolacrima crests. The left anterior process of the nasal can be determined by the premaxilla–nasal suture and is 3.5 cm in length. The right anterior process of the nasal is approximately 2.5 cm long.

In morphology, the nasal process of *Dilophosaurus wetherilli* (UCMP 37302; Welles, 1954; 1970; 1983; 1984) is more pronounced than any of those of KMV 8701, LDM–L10 and ZLJT01, and in lateral view there is a distinct bulge on the dorsomedial surface. The narrow and elongate nasal processes of ZLJT01 are more similar to those of LDM–L10. The shorter, wider nasal processes of KMV 8701 represent a minor difference that may be attributable to individual variation.

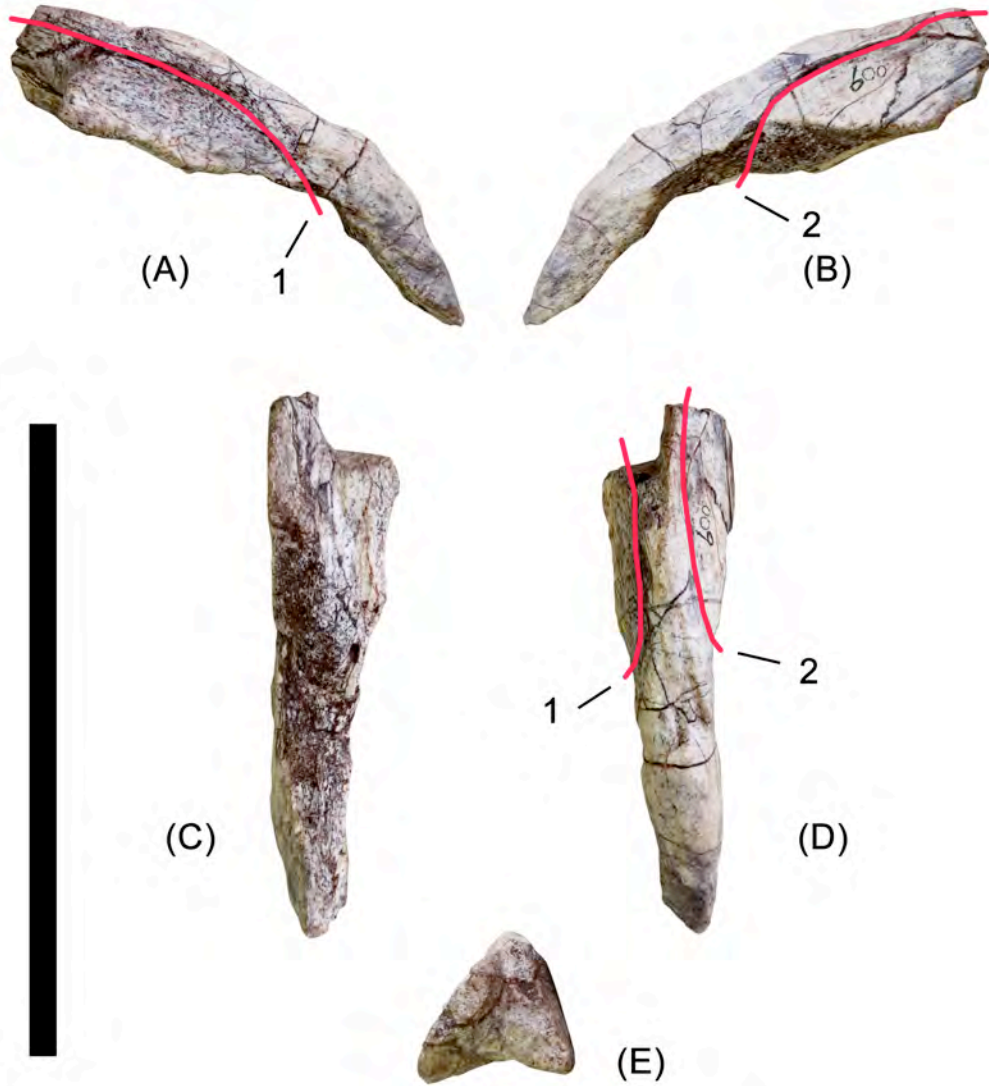


**FIGURE 1.3.** *Sinosaurus triassicus* (ZLJT01). Fused nasal processes of the premaxillae in right lateral (A), left lateral (B), posterior (C), anterior (D), and proximal (cross section; E) views. 1, right premaxilla–nasal suture; 2, left premaxilla–nasal sutures. Scale bar=10 cm

**(2) Maxilla.**

The maxilla of ZLJT01 is composed of three fragments with several partial teeth in position (Figs. 4, 5). As preserved, the right maxilla is composed of a large anterior segment separated by a short but indeterminate distance from a smaller posterior segment. Only the central, anterior portion of the left maxilla is preserved. The anterior segment of right maxilla lacks the upper process where it would have contacted the nasolacrimal crest, and the posterior fragment includes the posterior region of the alveolar ridge. In overall form, the maxilla is similar to that of *Sinosaurus triassicus* (KMV 8701 and LDM-L10)

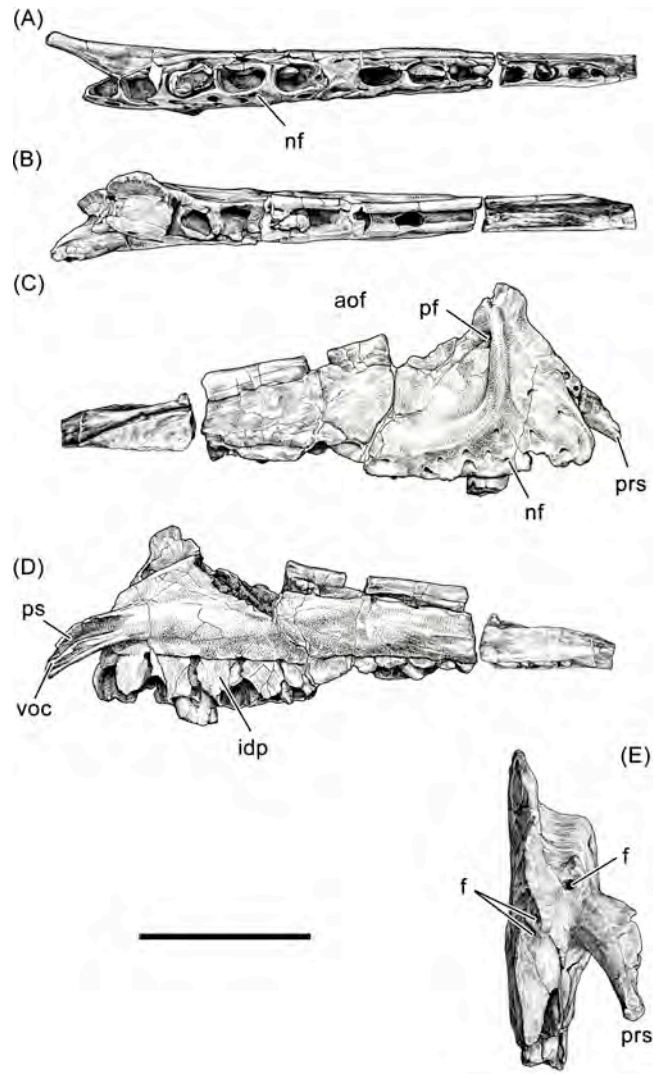


**FIGURE 1.4.** *Sinosaurus triassicus* (ZLJT01). Right maxilla in ventral (A), dorsal (B), lateral (C), medial (D) and anterior (E) views. Anatomical abbreviations: **aof**, antorbital fenestra; **f**, foramen; **idp**, interdental plates; **nf**, nutrient foramina; **pf**, promaxillary fenestra; **prs**, premaxillary suture of anteromedial process of the maxilla; **ps**, pterygoid suture on anteromedial process of the maxilla; **voc**, slot for vomer on anteromedial process of the maxilla. Scale bar=10 cm

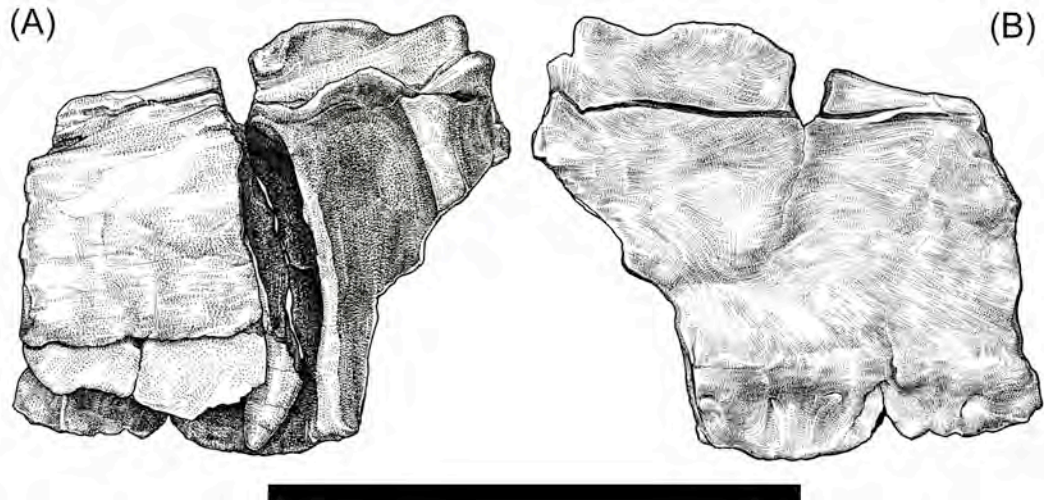


**FIGURE 1.5.** *Sinosaurus triassicus* (ZLJT01). Left maxilla fragment in medial (A) and lateral (B) views. Scale bar=10 cm

In ZLJT01, the posterior tip of the maxilla is not preserved, so the contacts between the maxilla, jugal and lacrimal cannot be observed.

A single opening is visible on the maxilla anterior to the edge of the antorbital fenestra along the anterior rim of the antorbital fossa. This opening is relatively large (13 by 8.5 mm), suggesting that it is the promaxillary fenestra. There is also a much smaller (4 by 2.5 mm) and more anterodorsal foramen that is still enclosed within the antorbital fossa.

The maxillary openings in KMV 8701 and LDM-L10 are similar to those of ZLJT01, although the promaxillary fenestrae are more posterior to the rims of the antorbital fossae. There are two accessory openings in *Dilophosaurus* (UCMP 77270), both positioned under the anterior rim of the antorbital fossa. In overall morphology, the maxillary fenestrae of UCMP 77270 are similar to those of ZLJT01, except that the former perforates the bone directly whereas they incline more gradually anteromedially in the latter.

In LDM-L10, there is a series of striations radiating downwards and backwards from the antorbital fossa, and it covers most of the lateral face of the ventrolateral surface of the maxilla and the lacrimal. This feature cannot be observed in KMV 8701 (where too much varnish covers the surface), and is not present on the maxillary fragments of ZLJT01.

The alveolar ridge on the lateral surface of ZLJT01 forms a clearly defined ventral limit to the antorbital fossa. In contrast, the horizontal ridges of KMV 8701, LDM-L10, and *Dilophosaurus* (UCMP 77270) are not pronounced. Nevertheless, the ventral margin of the antorbital fossa in ZLJT01 is not as well

demarcated as it is in most medium to large theropods. The ventral margin of the fossa is parallel to the alveolar margin as in *Coelophysis* (Colbert, 1989; 1990), *Liliensternus* (Huene, 1934; Ezcurra and Cuny, 2007), and *Syntarsus* (Tykoski, 1998). However, in *Dilophosaurus* the alveolar margin and the ventral rim of the antorbital fenestra diverge anteriorly (Currie et al., in progress). In *Sinosaurus triassicus* (KMV 8701, LDM–L10, and ZLJT01) the divergence of the alveolar margin and the ventral rim falls somewhere between these two extremes (Table 1.1).

**TABLE 1.1** Vertical distance (in mm) from the lateral edge of the alveolus to the ventral rim of the antorbital fossa.

	6 <sup>th</sup> alveolus	10 <sup>th</sup> alveolus	10 <sup>th</sup> /6 <sup>th</sup>
UCMP 77270	45	10	22%
UCMP 37303	40	9*	23%
LDM-L10	58.5	35	60%
KMV 8701	36.6	23	63%
ZLJT01	59	35	59%

\*below the 9<sup>th</sup> alveolus.

In ZLJT01, the anterior margin of the antorbital fossa inclines posteriorly at an angle of 93 degrees from horizontal. This inclination is closer to those in other *Sinosaurus triassicus* specimens (78 degrees in KMV 8701 and 75 degrees in LDM–L10) than it is to *Dilophosaurus* UCMP 77270 (70 degrees; Currie et al., in progress).

Two rows of nutrient foramina are positioned between the alveolar margin and the ventral margin of the antorbital fossa, whereas only one row is present in LDM–L10.

The 10<sup>th</sup> alveolus is incomplete in the right maxilla, and it is possible that one more alveolus may have been present in the missing central fragment. However, there were probably 13 maxillary tooth positions in ZLJT01. This is the same number as in other *Sinosaurus* specimens (KMV 8701), but is one less than in *Sinosaurus* (LDM–L10) and *Dilophosaurus* (UCMP 37302 and 37303).

As in *Dilophosaurus wetherilli* (Welles, 1984), *Sinosaurus triassicus* (KMV 8701 and LDM–L10) and *Syntarsus kayentakatae* (Rowe, 1989), there is a subnarial gap or groove separating the external surfaces of the premaxilla and maxilla above the alveolar margin. ZLJT01 probably shares this characteristic, because on the anterior edge of the maxilla, the area ventral to the anteromedial process is smooth, and lacks an identifiable premaxillary suture. This feature is similar to KMV 8701 and LDM–L10. The subnarial gaps of KMV 8701 and LDM–L10 share a common characteristic in having a premaxilla with a posterior region that is nearly parallel to the anterior portion of the maxilla; this is different from the condition in *Dilophosaurus wetherilli* (UCMP 37303, UCMP 77270),

where the posterior region of the premaxilla has a greater tilt. In this matter, ZLJT01 is similar to KMV 8701 and LDM–L10, with a straighter anteroventral maxillary edge.

In ZLJT01, *Dilophosaurus* (UCMP 37303, UCMP 77270), and *Sinosaurus triassicus* (KMV 8701 and LDM–L10), only the posterior portion of the ventral margin of the antorbital fossa is close to the alveolar margin. However, in *Coelophysis* (Colbert, 1989; 1990), *Liliensternus* (Ezcurra and Cuny, 2007), *Syntarsus* (Tykoski, 1998), and *Zupaysaurus* (Ezcurra, 2006; Ezcurra and Novas, 2007), there is a relatively shallow alveolar ridge that closely follows the ventral margin of the maxilla below the antorbital fossa.

### **(3) Lacrimal**

The paired crests in *Dilophosaurus* and *Sinosaurus* are formed by the nasals anteriorly, and the lacrimals posteriorly (Currie et al., in progress). The left crest of ZLJT01 only preserves the axe-shaped posterior section, which is formed by the lacrimal; it is well preserved (Fig. 1.6). The partial crest is 110 mm in length, and rises to a height of 73 mm above the postorbital contact of the lacrimal. The back of the crest extends posterolaterally above the rim of the orbit. In its morphology, ZLJT01 probably possessed a strongly convex dorsal margin that is similar to KMV 8701 but different from LDM–L10. The posterodorsal margins of ZLJT01 are thickened slightly in comparison with the main body of the crest, which is similar in degree to that of KMV 8701 but less like that of LDM–L10.

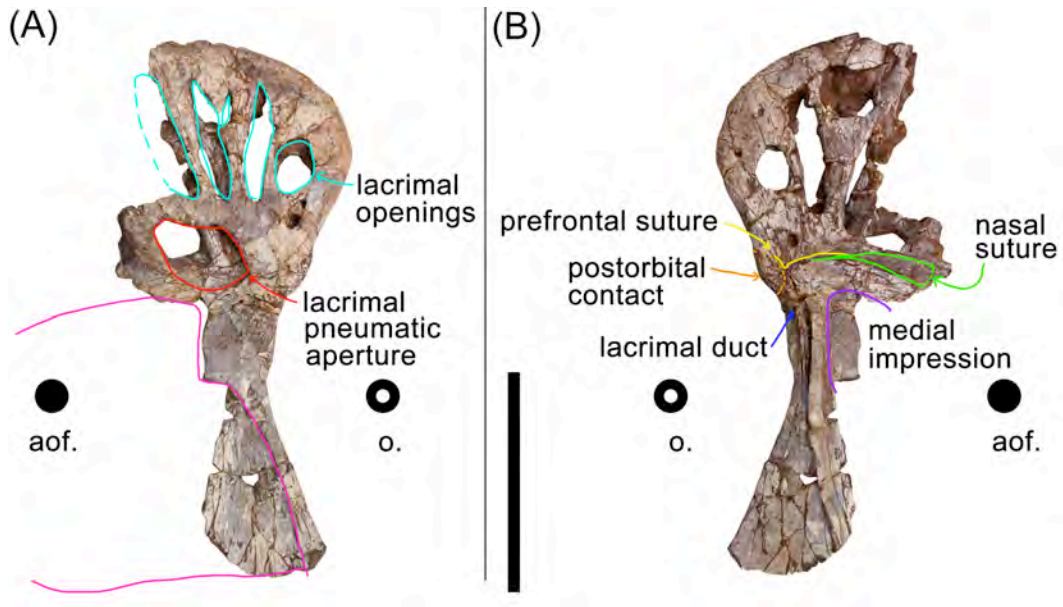


**FIGURE 1.6.** *Sinosaurus triassicus* (ZLJT01). Left lacrimal in lateral (A) and medial (B) views. Anatomical abbreviations: **aof**, antorbital fenestra; **o**, orbital fenestra. **Blue line**: lacrimal duct; **Light blue line**: lacrimal openings; **Green line**: nasal suture; **Orange line**: postorbital contact; **Pink line**: edge of the antorbital fenestra; **Purple line**: medial impression; **Red line**: lacrimal pneumatic aperture; **Yellow line**: prefrontal suture. **o**: orbital. Scale bars = 10 cm

The medial surface of the lacrimal portion of the crest has a series of oval openings near the dorsal margin of the crest. The bone between ridges is thin and ranges between 2.5 to 7 mm in thickness. These openings do not all penetrate the bone completely, and there are three lacrimal openings in lateral view and four openings in medial view. The long axis of each of these openings points towards the preorbital bar of the lacrimal. Below these lacrimal openings, near the posterodorsal corner of the antorbital fossa, is the ovoid lacrimal pneumatic aperture. It has a maximum length of 45 mm in lateral view, and is separated into anterior and posterior portions by a ridge. The posterior portion of the lacrimal pneumatic aperture is further divided into two upper lacrimal openings.

Well-defined, small holes are visible on the posterolateral margin of the medial surface of the crest; the width of each ranges between 3 and 16 mm. CT scans suggest that these small holes are connected with the larger lacrimal openings in the crest.

In the posterodorsal corner of the antorbital fossa, the lacrimal duct penetrates the preorbital bar. The antorbital fossa extends onto the lateral surface of the lacrimal in the posterodorsal corner. This extends dorsomedially into the pair of lacrimal pneumatic apertures as in most theropods. The lateral surface of the lacrimal extends to the edge of the antorbital fenestra as a projection below the posterodorsal portion of the antorbital fossa. This is similar to many other theropods including coelophysoids, and allosauroids.

Below that point, the antorbital fossa covers all the outer surface of the lacrimal except for an anteroposteriorly thin region along the orbital margin. This

character is similar to many other theropods including coelophysoids *Coelophysis bauri* (CM 31374; Downs, 2000), *Cryolophosaurus ellioti* (FMNH PR1821; Smith et al., 2007), *Dilophosaurus wetherilli* (UCMP 37302; Welles, 1984), *Syntarsus kayentakatae* (MNA V2623; Tykoski, 1998), and *Zupaysaurus rougieri* (PULR 076; Ezcurra, 2006); sinraptorids *Sinraptor dongi* (IVPP 10600; Currie and Zhao, 1993); and tyrannosaurids *Nanotyrannus lancensis* (CMNH 7541; Carr, 1999). This character is also similar to *Ceratosaurus magnicornis* (MWC 1; Madsen and Welles, 2000), although it also has another lacrimal recess in this area.

#### **(4) Dentary**

The lower jaws are represented by only the largely fragmentary left dentary (Fig. 1.7). As preserved, it is 277 mm long, with a maximum depth of 61 mm. The lateral surface of the dentary is pierced by a row of approximately eight mental foramina for innervation of the skin and lips of the lower jaw by the inferior alveolar nerve. An estimated twelve less prominent and smaller foramina are present close to the anteroventral margin of the lateral surface. The dental shelf is thick, and splits posterior to the last alveolus (the 13th) to accept the anterior end of the surangular. It appears that the dental shelf would have extended for at least another couple of centimetres beyond the persevered part. The supradentary was not recovered with ZLJT01, but the contact surface is present on the posteromedial surface of the dental shelf.

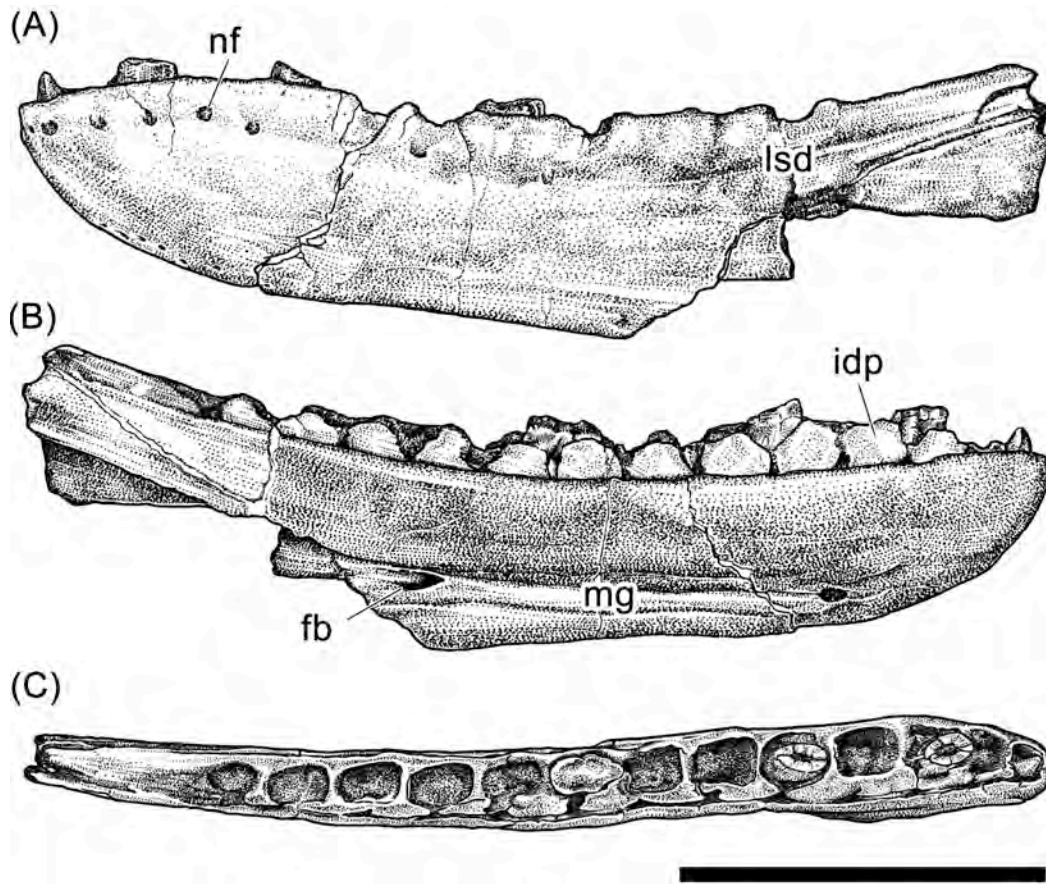


**FIGURE 1.7.** *Sinosaurus triassicus* (ZLJT01). Left dentary in lateral (A), medial (B) and dorsal (C) views. Anatomical abbreviations: **fb**, foramen for branch of inferior alveolar nerve; **idp**, interdentary plate; **lsd**, lateral sulcus of the dentary; **mg**, Meckelian groove; **mf**, mental foramen; **mkf**, Meckelian foramen; **ms**, medial symphysis. Scale bars = 10 cm

The dentary has 13 alveolar positions, which is the same as KMV 8701 (Hu, 1993). As displayed, LDM–L10 has 16 alveolar positions (Currie et al., in progress); however, it is likely that some of these teeth are the result of artistic license and were added in by the fossil preparator (Tao WANG, Lufeng Dinosaur Museum, pers. comm.). *Dilophosaurus wetherilli* (UCMP 37303) probably has 17 alveoli (Welles, 1984). Allosaurids and sinraptorids also appear to have had more alveolar positions than *Sinosaurus triassicus*. *Allosaurus* (Madsen, 1976) and *Sinraptor dongi* (IVPP 10600) have 16 alveoli (Currie and Zhao, 1993), and *Yangchuanosaurus shangyuensis* (CV 00215) has 14 (right) to 15 (left) alveoli (Dong et al., 1978, 1983).

Like *Sinraptor dongi* (Currie and Zhao, 1993), the interdental plates of ZLJT01 are separate. The interdental plates in *Dilophosaurus wetherilli* (UCMP 37303) are relatively lower than ZLJT01. The medial surfaces of the interdental plates of *Sinosaurus triassicus* (KMV 8701 and LDM–L10) are poorly preserved.

A distinct foramen is present underneath the tenth alveolus of the medial surface of the dentary. This foramen is attributed to the point where the Meckelian canal passes between the dentary and splenial to become the medially open Meckelian groove. In the dentary of *Dilophosaurus wetherilli* (UCMP 37303), this foramen is also present underneath the tenth alveolus. The lower jaws of *Dilophosaurus wetherilli* (UCMP 37302, UCMP 77270) and *Sinosaurus triassicus* (KMV 8701 and LDM–L10) are too poorly preserved for the presence or absence of this character to be verified. *Allosaurus* (Madsen, 1976) and *Sinraptor* (Currie and Zhao, 1993) each have two such foramina. The Meckelian

groove is shallow as in all theropods except troodontids (Currie, 1987). A Meckelian foramen exits the lingual surface of the bone at the anterior end of the Meckelian groove.

In lateral view, the dentary fragment has a generally concave upper margin and a straight lower margin. The dentary increases in depth posteriorly from the symphysis to about the level of the fourth dentary tooth, where it is 55.5 mm deep. The dentary height slightly decreases to 54.2 mm at about the seventh tooth position. After this position, it increases progressively to reach its maximum depth. However, the maximum depth cannot be measured because the intramandibular process (Currie and Zhao, 1993) is not present. The ZLJT01 dentary is different from those of *Dilophosaurus wetherilli* (UCMP 37303) and *Sinosaurus triassicus* (KMV 8701 and LDM-L10), in each of which there is a distinct decrease in dentary depth from the fourth to tenth dentary tooth.

#### **(5) Teeth.**

The teeth of ZLJT01 are poorly preserved, but include both erupted and germ (replacement) teeth (Fig. 1.8). Both the anterior and posterior carinae are well developed on all teeth, and have small denticles.

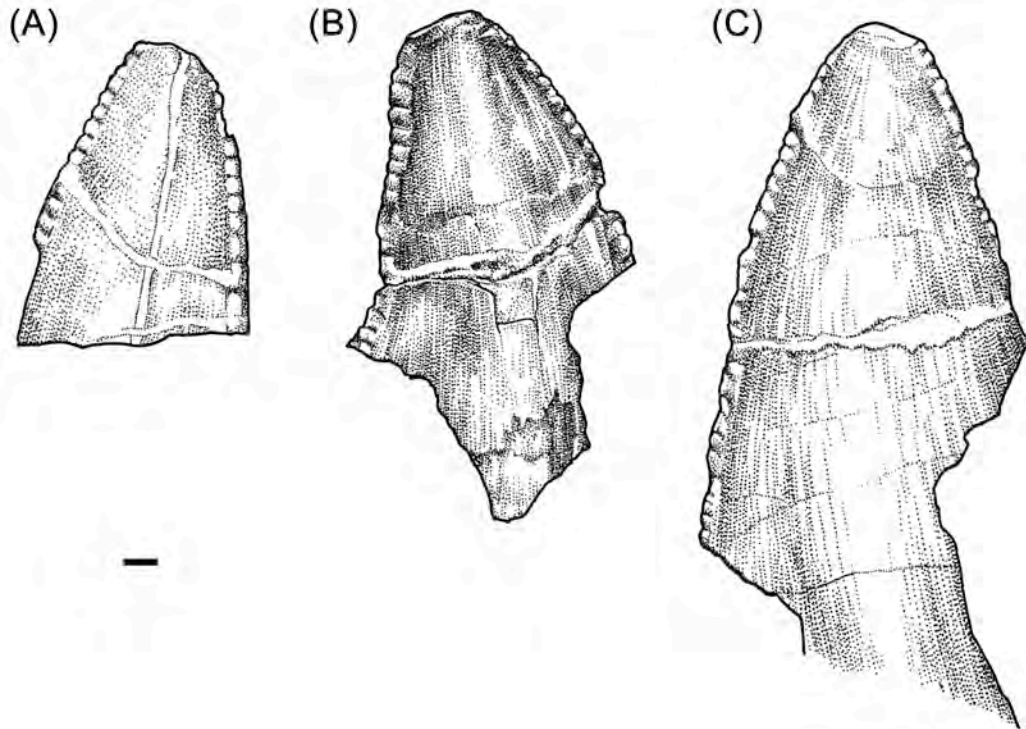


**FIGURE 1.8.** *Sinosaurus triassicus* (ZLJT01). The first left dentary tooth (A), fifth right maxillary tooth (B), and fourth left maxillary tooth (C). Scale bars = 1 mm

The teeth of the right maxilla are preserved in the third, fifth, eighth and eleventh alveoli. The third maxillary tooth (mx3) is fractured in the middle so that most of the crown is not preserved and only 20 mm of the base is present. The crown base length (CBL) and crown base width (CBW) are 24 mm and 11 mm, and the crown base ratio (CBR) is 0.46. CBR values have been used to measure the basal shape changes from circular (a value of 1.0) to increasingly bladelike structures (Smith et al., 2005). The value 0.46 is slightly less than the CBR of *Dilophosaurus* teeth (UCMP 37303), which range from 0.54 to 0.62 (Smith et al., 2005).

Mx5, mx8, and mx11 are newly exposed replacement teeth, but were not fully erupted. Crown heights (CH) are 17, 15 and 8 mm, respectively. The anterior and posterior carinae of mx5 have 2.2 denticles per millimeter. The denticles of mx8 are poorly preserved but are basically similar to those of mx5. The anterior and posterior carinae have 3 and 3.5 denticles per millimeter, respectively.

Part of the fourth tooth of the left maxilla is exposed in its damaged alveolus. The base of the crown is strongly compressed mediolaterally, and the anterior and posterior carinae are finely denticulate. There are two denticles per millimeter along the carinae.

Teeth of the left dentary are preserved in the first, third, fifth and eighth alveoli. D1 is a replacement tooth and has 1.6 and 2 denticles per millimeter on the anterior and posterior carina, respectively. The other three teeth were erupted but broken off at mid-height. The fore-aft basal lengths (FABL) of these teeth are 14, 15 and 17 mm, and the basal width of each is 8 mm. Only the anterior carina

of d3 preserves denticles, and it has 2.8 denticles per millimeter.

Generally, the denticles along the posterior carina are slightly larger than anterior ones in labial or lingual view. Each denticle is roughly rectangular and chisel-like in form. Blood grooves between the adjacent denticles do not extend far onto the crown surface. Enamel wrinkles are not present on either the labial or lingual surfaces. Almost all crowns have longitudinal striations in the enamel.

Most teeth of KMV 8701 (*Sinosaurus triassicus*) are in poor condition and provide little information. In LDM-L10 (*Sinosaurus triassicus*), a partial crown of the left mx5 has 3.2 denticles per mm on the posterior carina. This is similar to the denticle counts of *Cryolophosaurus* and *Dilophosaurus*, but larger than those of mx5 of ZLJT01, which has 1.8–2 denticles per mm. The teeth of IVPP V34 (*Sinosaurus triassicus*) are well-preserved, and there are 2.4–3 denticles per mm on the anterior carina, and 2.8–3 on the posterior carina (Currie et al., in progress). The counts are slightly more than 1.6–3 per mm of ZLJT01 on the anterior carina, and 2–3.6 on the posterior carina.

### **1.3.3.2 Postcranial Skeleton**

#### **(1) Atlantal intercentrum**

Most of the atlas-axis complex is missing, and only the atlantal intercentrum is completely preserved (Fig. 1.10). The atlantal intercentrum is close in overall morphology to that of *Sinraptor* (Currie and Zhao, 1993). The odontoid concavity in the dorsal surface is smoother and deeper than in other large Jurassic theropods, including *Allosaurus* (Madsen, 1976), *Ceratosaurus*

(Madsen and Welles, 2000), and *Torvosaurus* (Britt, 1991). As in *Sinraptor* and *Torvosaurus*, the ventrolateral process on the atlantal intercentrum is distinct, but weaker than that of *Allosaurus*. The surface of the process is smooth, and it would not have articulated with a cervical rib. The ventral axial articulation on the atlas preserves a tongue-shaped process that is more pronounced than it is in *Sinraptor*. A pair of pneumatic foramina is present on each side of this process and is medial to the ventrolateral process.

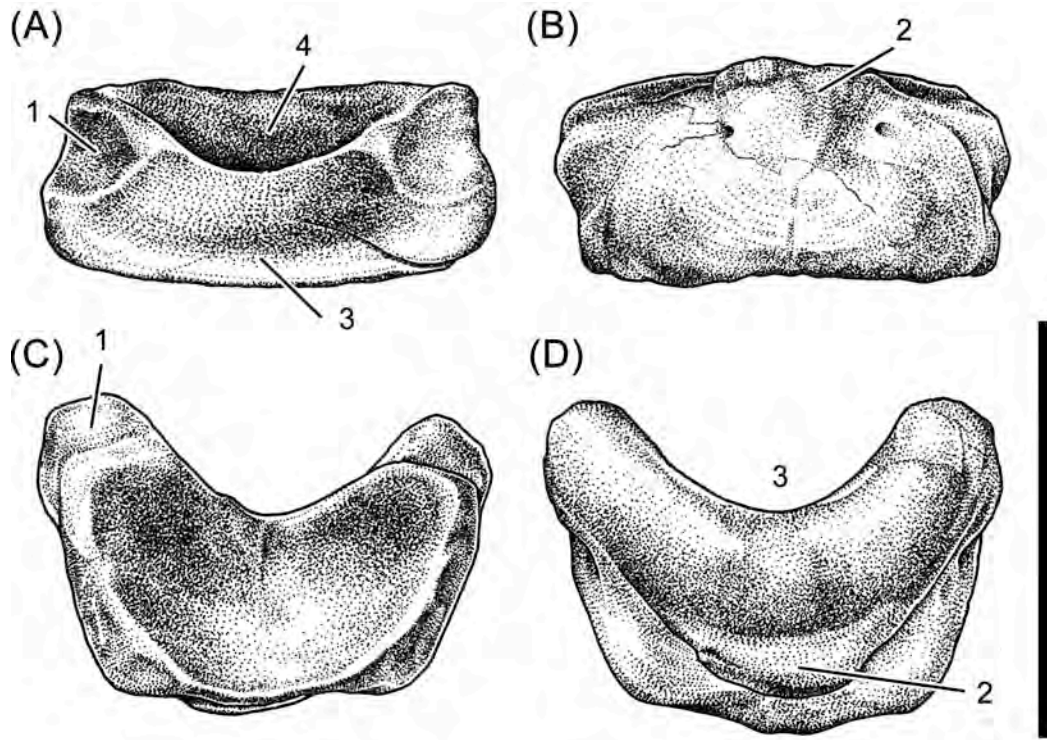


**FIGURE 1.10.** *Sinosaurus triassicus* (ZLJT01). Atlantal intercentrum in dorsal (A), ventral (B), anterior (C), and posterior (D) views. 1, suture for neurapophysis; 2, axial articulation on atlas; 3, odontoid concavity; 4, articular surface on atlantal intercentrum for occipital condyle. Scale bars = 5 cm.

The skull of KMV 8701 is articulated with the atlantal intercentrum, making it difficult to see details of the latter. The atlantal intercentrum of LDM-L10 was recognized when the specimen was re-examined in 2011. The atlantal intercentrum differs from ZLJT01 in that:

- 1) the odontoid concavity of the dorsal surface is shallower than in ZLJT01;
- 2) the articular surface on the atlantal intercentrum for the occipital condyle is much shallower than in ZLJT01, and there is a weak process on the dorsum of the articular surface;
- 3) there is no tongue-shaped process on the ventral edge of the axial articulation.

## **(2) Caudal vertebra**

A fragment of a vertebra was recovered, consisting of part of the neural arch, lacking the centrum, with a height of 6 cm and a width of 10.5 cm (Fig. 1.11). Only part of the ventral portion of the neural spine is preserved. The postspinal trough is well preserved and has an oval shape. The postspinal trough is continuous with a postspinal groove. Only the right postzygopophysis is preserved, extending from the edge of the postspinal trough. The proximal portion of the transverse process is preserved, extending laterodorsally. The hyposphene of ZLJT01 is damaged, but its existence is inferred. Hyposphenes do not persist into the tail of *Allosaurus* as they do in more primitive forms like *Monolophosaurus* and *Sinraptor* (Currie and Zhao, 1993).

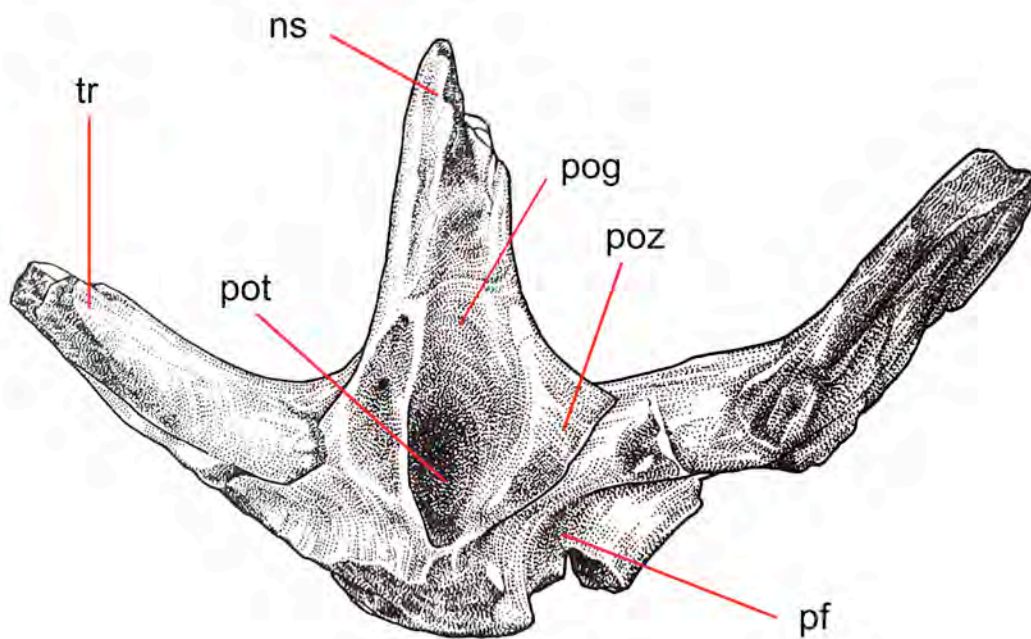


**FIGURE 1.11.** *Sinosaurus triassicus* (ZLJT01). Caudal vertebra in posterior view.

Anatomical abbreviations: **ns**, neural spine; **pf**, pneumatic foramina; **pog**, postspinal groove; **pot**, postspinal trough; **poz**, postzygopophysis; **tr**, transverse process. Scale bars = 10 cm

In posterior view, the articular surface of the postzygopophysis is roughly parallel to the dorsoventral angle of the transverse process. In this regard, it is similar to the anterior caudal vertebrae of *Sinosaurus triassicus* (LDM–L10) and *Dilophosaurus wetherilli* (UCMP 37302), which suggests the vertebra is probably from the anterior region of the caudal series.

Pneumatic foramina are nearly ubiquitous on the lateral surfaces of anterior presacral vertebrae of saurischian dinosaurs (Yates et al., 2012), and can extend posteriorly as far as the anterior caudals. One pneumatic foramen can be observed on the anteroventral surface of the transverse process of ZLJT01, which is consistent with the interpretation that the specimen represents an anterior caudal.

### **(3) Ribs.**

Only two fragmentary ribs are preserved (Fig. 1.12) with ZLJT01. Based on the characteristics of large theropods (Bakker et al. 1992), these rib fragments are best referred to as dorsal ribs. One of the fragmentary ribs is a proximal rib, with a capitulum (2.1 cm X 1.9 cm) and tuberculum (1.5 cm X 0.9 cm). There are distinct depressions on the posteromedial surface of the web between the bases of the capitulum and tuberculum. The second fragment is the middle part of a shaft. Its maximum cross-sectional diameters are 1.9 cm X 1.5 cm at the proximal end, compared with 1.1 cm X 1.1 cm at the distal end of the preserved section.

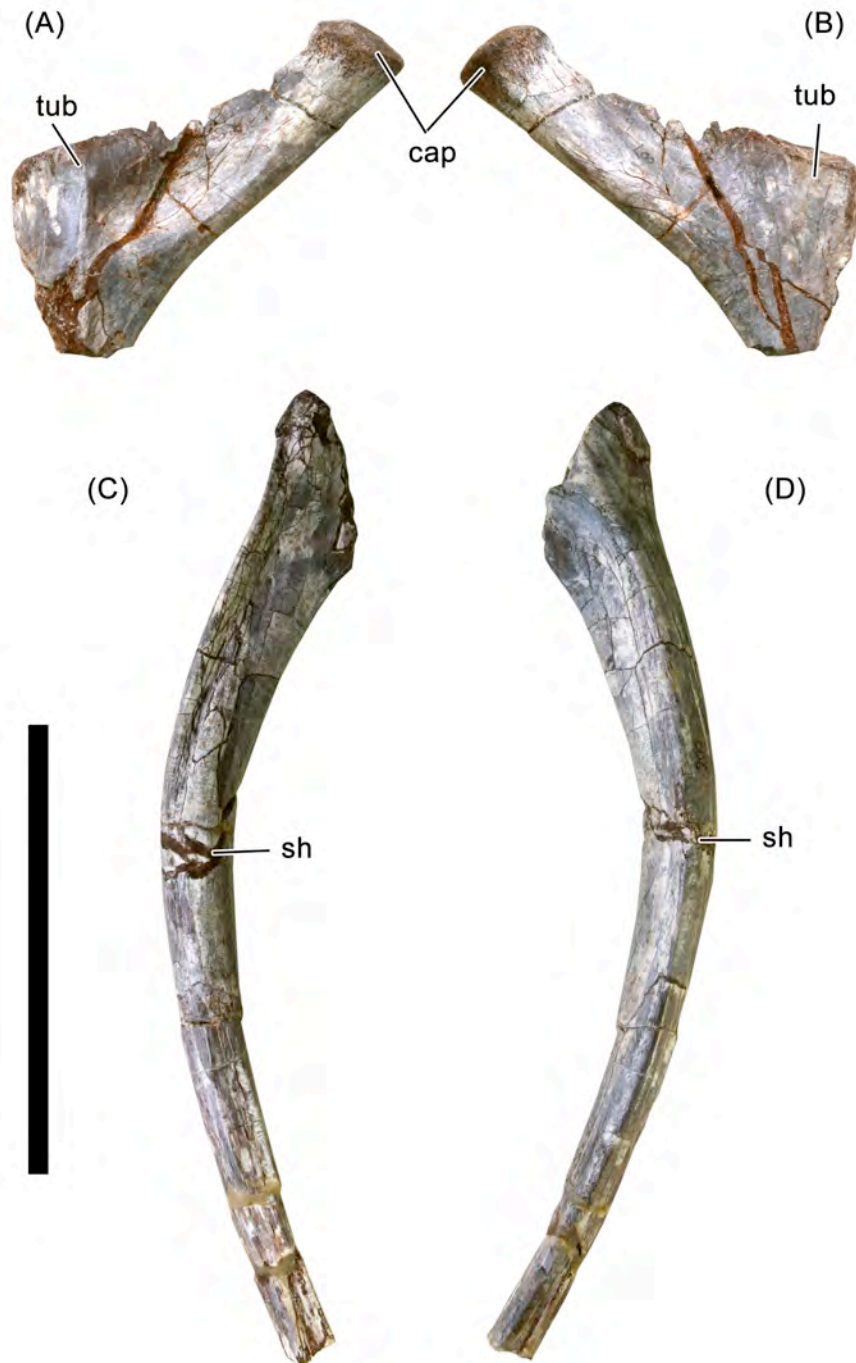


**FIGURE 1.12.** *Sinosaurus triassicus* (ZLJT01). Ribs in anteroventral (A and C) and posterodorsal (B and D) views. Anatomical abbreviations: **cap**, capitulum; **sh**, shaft; **tub**, tuberculum. Scale bars = 10 cm

The rib fragments of ZLJT01 are difficult to compare in a meaningful way with those of other theropods. There is nothing obvious that suggests any differences from the articulated specimens of *Sinosaurus triassicus* (KMV 8701, LDM–L10), which have abundant ribs.

#### **1.3.4 Discussion**

The lacrimal crest included the more special characteristics than the other materials in the ZLJT01, and can compare with the other theropod. Many theropod genera developed cranial crests, including *Ceratosaurus*, *Cryolophosaurus*, *Dilophosaurus*, *Guanlong*, *Monolophosaurus*, and *Oviraptor*. Most theropods, including allosaurids, carcharodontosaurids, sinraptorids, tyrannosaurids and many other lineages develop a pair of low ridges on the nasals that extend onto the lacrimals near the anterior margins of the orbits.

The theropods with paired, sheet-like cranial crests include *Dilophosaurus wetherilli* and *Syntarsus kayentakatae* from Arizona, *Dracovenator regenti* from South Africa, *Sinosaurus triassicus* from China, and *Zupaysaurus rougieri* from Patagonia. All these five species have been referred to as dilophosaurids, and come from the Lower Jurassic strata.

Each of the crests of KMV 8701 is formed by the nasal anteriorly, and the lacrimal posteriorly. The surface is poorly preserved, because of the conditions of preservation and/or poor preparation. The technicians at the Kunming City Museum applied too much varnish to the fossil, making it unfavorable for observation. There is no distinct border between the nasal and lacrimal portions of

the left crest, although its assumed position suggests that the number of depressions of the nasal portion exceeds those of the lacrimal. In lateral view, the nasal (front) portion has six elongate, oval depressions, whereas the lacrimal portion has only three distinct oval depressions. The most anterior lacrimal depression is twice the size of the other two. Moreover, there are three elongate, small, oval depressions close to each other between the most anterior and second lacrimal depression. Currently, the skull of KMV 8701 is preserved on a plaster base so that it is difficult to observe the base of the right crest. Although depressions are observed on the medial surface of the left crest, they are presumably asymmetric with the lateral depressions.

LDM-L10 has the best preservation of the crest on the left side. No distinct border was observed between the nasal and lacrimal portions of the left crest. In lateral view, the depressions in the nasal portion of the crest are more widely spaced than those in the lacrimal portion, although they are almost the same size. However, in medial view, the depressions are smaller than those on the lateral side. In this specimen, there are more depressions in the lacrimal portion of the crest than there are in the nasal portion. The left crest of this specimen is penetrated by only one opening, and it is infilled with plaster. The opening was probably caused by damage during excavation rather than being natural. A transverse section in the middle of the left crest shows that the interior is hollow (Fig. 1.12).

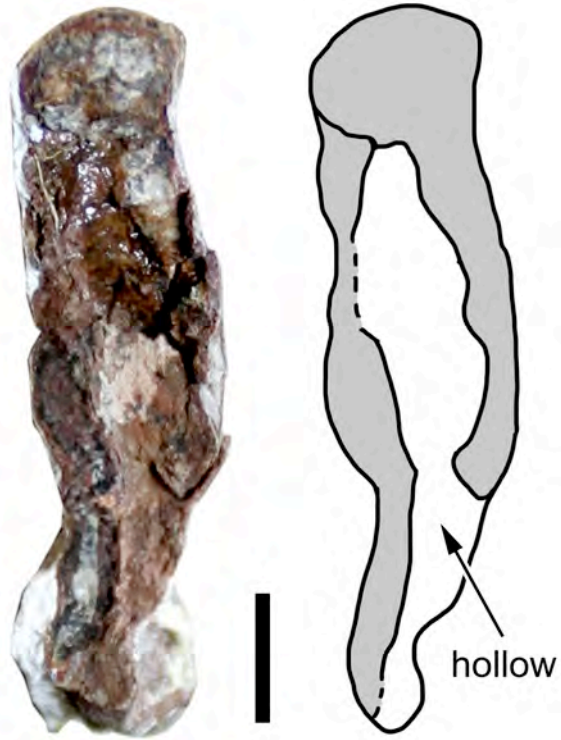


**FIGURE 1.12.** *Sinosaurus triassicus* (LDM-L10). A transverse section in the middle of the left crest. Scale bars = 5 mm

In morphology, the crest of ZLJT01 is similar to, but taller than the crest of KMV 8701. In the lacrimal portion of the crest, the most apparent differences amongst KMV 8701, LDM–L10, and ZLJT01 are in the shapes and sizes of the many lacrimal recesses. Although the depressions of the lacrimal portions of both KMV 8701 and LDM–L10 probably actually invade the interiors of the crests, there is no evidence of the large, lacrimal pneumatic apertures in the posterodorsal corners of the antorbital fossae.

The original *Dilophosaurus wetherilli* specimens (UCMP 37302, UCMP 37303) described by Welles (1954) lacked well-preserved crests, and Welles (1984) suggested that the crested specimens pertained to a different species. *Dilophosaurus "breedorum"* (Welles and Pickering, 1999) was based upon a crested specimen (UCMP 77270), but this species has been considered as nomen nudum in other reviews of the genus (Gay, 2001), and only one species of *Dilophosaurus* is considered valid. The most distinct difference between the crests of UCMP 77270 and ZLJT01 lies in the fact that the latter possessed distinct lateral lacrimal openings and a lacrimal pneumatic aperture in the posterodorsal corner of the antorbital fossa. UCMP 77270 probably possessed depressions only, similar to those of KMV 8701. Furthermore, the postorbital contact in UCMP 77270 is extended into a short, angular-shaped process that is not present in ZLJT01.

*Cryolophosaurus ellioti* (Hammer and Hickerson, 1994; Smith et al., 2007) has a large, posterodorsally curving transverse crest – formed by dorsal expansions of lacrimals – that has fluted anterior and posterior surfaces (Smith et

al., 2007). The transverse crest is quite different from the dilophosaur type of longitudinal and sheet-like crests of ZLJT01.

The paired parasagittal crests of *Zupaysaurus rougieri* (PULR 076; Arcucci and Coria, 2003) are restricted to the nasal and do not extend onto the lacrimal. However, this interpretation was dismissed by Ezcurra and Novas (2005) and Ezcurra (2007), who suggest that the right nasal is disarticulated from the left to give the false appearance of a long parasagittal crest. Based on the description by Arcucci and Coria, the crests of PULR 076 are low, and are different from the dilophosaur type of crest of ZLJT01 that is formed by the nasals anteriorly and the lacrimal posteriorly. PULR 076 has at least five lacrimal recesses in the posterodorsal corner of the antorbital fossa (Ezcurra and Novas 2006: Fig 10). The most posterior lacrimal recess is largest, and is similar with the large lacrimal pneumatic aperture.

*Dracovenator regenti* (Yates, 2005) has a sharp, low dorsolateral crest that is developed at the tip of the posterior end of the nasal. It is poorly preserved but suggests that there was probably a pair of nasolacrimal crests that were lower than those of *Dilophosaurus wetherilli* and ZLJT01.

"*Syntarsus*" *kayentakatae* (MNA V2623) has a pair of low, exceptionally thin, longitudinal crests (Tykoski, 1998). These crests are similar with those of *Dilophosaurus wetherilli* in morphology (Rowe, 1989), although the crests in MNA V2623 have little or no contributions from the lacrimals (Tykoski, 1998). A juvenile *Syntarsus* (QG165) has a incipient parasagittal crest, but it much smaller than that of MNA V2623; however, this small 'crest' may be an artifact of

displacement and distortion of the thin and plastic lacrimal and nasal bones according to Bristowe and Raath (2004). The most distinct difference between the crests of MNA V2623 and ZLJT01 lies in the fact that the latter has openings, and is formed by the nasal anteriorly, and the lacrimal posteriorly.

### **1.3.5 Conclusions**

In the Hewanzi specimen (ZLJT01), the morphological characteristics of the premaxilla, maxilla, lacrimal, dentary, and postcranial skeleton (atlantal intercentrum, caudal vertebra, and rib) suggests this specimen shares a number of characters with two other *Sinosaurus triassicus* specimens (KMV 8701, LDM–L10). These characters include the similar positions of the promaxillary fenestrae, a similar vertical distance from the lateral edge of the alveolus to the ventral rim of the antorbital fossa, the same number of dentary and maxillary alveol (KMV 8701), and the similar structure of the anterior caudal vertebrae.

In addition, the Hewanzi specimen (ZLJT01) also reveals several previously unknown characters, including the presence of a series of oval openings on the medial surface of the lacrimal portion of the crest, and an ovoid lacrimal pneumatic aperture near the posterodorsal corner of the antorbital fossa.

In conclusion, the Hewanzi specimen (ZLJT01) can undoubtedly be referred to *Sinosaurus triassicus*, but is more similar to the Qinglongshan specimen (KMV 8701) than it is to the Heilongtan specimen (LDM–L10).

## References

- Arcucci AB, Coria RA. 2003. A new Triassic carnivorous dinosaur from Argentina. *Ameghiniana* 40: 217–228.
- Bakker RT, Siegwarth J, Kralis D, Filla J. 1992. *Edmarka rex*, a new, gigantic theropod dinosaur from the middle Morrison Formation, Late Jurassic of the Como Bluff outcrop region. *Hunteria* 2: 9–24.
- Barrett PM. 1999. A sauropod dinosaur from the Lower Lufeng Formation (Lower Jurassic) of Yunnan Province, People's Republic of China. *Journal of Vertebrate Paleontology* 19(4): 785–787.
- Barrett PM, Xu X. 2005. A reassessment of *Dianchungosaurus lufengensis* Yang, 1982a, an enigmatic reptile from the Lower Lufeng Formation (Lower Jurassic) of Yunnan Province, People's Republic of China. *Journal of Paleontology*, 79(5): 981–986.
- Bien MN. 1941. “Red Beds” of Yunnan. *Bulletin of the Geological Society of China* 21: 159–198.
- Bristowe A, Raath MA. 2004. A juvenile coelophysoid skull from the Early Jurassic of Zimbabwe, and the synonymy of *Coelophysis* and *Syntarsus*. *Palaeontologia Africana*.40: 31–41.

- Britt B. 1991. Theropods of Dry Mesa Quarry (Morrison Formation, Late Jurassic), Colorado, with emphasis on the osteology of *Torvosaurus tanneri*, Brigham Young University Geology Studies 37: 1–72.
- Carr TD. 1999. Craniofacial ontogeny in Tyrannosauridae (Dinosauria, Coelurosauria). *Journal of Vertebrate Paleontology* 19: 497–520.
- Chao S. 1985. The reptilian fauna of the Jurassic in China. In: Wang S, Cheng Z. and Wang N. (eds.), *The Jurassic System of China*. Geological Publishing House, Beijing. 286–289, 347.
- Cheng Z, Li P, Pang Q, Zhang Z, Zhang Z, Jin Y, Lu L, Fang X. 2004. New progress in the study of the Jurassic of central Yunnan, *Geological Bulletin of China* 23(2): 154–159.
- Colbert EH. 1989. The Triassic dinosaur, *Coelophysis*. Museum of Northern Arizona, Bulletin 57: 1–160.
- Colbert EH. 1990. Variation in *Coelophysis bauri*. In: Carpenter K and Currie PJ. (eds.), *Dinosaur Systematics: Approaches and Perspectives*. Cambridge University Press, New York. 81–89.

- Currie PJ. 1987. Bird-like characteristics of the jaws and teeth of troodontid theropods (Dinosauria: Saurischia). *Journal of Vertebrate Paleontology* 7: 72–81.
- Currie PJ. and Zhao XJ. 1993. A new carnosaur (Dinosauria, Theropoda) from the Jurassic of Xinjiang, People's Republic of China. *Canadian Journal of Earth Sciences* 30(10–11): 2037–2081.
- Currie PJ, Xing LD, Wu XC, Dong, ZM. In progress. Anatomy and relationships of *Sinosaurus triassicus* (“*Dilophosaurus sinensis*”) from the Lufeng Formation (Lower Jurassic) of Yunnan, China.
- Dong ZM. 2001. Primitive armored dinosaur from the Lufeng Basin, China. In: Tanke DH. and Carpenter K. (eds.), *Mesozoic Vertebrate Life*. Indiana University Press, Bloomington. 237–242.
- Dong ZM. 2003. Contributions of new dinosaur materials from China to dinosaurology. *Memoir of the Fukui Prefectural Dinosaur Museum* 2: 123–131.
- Dong, ZM, Zhang YH, Li X and Zhou. SW. 1978. A new carnosaur from Yongchuan County, Sichuan Province. *Science Newsletter* 23(5): 302–304.

- Dong ZM, Zhou SW, Zhang, YH. 1983. Dinosaurs from the Jurassic of Sichuan. *Palaeontologica Sinica, New Series C* 162 (23): 1–136.
- Downs A. 2000. *Coelophysis bauri* and *Syntarsus rhodesiensis* compared, with comments on the preparation and preservation of fossils from the Ghost Ranch *Coelophysis* quarry: New Mexico Museum of Natural History and Science, Bulletin 17: 27–32.
- Ezcurra MD. 2006. A review of the systematic position of the dinosauriform archosaur *Eucoelophysis baldwini* Sullivan and Lucas, 1999 from the Upper Triassic of New Mexico, USA. *Geodiversitas* 28(4): 649–684
- Ezcurra MD, Novas FE. 2005. Phylogenetic relationships of *Zupaysaurus rougieri* from NW Argentina. *Boletim de Resumos, II Congresso Latino-Americano de Paleontologia de Vertebrados*. 102–104.
- Ezcurra MD, Novas FE. 2007. Phylogenetic relationships of the Triassic theropod *Zupaysaurus rougieri* from NW Argentina. *Historical Biology* 19: 35–72.
- Fang XS, Pang QJ, Lu LW, Zhang ZX, Pan SG, Wang YM, Li XK, Cheng ZW. 2000. Lower, Middle, and Upper Jurassic subdivision in the Lufeng region, Yunnan Province. in *Proceedings of the Third National Stratigraphical Congress of China*. Geological Publishing House, Beijing, 208–214.

- Galton PM, Upchurch P. 2004. Prosauropoda. In: Weishampel DB, Dodson P, Osmólska H (eds.), *The Dinosauria* (2nd Edition). University of California Press, Berkeley, 232–258.
- Gay R. 2001. New specimens of *Dilophosaurus wetherilli* (Dinosauria: Theropoda) from the early Jurassic Kayenta Formation of northern Arizona: Mesa Southwest Museum, Bulletin 8, 19–23.
- Hammer WR, Hickerson WJ. 1994. A crested theropod dinosaur from Antarctica. *Science* 264: 828–830.
- Hu SJ. 1993. A short report on the occurrence of *Dilophosaurus* from Jinning County, Yunnan Province. *Vertebrata Palasiatica* 31: 65–69.
- Huene Fv. 1934. Ein neuer Coelurosaurier in der thüringischen Trias. *Paläontologische Zeitschrift* 16(3–4): 145–170
- Irmis RB. 2004. First report of *Megapnosaurus* (Theropoda: Coelophysoidea) from China. *PaleoBios* 24 (3): 11–18.
- Madsen JH. 1976. *Allosaurus fragilis*: A revised osteology. Utah Geological and Mineralogical Survey Bulletin 109: 1–163.

- Madsen JH, Welles SP. 2000. *Ceratosaurus* (Dinosauria, Theropoda), a revised osteology. Miscellaneous Publication. Utah Geological Survey. 1–80.
- Norman DB, Butler RJ, Maidment SCR. 2007. Reconsidering the status and affinities of the ornithischian dinosaur *Tatisaurus oehleri* Simmons, 1965. *Zoological Journal of the Linnean Society* 150(4): 865–874.
- Rauhut OWM. 2000. The interrelationships and evolution of basal theropods (Dinosauria, Saurischia). Ph.D. dissertation, University of Bristol, U.K. 440.
- Rowe T. 1989. A new species of the theropod *Syntarsus* from the Early Jurassic Kayenta Formation of Arizona. *Journal of Vertebrate Paleontology* 9: 125–136.
- Sheng SF, Chang LQ, Cai SY, Xiao RW. 1962. The problem of the age and correlation of the red beds and the coal series of Yunnan and Szechuan. *Acta Geologica Sinica*, 42(1): 31–56.
- Simmons DJ. 1965. The non–therapsid reptiles of the Lufeng Basin, Yunnan, China. *Fieldiana: Geology*, 15 (1): 1–93.
- Smith JB, Vann DR, and Dodson P. 2005. Dental morphology and variation in

theropod dinosaurs: implications for the taxonomic identification of isolated teeth. *The Anatomical Record Part A* 285: 699–736.

Smith ND, Makovicky PJ, Hammer WR, Currie PJ. 2007. Osteology of *Cryolophosaurus ellioti* (Dinosauria: Theropoda) from the Early Jurassic of Antarctica and implications for early theropod evolution. *Zoological Journal of the Linnean Society* 151 (2): 377–421.

Tykoski RS. 1998. The osteology of *Syntarsus kayentakatae* and its implications for ceratosaurid phylogeny. MSc thesis, University of Texas, Austin, 1–217.

Tykoski RS, Rowe T. 2004. Ceratosauria. In: Weishampel DB, Dodson P, Osmolska H. (eds.), *The Dinosauria* (2nd Edition). University of California Press, Berkeley. 47–70.

Upchurch P, Barrett PM, Galton PM. 2007. A phylogenetic analysis of basal sauropodomorph relationships: implications for the origin of sauropod dinosaurs. In: Barrett PM. and Batten DJ. (eds.), *Evolution and Palaeobiology of Early Sauropodomorph Dinosaurs*. *Special Papers in Palaeontology* 77: 57–90.

Welles SP. 1954. New Jurassic dinosaur from the Kayenta formation of Arizona. *Bulletin of the Geological Society of America* 65: 591–598.

- Welles SP. 1970. *Dilophosaurus* (Reptilia: Saurischia), a new name for a dinosaur. *Journal of Paleontology* 44: 989.
- Welles SP. 1983. Two centers of ossification in a theropod astragalus. *Journal of Paleontology* 57(2): 401.
- Welles SP. 1984. *Dilophosaurus wetherilli* (Dinosauria, Theropoda): Osteology and comparisons. *Palaeontographica Abteilung A* 185: 85–180.
- Welles SP, Pickering S. 1999. *Megalosaurus bucklandii*. Private publication of Stephen Pickering, An extract from Archosauromorpha: Cladistics & Osteologies. A Fractal Scaling in Dinosaurology Project 1–119.
- Xu X, Zhao X, Clark JM. 2001. A new therizinosaur from the Lower Jurassic Lower Lufeng Formation of Yunnan, China. *Journal of Vertebrate Paleontology* 21(3): 477–483.
- Xing LD, Harris JD, Toru S, Masato F, Dong ZM. 2009. Discovery of Dinosaur Footprints from the Lower Jurassic Lufeng Formation of Yunnan Province, China and New Observations on *Changpeipus*. *Geological Bulletin of China* 28(1): 16–29.

- Yang ZJ. 1982. A new genus of dinosaur from Lufeng County, Yunnan Province.  
In: Zhou MZ. (ed.), Collected works of Yang Zhongjian. Academia Sinica,  
Beijing. 38–42.
- Yates AM. 2005. A new theropod dinosaur from the Early Jurassic of South  
Africa and its implications for the early evolution of theropods.  
*Palaeontologia Africana* 41: 105–122.
- Yates AM, Wedel MJ, Bonnan MF. 2012. The early evolution of postcranial  
skeletal pneumaticity in sauropodomorph dinosaurs. *Acta Palaeontologica  
Polonica* 57: 85–100.
- Young CC. 1941. A complete osteology of *Lufengosaurus huenei* Young (gen. et  
sp. nov) from Lufeng, Yunnan, China. *Palaeontologia Sinica, New Series C* 7:  
1–53.
- Young CC. 1942. *Yunnanosaurus huangi* (gen. et sp. nov.), a new Prosauropoda  
from the Red Beds at Lufeng, Yunnan. *Bulletin of the Geological Society of  
China* 22 (1–2): 63–104.
- Young CC. 1947. On *Lufengosaurus magnus* Young (sp. nov.) and additional  
finds of *Lufengosaurus huenei* Young. *Palaeontologia Sinica, New Series C*  
12: 1–53.

- Young CC. 1948. On two new Saurischia from Lufeng, Yunnan. Bulletin of the Geological Society of China 28(1-2): 75-90.
- Young CC. 1951. The Lufeng saurischian fauna in China. Palaeontologia Sinica, New Series C 13: 1-96.
- Zhang YH, Yang ZL. 1995. A complete osteology of Prosauropoda in Lufeng basin Yunnan China: *Jingshanosaurus*. Yunnan Scientific and Technological Publishing House, Kunming, 1-100.
- Zhang ZX, Li XK. 1999. A study on the stratigraphic section bearing the new sauropoda fauna in Laochangjing, Lufeng. Yunnan Geology 18(1): 72-82.

## CHAPTER 2

### **Braincase anatomy of *Sinosaurus triassicus* from the Lufeng Formation (Lower Jurassic) of Yunnan, China.**

#### **2.1 Introduction**

Dilophosaurid theropods are known from the Lower Jurassic sediments of Africa, Antarctica, China and North America (Smith et al., 2007). Partial braincases are known for *Cryolophosaurus ellioti* (Smith et al., 2007), *Dilophosaurus wetherilli* (Welles, 1984), *Dracovenator regenti* (Yates, 2006), *Syntarsus kayentakatae* (Rowe, 1989) and *Zupaysaurus rougieri* (Ezcurra, 2006). Complete braincases are known for three Chinese specimens of *Sinosaurus triassicus* ("*Dilophosaurus sinensis*" of Hu, 1993).

Dilophosauridae includes several medium-sized, Early Jurassic theropods, such as *Cryolophosaurus*, *Dilophosaurus*, *Dracovenator*, and *Sinosaurus*. They were traditionally assigned to the superfamily Coelophysoidea, although recent phylogenetic analyses suggest that dilophosaurids may have been more closely related to the Tetanurae, comprising the more advanced megalosaurs, carnosaurus and coelurosaurs (Smith et al., 2007). However, the interrelationships within the group are not yet completely understood.

Although two specimens of *Sinosaurus triassicus* (KMV 8701 and LDM-L10) have preserved braincases, they are poorly prepared and many areas are obscured by sediment, which is the reason why this part of the skull remains undescribed for this taxon (Hu, 1993). A new partial braincase of *Sinosaurus*

*triassicus* (ZLJT01) was prepared in 2011. It is exceptionally well preserved, although the frontals and orbitosphenoids are missing. This specimen allows the description of almost all the cranial nerve foramina, as well as the delicate structures that are often missing in other theropod braincases (Currie, 1997).

In this chapter, the braincase and endocranial morphology of *Sinosaurus* (ZLJT01) is described. New comparative data on braincase anatomy may provide a useful source of character information for phylogenetic analyses of dilophosaurids.

## **2.2 Methods**

In order to supplement observations on the external surfaces of the braincase, the specimen was subjected to X-ray computed tomographic (CT) imaging. It was scanned helically using a SOMATOM Definition AS/AS+ with FAST CARE (64-slice and 128-slice configurations) at Central Hospital, Chaozhou City, Guangdong Province, China. The slice thickness was 600  $\mu\text{m}$  at 120 kV and 350 mA. The three-dimensional reconstruction was made using the software Mimics (version 14) and Geomagic, and the illustrations were generated with Adobe Photoshop (version SC4).

Based a three-dimensional reconstruction was done of the *Sinosaurus* (ZLJT01) braincase, permitting study of the structure of the endocranial cavity and inner ear. The new information on the braincase of *Sinosaurus* will facilitate comparison with *Cryolophosaurus* (Smith et al., 2007), *Sinraptor* (Paulina Carabajal and Currie, 2011), and other theropods, which is important from both

anatomical and systematic points of view.

### **2.3 Anatomical Abbreviations**

**apf**, fenestra rostral to the pituitary fossa;

**bo**, basioccipital;

**bsph**, basisphenoid;

**bt**, basal tuber;

**btp**, basipterygoid process;

**bw**; basipterygoid web;

**col**, columellar recess;

**ctr**, caudal tympanic recess;

**cul**, cultriform process;

**eo–op**, exoccipital–opisthotic;

**f**, frontal;

**fm**, foramen magnum;

**lsph**, laterosphenoid;

**ltr**, lateral tympanic recess;

**met**, metotic foramen;

**oc**, occipital condyle;

**p**, parietal;

**psph**, parasphenoid;

**pop**, paroccipital process;

**pp**, preotic pendant;

**pcr**, paracondylar recess;

**pro**, prootic;

**so**, supraoccipital;

**sr**, subsellar recess;

**I–XII**, cranial nerve foramina.

#### **2.4. Description and Comparisons**

The skull roof is complete, preserving the frontals and parietals. The occiput is well preserved, although the parietal of the skull roof and the exoccipital–opisthotic complex are crushed. The foramen magnum, as preserved, is approximately 3.2 cm wide and 1.7 cm high. The occipital condyle is 4 cm across, and 3 cm in height. The sutures of the occiput are not closed, suggesting immaturity.

Most of the right frontal is preserved (Figs. 2.1 and 2.2) as a separate bone. As in *Sinosaurus triassicus* (KMV 8701 and LDM–L10), the frontal of ZLJT01 does not contribute to the lacrimal crest. It is relatively broad posteriorly, with a maximum width of 72 mm, and a maximum length of 82 mm. The anterior tip of the frontal is broken, and the nasofrontal suture cannot be observed.

In dorsal view, the lateral edge of the anterior tip of the frontal contacts the prefrontal and the lacrimal crest. The latter is an interlocking suture. The frontals also make a minor contribution to the back of the crest in *Monolophosaurus* (Zhao and Currie, 1993). The posterolateral corner of the frontal contacts the anteromedial edge of the postorbital. Posteriorly, the parietal suture is complex

and mostly transverse. The frontal has a small participation on the anterior margin of the supratemporal fossa, as in *Sinosaurus triassicus* (KMV 8701 and LDM–L10), *Zupaysaurus rougieri* (Ezcurra, 2006), and probably *Cryolophosaurus ellioti* (Smith et al., 2007).

The dorsal surface of the frontal has a shallow, bowl-like depression anterior to the parietal/frontal suture and medial to the postorbital suture. Several authors (Coria and Currie, 2002) believe that the adductor musculature (m. pseudotemporalis superficialis) attached to this region, whereas others (including Holliday, 2009) have suggested the m. pseudotemporalis superficialis attached within the supratemporal fossa proper.

In ventral view, the posteromedial region of the frontal has a somewhat circular cerebral impression. The posterolateral region has a smooth olfactory bulb impression. Posteriorly, the laterosphenoid contact is an oblate triangular shape.

Overall, the characteristics of the frontal of ZLJT01 are similar to those of *Sinosaurus triassicus* (LDM–L10 and KMV 8701). However, the frontals of *Dilophosaurus wetherilli* (UCMP 37302) are poorly preserved and too badly distorted for description (Welles, 1984) and comparison.

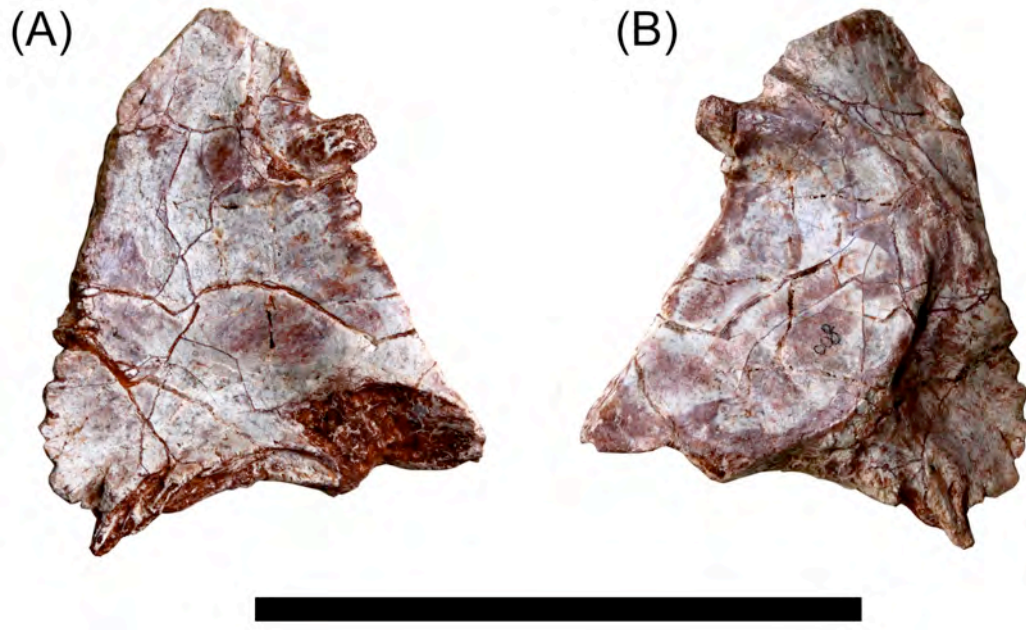


**FIGURE 2.1.** *Sinosaurus triassicus* (ZLJT01). Right frontal in dorsal (A) and ventral (B) views. Scale bars = 10 cm

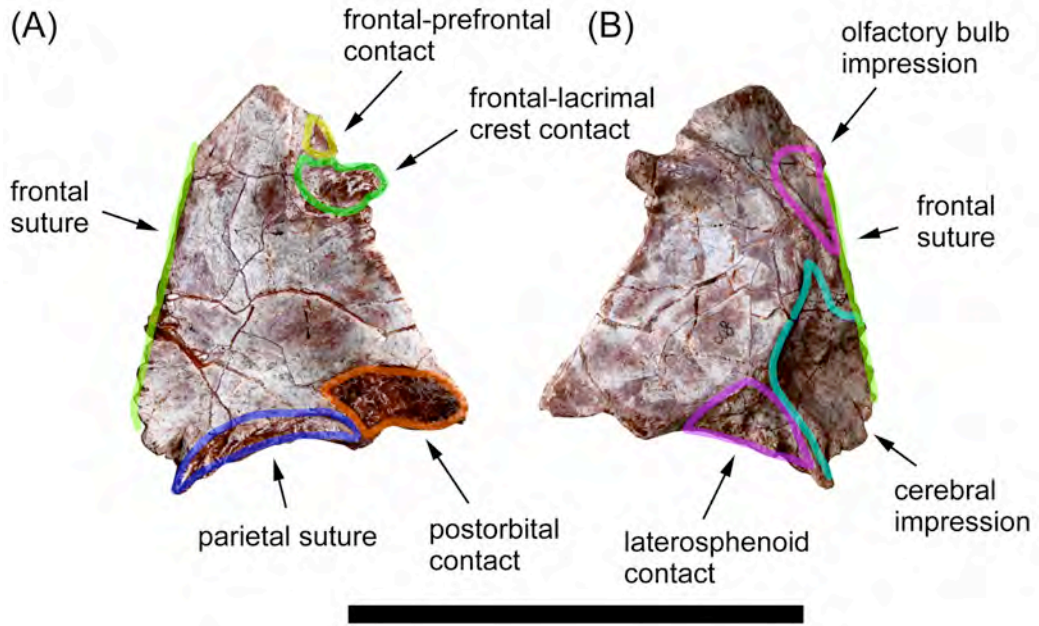
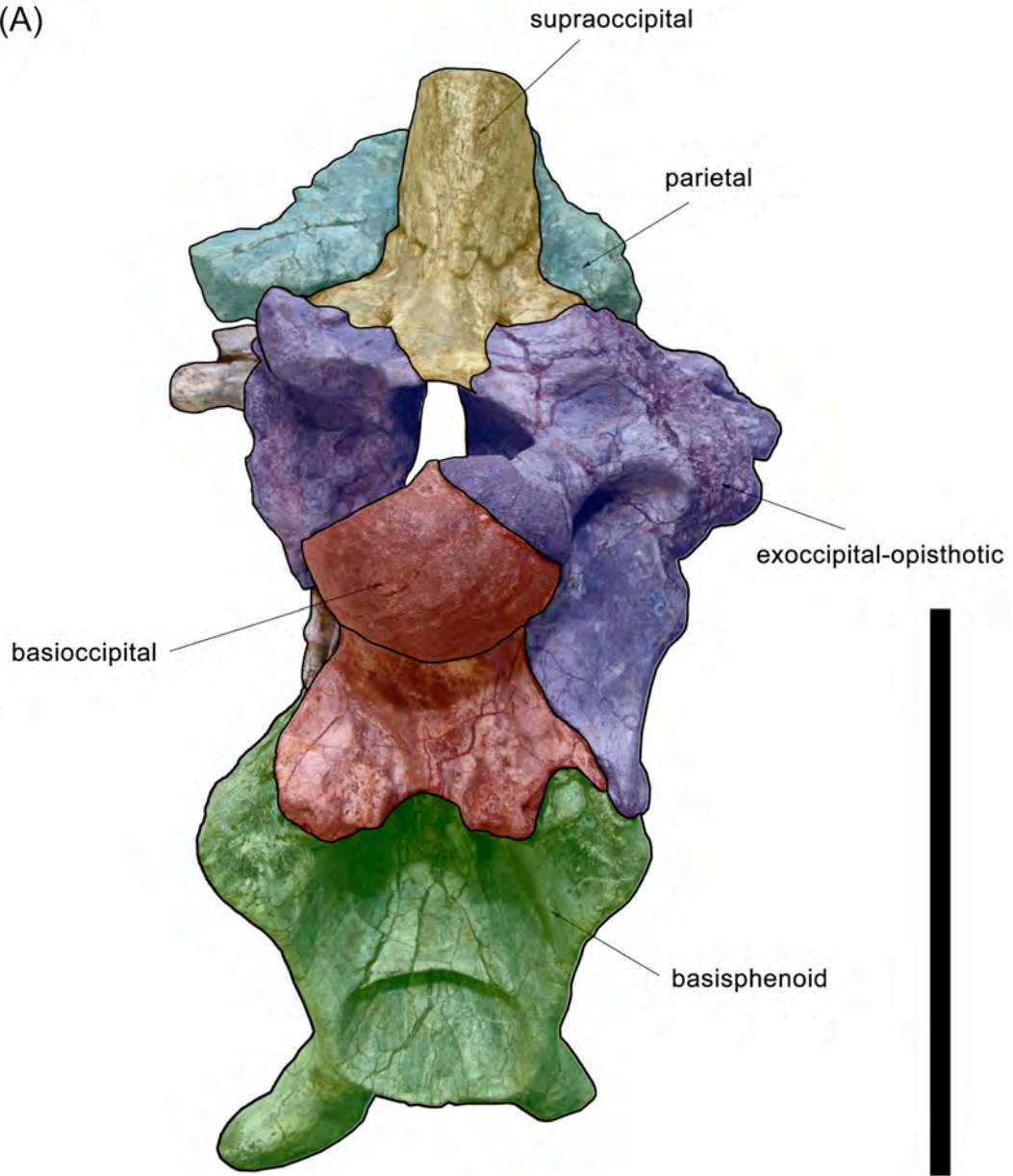


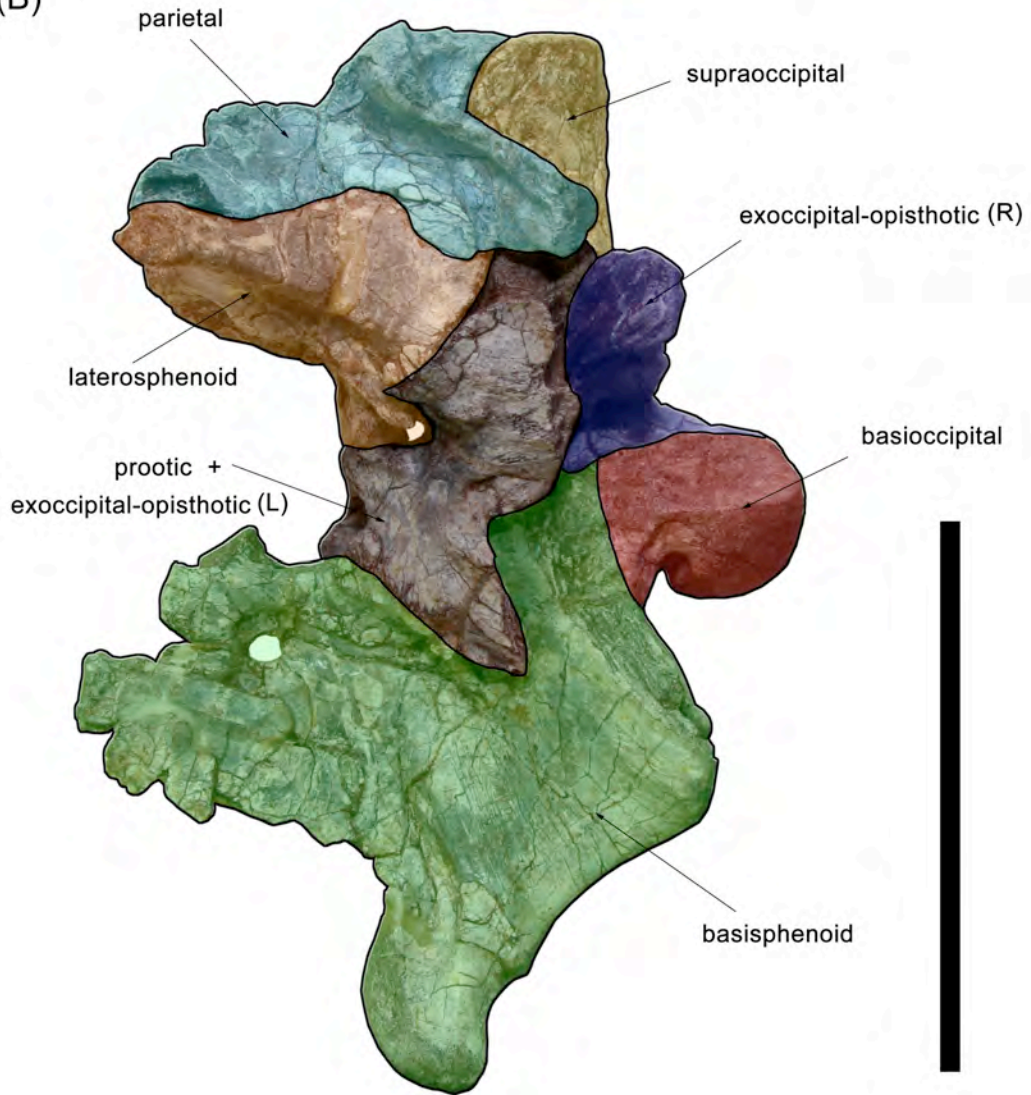
**FIGURE 2.2.** Right frontal of *Sinosaurus triassicus* (ZLJT01) in dorsal (A) and ventral (B) views. Scale bars = 10 cm

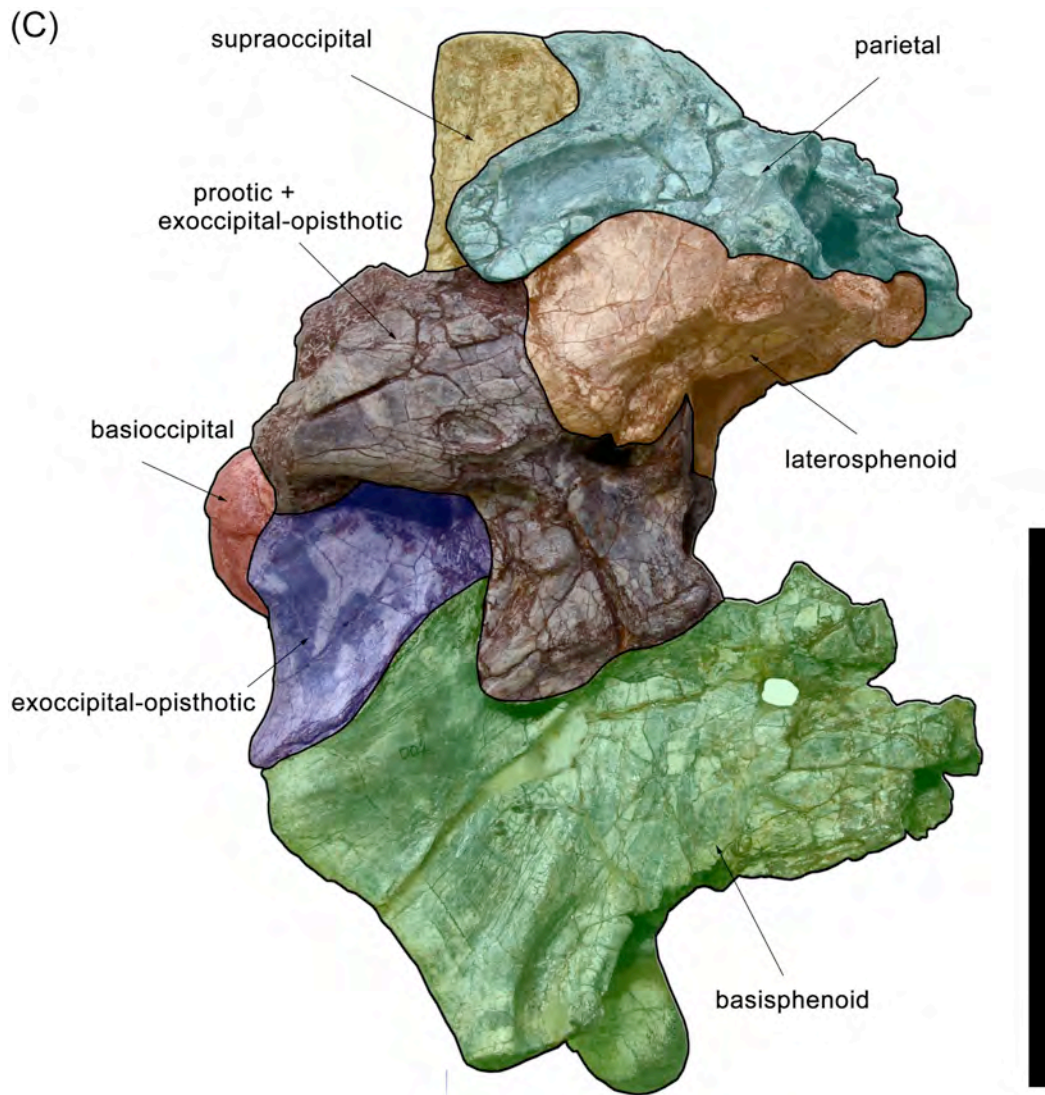
The fused parietals have a pair of low parasagittal ridges that are separated in the midline by a longitudinal trough. The trough extends from the frontal suture to end posteriorly on the flange of the parietal that overlaps the supraoccipital knob, as in KMV 8701 and LDM-L10 (Currie et al., in progress; Figs. 2.3 and 2.4). At the narrowest point between the supratemporal fenestrae, the ridges are separated by 27 mm. This width is similar to that of KMV 8701 (34 mm), but is larger than that of LDM-L10 (10 mm). Posteriorly, the nuchal crest is relatively low in comparison with the skull roof, and V-shaped in dorsal view, as in *Cryolophosaurus ellioti* (Smith et al., 2007), *Sinosaurus triassicus* (KMV 8701 and LDM-L10), *Syntarsus kayentakatae* (Rowe, 1989), and *Zupaysaurus rougieri* (Ezcurra, 2006).

(A)

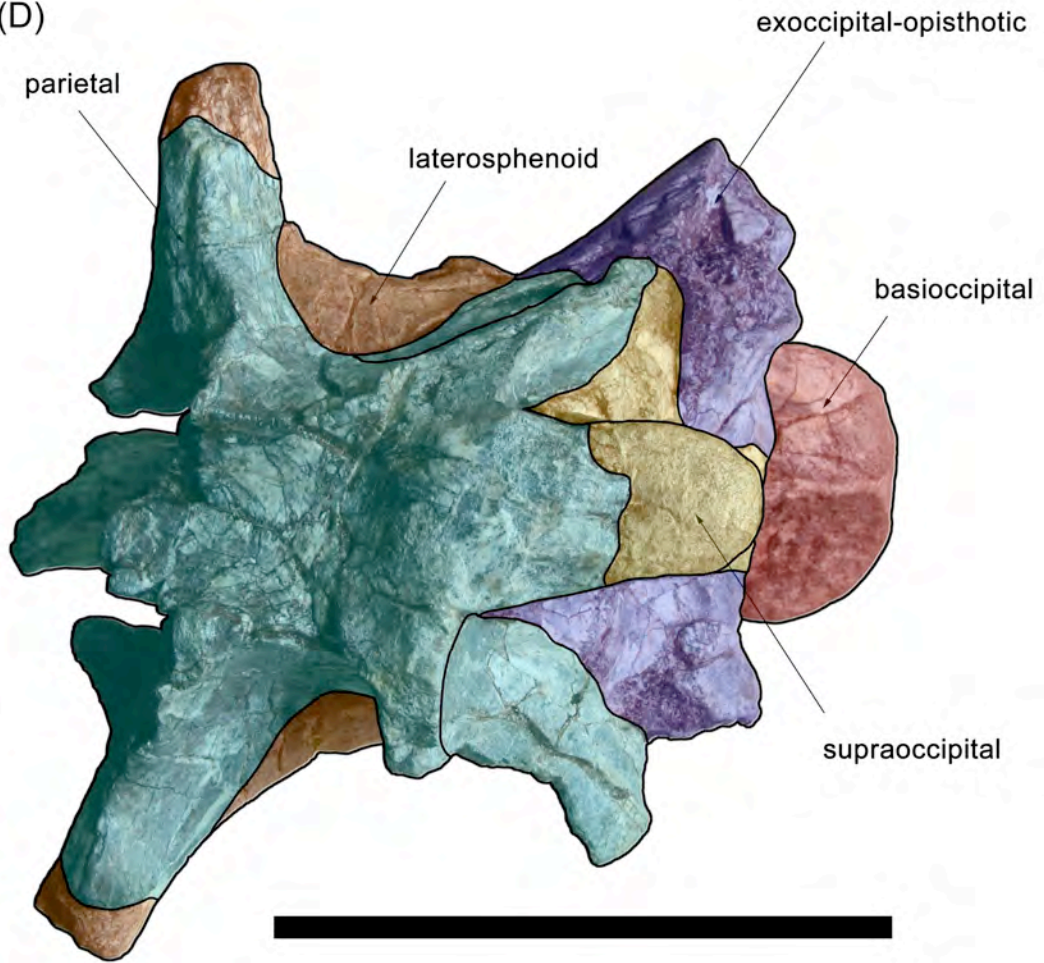


(B)





(D)



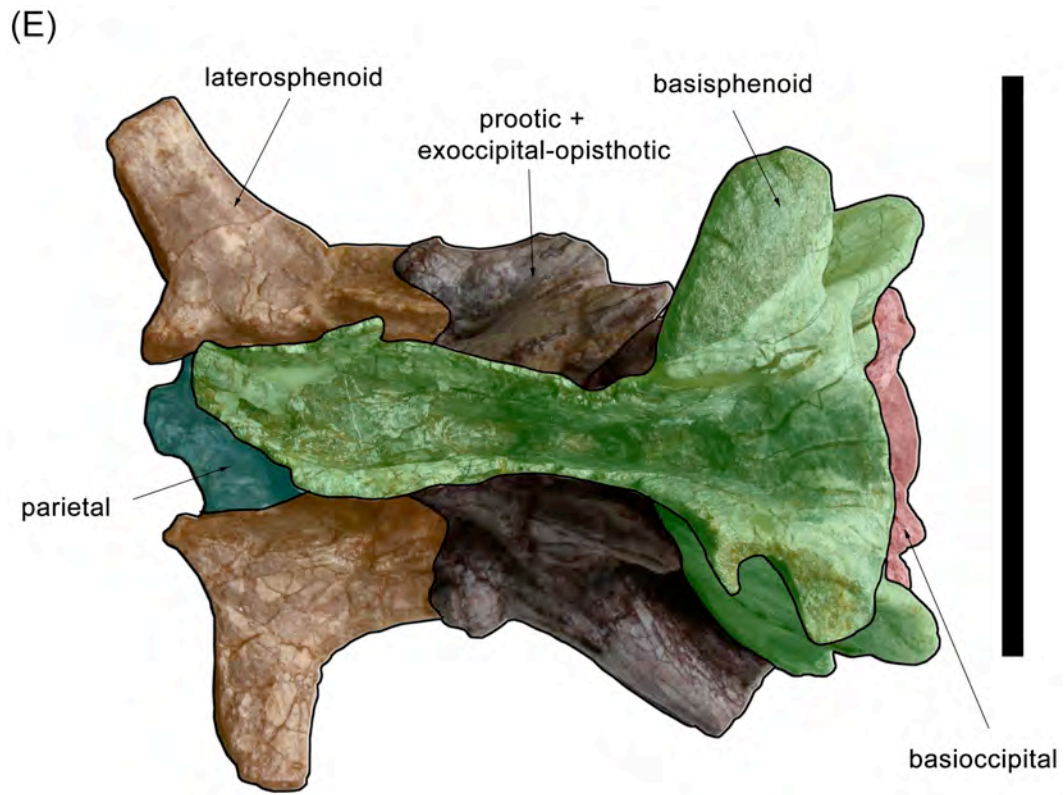
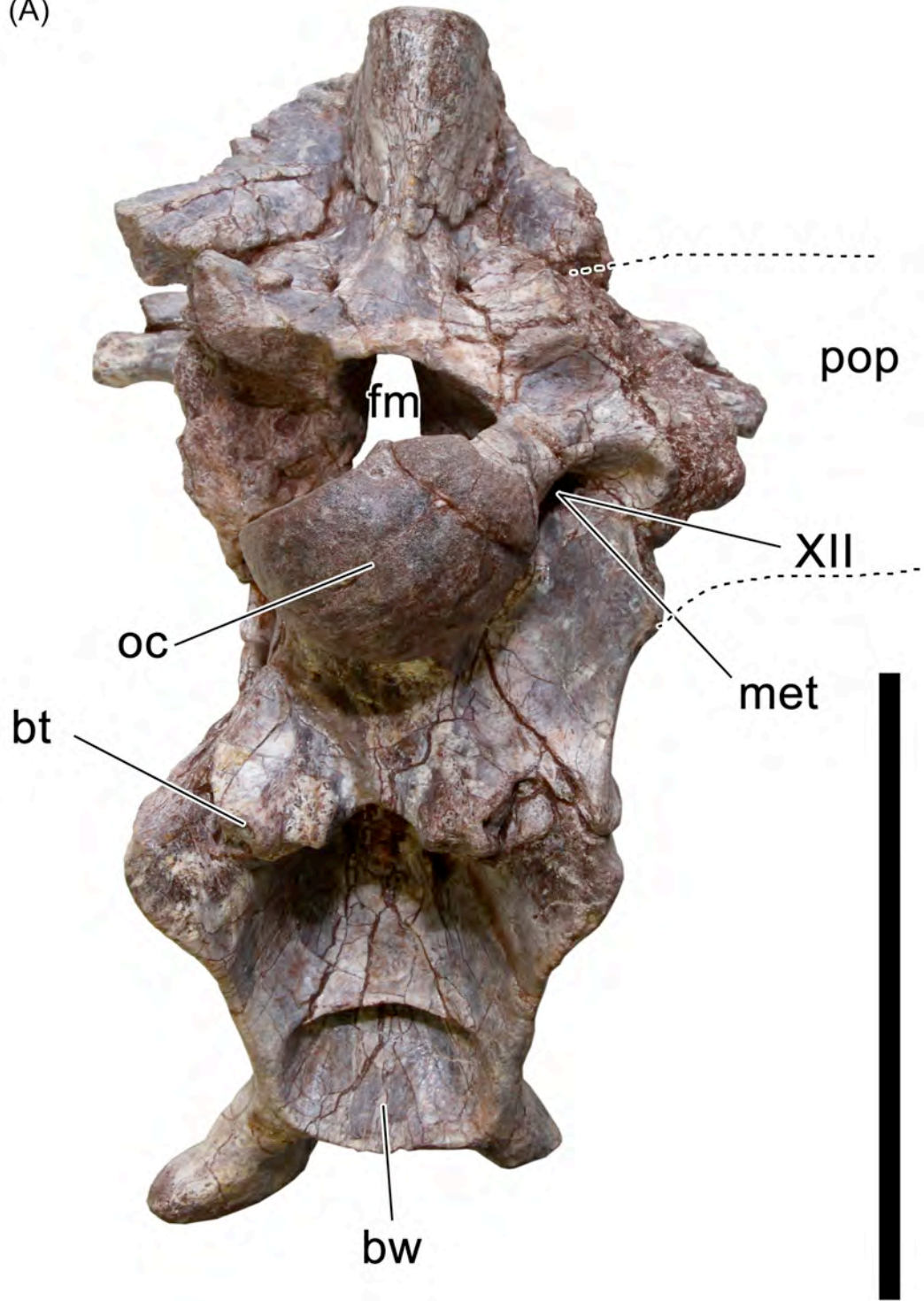


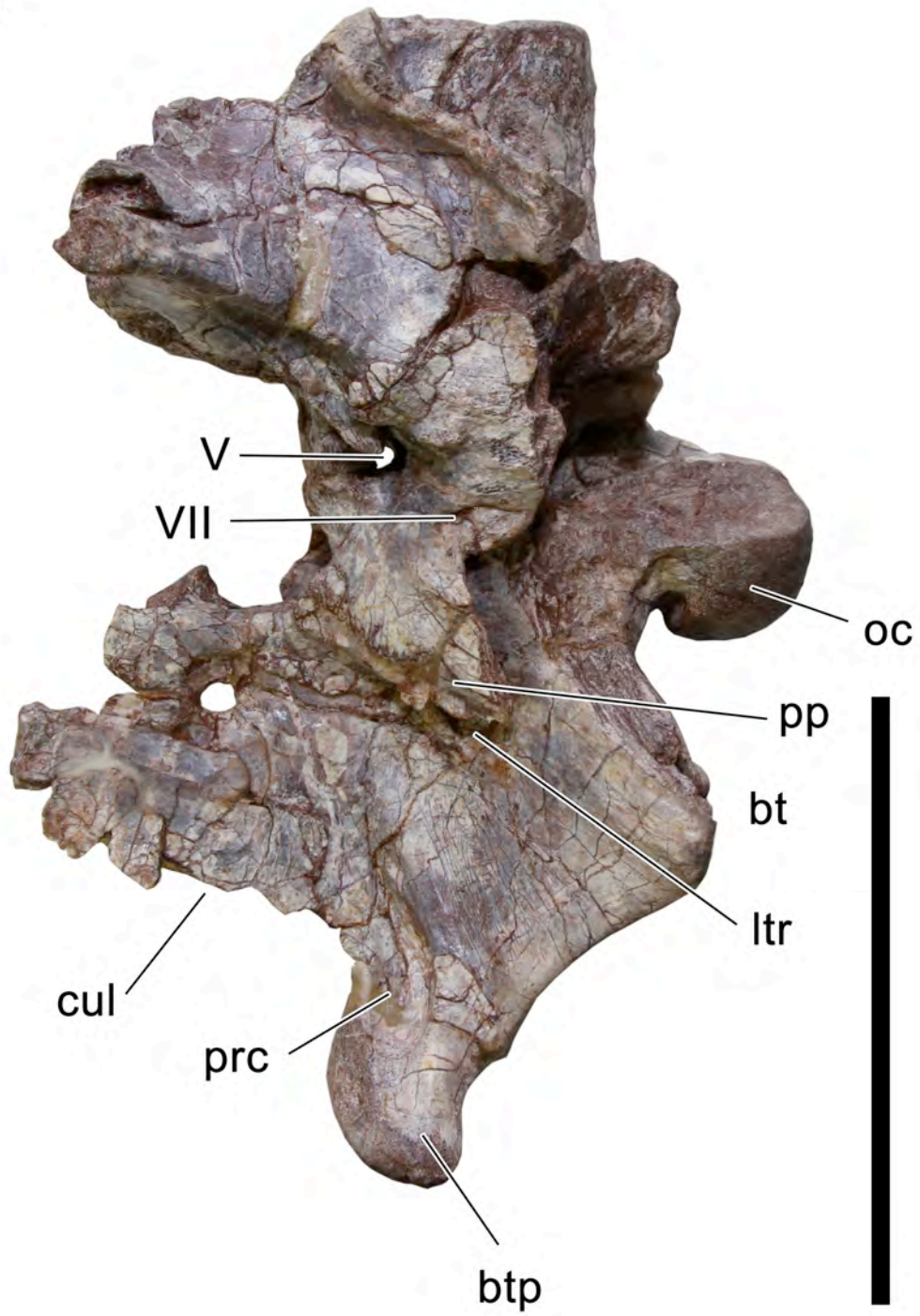
**FIGURE 2.3.** Braincase of *Sinosaurus triassicus* (ZLJT01) in occipital (A), left lateral (B), right lateral (C), dorsal (D), and ventral (E) views. Scale bar = 10 cm.

(A)

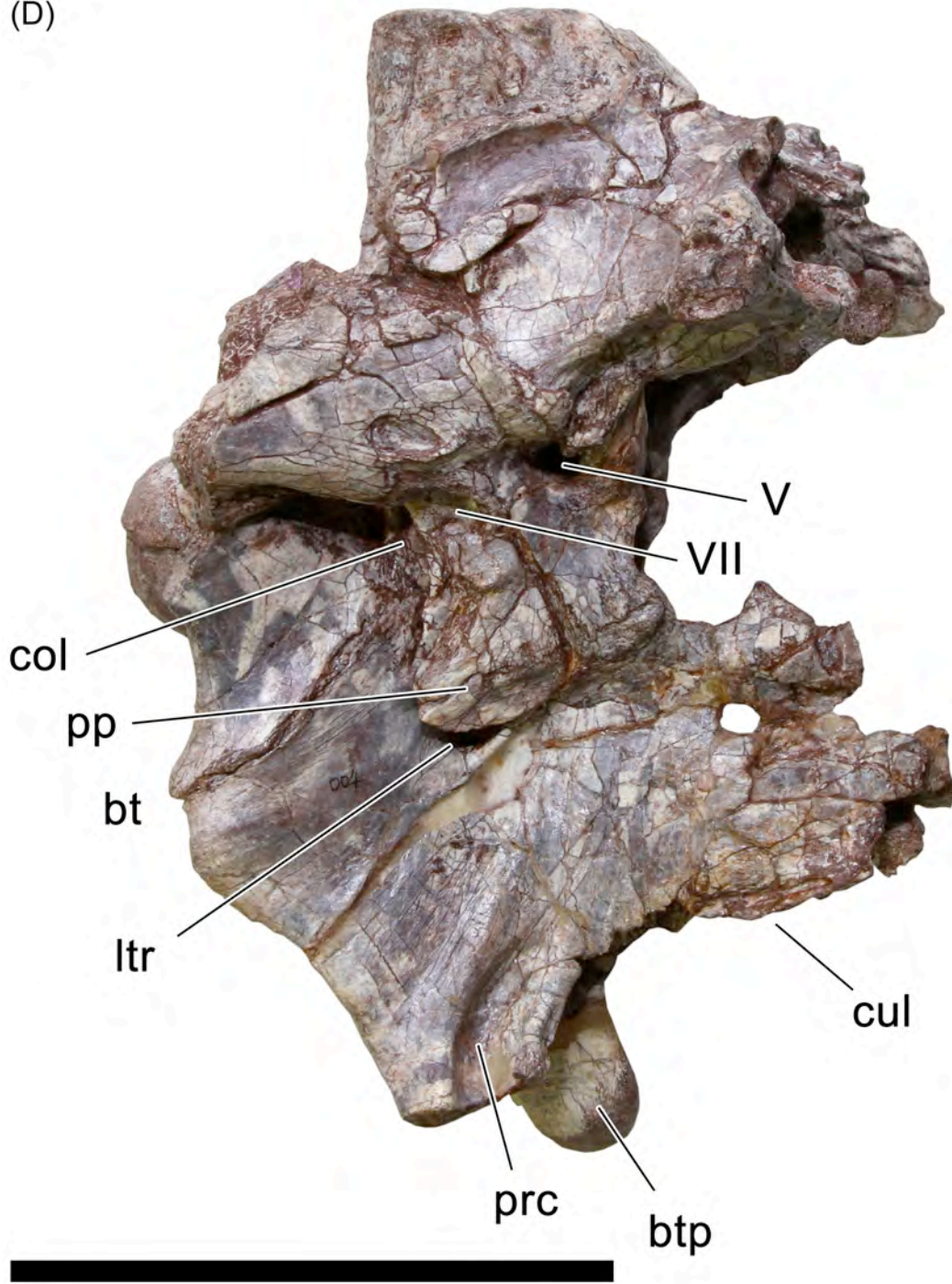




(C)



(D)



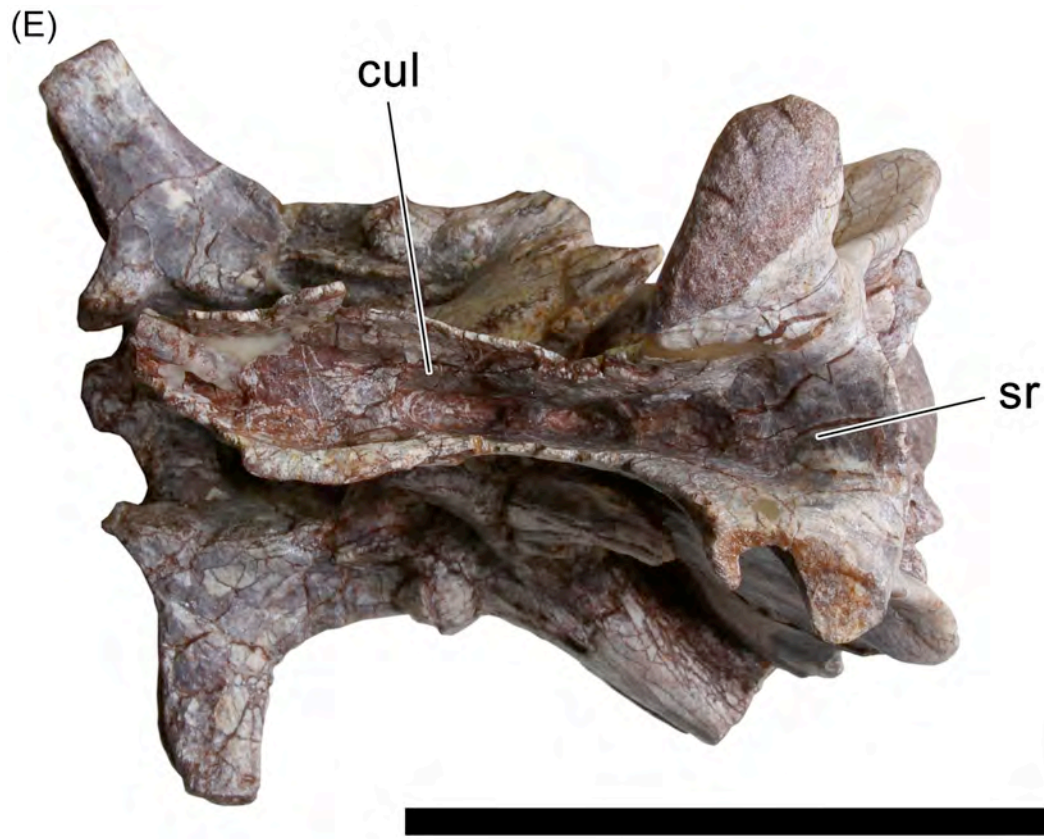


**FIGURE 2.4.** Illustration of a *Sinosaurus triassicus* (ZLJT01) braincase in posterior (A), posteroventral (B), left lateral (C), right lateral (D), and ventral (E) views. Scale bar = 10 cm.

The distinct median ridge of the supraoccipital expands slightly posterodorsally (Figs. 2.3 and 2.4) as in KMV 8701 (*Sinosaurus*), whereas the supraoccipital expands into a double knob of bone in LDM–L10. The dorsal expansion is somewhat weaker than those of *Allosaurus* (Madsen, 1976), *Sinraptor* and *Yangchuanosaurus* (Currie and Zhao, 1993). The supraoccipital extends posteriorly almost 1.8 cm from the nuchal crest of the parietal, and is level with the top of the parietal on the midline. The top of this knob is flat, as in KMV 8701, whereas in LDM–L10 it is smoothly convex. This knob is partially capped by a posterior lappet from the parietal, as in LDM–L10. This was probably the same as in KMV 8701, although this specimen has a breach between the knob and parietals.

The supraoccipital encloses two foramina (one is much smaller than the other), for the dorsal head veins. The foramina for the dorsal head veins are enclosed by the supraoccipital only, as in *Sinraptor*. In most theropods, the foramina pass between the supraoccipitals and parietals. The other two specimens of *Sinosaurus* (KMV 8701 and LDM–L10) are poorly preserved in this area.

The supraoccipital has a limited participation in the dorsal border of the foramen magnum, as in KMV 8701 and LDM–L10 (Currie et al., in progress). However, this bone is excluded from the margin in *Dilophosaurus* (Welles, 1984).

The foramen magnum is wider than high. The occipital condyle is formed by the basioccipital and exoccipitals, and is semicircular in posterior view. The occipital condyle is larger than the foramen magnum. The occipitofrontal angle (Coria and Currie, 2002) is 90° or less.

There is a long, relatively smooth suture with the parietal, which does not make a sharp incursion into the supraoccipital as it does in *Cryolophosaurus* (Smith et al., 2007), *Dilophosaurus* (Welles, 1984), *Sinosaurus* (KMV 8701 and LDM-L10; Currie et al., in progress), *Sinraptor* (Currie and Zhao, 1993; Paulina Carabajal and Currie, 2012), and *Syntarsus* (Tykoski, 1998).

The basioccipital is the main component of the occipital condyle (Figs. 2.3 and 2.4). The basioccipital forms the posterior portions of the basal tubera. The distance between each basal tuber (5.2 cm) is more than the transverse diameter of the occipital condyle (4.2 cm), unlike the conditions observed in *Allosaurus* and *Sinraptor* (Currie and Zhao, 1993), dromaeosaurids (Colbert and Russell, 1969), troodontids (Currie, 1985), and tyrannosaurids (Bakker et al. 1988). In these animals, the width across the basal tuber is larger than the transverse diameter of the occipital condyle. The basal tubera are fused but still distinguishable, with free distal ends.

The neck of the occipital condyle is flat and there is no longitudinal groove, as in *Sinraptor* (Paulina Carabajal and Currie, 2012), but unlike the situation in *Dilophosaurus* (Welles, 1984). The crista tuberalis is well developed and reaches distally to the end of the basal tuber, as in *Sinraptor*. A shallow paracondylar recess is lateral to the occipital condyle, whereas *Cryolophosaurus*, *Dilophosaurus*, "*Syntarsus*" *kayentakatae*, have well developed paracondylar pockets (Welles, 1984; Tykoski, 1998; Smith et al., 2007).

There is no evident division between the exoccipital and opisthotic in any known theropod (Currie and Zhao, 1993). The exoccipitals are separated from

each other by the supraoccipital above the foramen magnum and by the basioccipital below. The paroccipital processes of ZLJT01 are poorly preserved (Figs. 2.3 and 2.4). The left exoccipital–opisthotic is missing, leaving the suture on the basioccipital exposed. In posterior view, the exoccipital–opisthotic–basisphenoid suture is distinct and rough. The suture for the supraoccipital is overlapped by about a centimeter of the proximal end of the left exoccipital–opisthotic.

Only the proximal end of the right exoccipital–opisthotic is preserved. The base of the paroccipital process is 8.4 cm tall. In posterior view, the ventral border of the remaining paroccipital process is level with the ventral border of the occipital condyle, as in *Cryolophosaurus* (Smith et al., 2007), *Sinosaurus* (KMV 8701, LDM–L10, Currie et al., in progress) and *Sinraptor* (Currie and Zhao, 1993; Paulina Carabajal and Currie, 2012), whereas the ventral border is level with the dorsal margin of the occipital condyle in *Carnotaurus* (Paulina Carabajal, 2011), *Dilophosaurus* (Welles, 1984), and *Syntarsus* (Tykoski, 1998).

A small horizontal notch (transverse width 0.6 cm) separates the basal tuber from the more anteroventral extension of the exoccipital–basisphenoid suture. This is different from allosaurids and *Sinraptor* (Currie and Zhao, 1993), each of which has greater separation of the regions on each side of the notch.

The basisphenoid–parasphenoid is a complex structure of thin webs of bone (Figs. 2.3 and 2.4). Anteriorly, the cultriform process is incomplete. However, the base of the process is formed by two longitudinal, thin (1.4 mm) webs of bone that converge and join dorsally, arching over a ventrally oriented longitudinal

trough, as in *Sinraptor*. The cultriform process is large, with a tall base; it seems to have projected horizontally when complete. The maximum central width (2.4 cm) of the preserved cultriform process is greater than the proximal part (1.4 cm). The preserved length of the cultriform process is equal to the anteroposterior length of the basicranial box, and it is safe to assume that it was longer when complete. A large fenestra opens dorsal to the base of the cultriform process.

The lateral tympanic recess is a deep, narrow pneumatic cavity excavated into the basisphenoid, posteroventral to the preotic pendant. The preotic pendant, probably formed mainly by the prootic, is well developed and overhangs the anterodorsal portion of the lateral tympanic recess. The recess is an oval chamber, and is separated from a ventral shallow depression by means of a low ridge. This condition is closer to that of *Sinraptor* than it is to other theropods such as *Abelisaurus* (Paulina Carabajal, 2011), *Piatnitzkysaurus* (PVL 4073), and *Troodon* (Currie, 1985), where the lateral tympanic recess is larger, deeper, and is subdivided in many chambers. The CT scans show that the foramen of the internal carotid is within this recess, as in *Sinraptor*. The internal carotid artery enters the pituitary fossa, separate from its counterpart. The foramina for cranial nerve VI (CN VI), which also enter the pituitary fossa, open dorsal to the internal carotid foramina.

The lateroventrally projecting basiptyergoid processes are well developed and finger-like. They are joined by a basiptyergoidal web, but have free distal ends. Laterally, there is a deep basiptyergoid recess, unlike the flat lateral surface observed in *Dilophosaurus* (Welles, 1984). The basiptyergoid recess is present in

many other theropods such as *Allosaurus* (Madsen, 1976), *Oviraptor* (Norell et al., 2001), *?Stokesosaurus* (Chure and Madsen, 1998), and *Velociraptor* (Barsbold and Osmólska, 1999).

The columellar recess is vertically aligned with the basipterygoid process, whereas in *Dilophosaurus* it is aligned with the basal tuber (Welles, 1984).

There are no visible sutures between the prootic and the exoccipital–opisthotic (Figs. 2.3 and 2.4). A large preotic pendant extends anteroventrally from the main body of the prootic, obscuring the foramen for the internal carotid. The fifth cranial nerve (CN V) from a large foramen between the prootic and laterosphenoid, and the groove clearly extended posteriorly and ventrally across the surface of the former bone. The opening for CN V is dorsoventrally constricted at one point. The prootic surrounds the foramen for seventh cranial nerve (CN VII) completely, but only forms the anterior border of the columellar recess.

The postorbital process of the laterosphenoid is dorsoventrally depressed and transversally projected (Figs. 2.3 and 2.4). The proximoventral part contacts the prootic and delimits anteriorly the foramen for the CN V.

## **2.5. Cranial nerves**

The foramina for first to third cranial nerves (CN I–III) not preserved because the orbitosphenoids and the main part of the laterosphenoids are missing.

The fifth cranial nerve (CN V) exited through a circular foramen between the prootic and laterosphenoid. It is the largest opening in the lateral wall of the

braincase, and is undivided. The ophthalmic branch left a marked impression in front of the opening.

The openings for the sixth cranial nerves (CN VI) are small in diameter, and would have continued out through the pituitary fossa. The condition is unknown in the other dilophosaurids with preserved braincases.

The seventh cranial nerve (CN VII) exited posterior to the foramen for CN V, dorsal to the preotic pendant. Based on the size of the opening, it would have been much smaller than CN V. In *Dilophosaurus*, the foramen for CN VII is shaped like a figure 8, showing the separation of the hyomandibular and palatine branches (Welles, 1984).

The metotic foramen within the exoccipital-opisthotic is large and opens in a shallow recess lateral to the occipital condyle. It would have accommodated CN IX to CN XI. A single opening for all the branches of CN XII also exits the depression. A groove extending posterolaterally from the metotic foramen indicates the direction followed by the nerves and blood vessels that exited the braincase through this foramen.

## **2.6. Pneumatic recesses**

The subsellar recess is well developed anterior to the basipterygoid process. It is continuous with a longitudinal recess that extends below the parasphenoidal rostrum, as observed in *Sinraptor* (Paulina Carabajal and Currie, 2012).

The basal tubera and basipterygoid processes enclose the basisphenoidal recess, which is deep and subdivided into a main depression and a smaller

opening just behind the basiptyergoid processes. The smaller recess is transversely oval and is delimited by the basiptyergoid web and a second, shorter lamina of bone. In *Dilophosaurus wetherilli* (UCMP 37302), there is a single basisphenoidal recess (Welles, 1984) that is otherwise similar to that of ZLJT01.

## **2.7. Discussion and Conclusions**

In most respects, comparison of the multiple specimens of *Sinosaurus triassicus* suggests that ZLJT001 is more similar to KMV 8701 than it is to LDM-L10. The most significant differences are in the morphology of the cranial crest and the atlantal intercentrum.

Morphological characters of the braincase and its pneumatic recesses suggest that ZLJT001 possesses advanced characters that are more derived than *Dilophosaurus*, and in some ways are more comparable with the Late Jurassic *Sinraptor*. These include the fact that the foramina for the dorsal head veins are enclosed by the supraoccipital only; the base of the cultriform process is formed by two longitudinal, thin webs of bone that converge and join dorsally, arching over a ventrally oriented longitudinal trough; the lateral tympanic recess is separated from a ventral shallow depression by means of a low ridge; a deep basisphenoid recess is subdivided into a main depression and a smaller opening behind the basiptyergoid processes.

## References

- Bakker RT, Siegwarth J, Kralis D, Filla J. 1992. *Edmarka rex*, a new, gigantic theropod dinosaur from the middle Morrison Formation, Late Jurassic of the Como Bluff outcrop region. *Hunteria* 2: 9–24.
- Barsbold R, Osmólska H. 1999. The skull of *Velociraptor* (Theropoda) from the Late Cretaceous of Mongolia. *Acta Palaeontologica Polonica* 44 (2): 189–219.
- Chure D, Madsen J. 1998. An unusual braincase (?*Stokesosaurus clevelandi*) from the Cleveland-Lloyd Dinosaur Quarry, Utah (Morrison Formation; Late Jurassic). *Journal of Vertebrate Paleontology* 18 (1): 115–125.
- Coria RA, Currie PJ. 2002. The braincase of *Giganotosaurus carolinii* from the Upper Cretaceous of Argentina. *Journal of Vertebrate Paleontology* 22: 802–811
- Colbert EH, Russell DA. 1969. The small Cretaceous dinosaur *Dromaeosaurus*. *American Museum Novitates* 2380: 1–49.
- Currie PJ. 1985. Cranial anatomy of *Stenonychosaurus inequalis* (Saurischia, Theropoda) and its bearing on the origin of birds. *Canadian Journal of Earth Sciences* 22: 1643–1658

- Currie PJ. 1997. Braincase anatomy. In: Encyclopedia of Dinosaurs. Currie P J, Padian K (eds.). Academic Press, San Diego. 81–85.
- Currie PJ. and Zhao XJ. 1993. A new carnosaur (Dinosauria, Theropoda) from the Jurassic of Xinjiang, People's Republic of China. Canadian Journal of Earth Sciences 30(10–11): 2037–2081.
- Currie PJ, Xing LD, Wu XC, Dong, ZM. In progress. Anatomy and relationships of *Sinosaurus triassicus* (“*Dilophosaurus sinensis*”) from the Lufeng Formation (Lower Jurassic) of Yunnan, China.
- Ezcurra MD. 2006. A review of the systematic position of the dinosauriform archosaur *Eucoelophysis baldwini* Sullivan and Lucas, 1999 from the Upper Triassic of New Mexico, USA. Geodiversitas 28(4): 649–684.
- Holliday CM. 2009. New insights into dinosaur jaw muscle anatomy. The Anatomical Record 292: 1246–1265.
- Hu SJ. 1993. A short report on the occurrence of *Dilophosaurus* from Jinning County, Yunnan Province. Vertebrata PalAsiatica 31: 65–69.
- Madsen JH. Jr. 1976. *Allosaurus fragilis*: A Revised Osteology. Utah Geological and Mineralogical. Survey Bulletin 109: 1–163.

Norell MA, Clark JM, Chiappe LM. 2001. An embryonic oviraptorid (Dinosauria: Theropoda) from the Upper Cretaceous of Mongolia. American Museum Novitates 3315: 1–17

Paulina Carabajal A. 2011. Braincases of abelisaurid theropods from the upper Cretaceous of north Patagonia. Palaeontology 54(4):793–806.

Paulina Carabajal A and Currie PJ. 2012. New information on the braincase and endocast of *Sinraptor dongi* (Theropoda: Allosauroidea): Ethmoidal region, endocranial anatomy and pneumaticity. Vertebrata Palasiatica 50(2): 85–101.

Rowe T. 1989. A new species of the theropod *Syntarsus* from the Early Jurassic Kayenta Formation of Arizona. Journal of Vertebrate Paleontology 9: 125–136.

Smith ND, Makovicky PJ, Hammer WR, Currie PJ. 2007. Osteology of *Cryolophosaurus ellioti* (Dinosauria: Theropoda) from the Early Jurassic of Antarctica and implications for early theropod evolution. Zoological Journal of the Linnean Society 151 (2): 377–421

Welles SP. 1984. *Dilophosaurus wetherilli* (Dinosauria, Theropoda): Osteology and comparisons. Palaeontographica Abteilung A. 185: 85–180.

Zhao XJ, Currie PJ. 1993. A large crested theropod from the Jurassic of Xinjiang, People's Republic of China. *Canadian Journal of Earth Sciences* 30: 2027–2036.

## CHAPTER 3

### The phylogenetic systematics of *Sinosaurus triassicus* from China

#### 3.1 Introduction

Theropod dinosaurs formed one of the most remarkable lineages of terrestrial vertebrates in the Mesozoic Era. They possessed a high level of taxonomic diversity, represented by a huge range of cranial morphologies (Weishampel et al., 2004; Foth and Rauhut, in press).

Numerous papers have been published on the phylogenetic relationships of non-avian theropods and basal birds (Gauthier, 1986; Rowe, 1989; Sereno, 1999; Holtz, 2000; Clark et al., 2002; Rauhut, 2003; Smith et al., 2007a; Choiniere et al., 2010). These analyses agree in the general interrelationships of major groups, but the phylogenetic position and validity of several clades -- such as Ceratosauria, Compsognathidae and Therizinosauridae -- and the detailed positions of many species are still controversial (Rauhut, 2003; Choiniere et al., 2010; Zanno, 2010; Xu et al., 2011).

#### 3.2 Coelophysoids and dilophosaurids

Theropods form a monophyletic group, within which *Eodromaeus* from the Late Triassic Ischigualasto Formation of Argentina is the most primitive theropod presently known (Martinez et al., 2011). Slightly more basal are the Herrerasauria, an exclusively Late Triassic group known from South and North America (Langer, 2004). *Tawa* from the Late Triassic of New Mexico provides a convincing

intermediate with the Neotheropoda, sharing with basal neotheropods a kink between the maxilla and the premaxilla (Nesbitt et al., 2009).

The remaining theropods (ceratosaurs, coelophysoids, dilophosaurids and tetanurines) form a clade called Neotheropoda (Holtz, 2012). Neotheropoda includes various primitive branches during the Late Triassic and Early Jurassic (Coelophysidae and Dilophosauridae, collectively known as coelophysoids); and then have two major clades by the Middle Jurassic (Ceratosauria and Tetanurae).

The oldest neotheropod known is *Camposaurus* of the middle Late Triassic (Ezcurra and Brusatte, 2011), but *Coelophysis* from the latest Triassic is more famous. These coelophysids were small to mid-sized carnivores (2–4 m long) with long and slender bodies, and slender skulls (Colbert, 1989; 1990; Downs, 2000; Holtz, 2012).

By the end of the Late Triassic, a larger (4–6 m long) primitive theropod *Zupaysaurus rougieri* (Arcucci and Coria, 2003) from Argentina seems to be intermediate in its phylogenetic position between coelophysids and dilophosaurids, based on the phylogenetic analysis of Smith et al. (2007).

The next phase of theropod evolution included relatively large forms (4–6 m long) during the Early Jurassic. These include *Cryolophosaurus* of Antarctica (Smith et al., 2007a), *Dilophosaurus* the North American (Welles, 1984); *Dracovenator* of South Africa (Yates, 2005), and *Sinosaurus triassicus* ("*Dilophosaurus sinensis*", Hu, 1993) of China. Charig and Milner (1990) first used the Dilophosauridae as a formal family, with reference to the informal term of dilophosaur used by Paul (1988). Madsen and Welles (2000) placed

*Dilophosaurus* as the sole member of the Dilophosaurinae within the Dilophosauridae. Smith et al. (2007) considered there to be affinities between these four medium-sized Early Jurassic theropods, although they did not use the name Dilophosauridae for this clade.

In addition, the late Early Jurassic *Berberosaurus* from northern Africa was considered the most primitive ceratosaur (Allain et al., 2007). A more recent paper suggests it is a member of the Dilophosauridae grade or clade (Xu et al., 2009).

Some studies considered dilophosaurids, coelophysids, and intermediate forms within the Coelophysoidea. The superfamily was found to be closer to Ceratosauria than Tetanurae (Gauthier, 1986; Holtz, 1994; Sereno, 1999; Ezcurra and Cuny, 2007). Other studies removed *Dilophosaurus wetherilli* from the Coelophysoidea, suggesting it was more closely related to neoceratosaurs and tetanurans (Carrano et al., 2002; Rauhut, 2003). Another analysis proposed the existence of a novel clade of early theropods that represents the sister-taxon to Neoceratosauria + Tetanurae (Yates, 2005). During the analysis of the new material of *Cryolophosaurus*, Smith et al. (2007) also considered the dilophosaurid clade as a sister-taxon to a Neoceratosauria + Tetanurae clade, rendering both a traditional Coelophysoidea and Ceratosauria non-monophyletic.

Nesbitt et al. (2009) considered Coelophysoidea and dilophosaurids paraphyletic, with coelophysoids occupying the most basal phase of neotheropod evolution, and dilophosaurids a more derived position.

Ezcurra and Brusatte (2011) recovered a polytomy at the base of

Neotheropoda, as most parsimonious trees disagreed in recovering a monophyletic or paraphyletic ‘traditional’ Coelophysoidea.

Carrano et al. (2012) support the successive placement of Ceratosauria and Tetanurae as more derived groups relative to Coelophysoidea. Several taxa were found to occupy stem positions relative to Tetanurae, including *Cryolophosaurus* and ‘*Dilophosaurus*’ *sinensis*.

The following analyses places Ceratosauria and Tetanurae in the clade Averostrans, which excludes coelophysoids (Holtz, 2012). The analysis also suggests that coelophysoids are a paraphyletic grade of primitive neotheropods, and that dilophosaurids were closer to Averostrans than to Coelophysoidea (Rauhut, 2003; Smith et al., 2007a; Xu et al., 2009; Holtz, 2012).

### **3.3 New materials of *Sinosaurus triassicus***

ZLJT01 (*Sinosaurus triassicus*) includes an incomplete premaxilla, partial maxilla, nasal crest, frontal, occiput, dentary, and some of the postcranial skeleton. It possesses two distinct characters that diagnose it as a Coelophysoidea (included taxa: Coelophysidae and *Dilophosaurus*, Holtz, 1994) -- the presence of a subnarial gap indicating a potentially mobile premaxilla–maxilla joint (Holtz, 1994; Rauhut, 2003), and a maxillary alveolar margin that curves sharply anteriorly (Rauhut, 2003). These observations, coupled with the results of earlier studies of *Sinosaurus triassicus* (=“*Dilophosaurus sinensis*”; Young, 1948; Hu, 1993; Currie et al., in progress), suggest that ZLJT01 is a coelophysoid.

In the theropod skull, certain evolutionary trends can be observed over the

course of their Mesozoic history. Pneumatization of the snout becomes more pronounced in advanced theropods, and accessory antorbital openings appear in front of the antorbital fenestra (Currie, 1999). However, generally speaking, the theropod skull was the most conservative part of the skeleton, and shows stability of its main features; these include the construction of the otic region of the endocranium (Barsbold, 1983), the morphology of the lacrimal, which borders the orbit anteriorly and extends onto the top of the skull (Currie, 1999), and the presence and form of the intramandibular joint in the lower jaw (Currie, 1999). The postcranial skeleton was changing progressively, but there is considerable convergence (Schachner et al., 2009). Because the skull expresses strong phylogenetic signals in theropod systematics, previous phylogenetic analyses of theropods are sometimes only based on skulls or braincases (Coria and Currie, 2002; Currie et al., 2003, Currie and Varricchio, 2004; Xu et al., 2006).

### **3.4 Methods**

ZLJT01 is composed mostly of skull bones, and the postcranial skeletons of other specimens of *Sinosaurus triassicus* are in poor condition, and difficult to study because they are mounted and on display in museums. In addition, in order to not simply repeat the analysis from Smith et al. (2007), the characters of the postcranial skeleton were removed. For these reasons, only cranial characters were used in the present phylogenetic analysis.

The software NDE (NEXUS Data Editor) version 0.5.0 was used to create and edit NEXUS format data files on a Windows-based computer, and

PAUP\*4.0b10 version (Swofford, 2002) was utilized on a Macintosh.

Similar to Smith et al. (2007), ingroup taxa were selected for the phylogenetic analysis with the primary goal of including multiple representatives of major groups at the base of Theropoda.

Most of the characters were coded using the data matrices of previous workers (Gauthier, 1986; Rowe, 1989; Rowe and Gauthier, 1990; Sereno et al., 1994, 1996, 1998; Harris, 1998; Sampson et al., 1998; Tykoski, 1998, 2005; Forster, 1999; Sereno, 1999; Currie and Carpenter, 2000; Holtz, 2000; Allain, 2002; Carrano et al., 2002; Coria and Currie, 2002; Rauhut, 2003; Hwang et al., 2004; Novas et al., 2005; Yates, 2005; Smith et al., 2007a; Xu et al., 2009; Xu et al., 2012). The studies by Carrano et al. (2002) and Smith et al. (2007) focused heavily on neoceratosaurs, and were therefore the most useful. The latter included coding for *Dilophosaurus wetherilli*, *Sinosaurus triassicus* ("Dilophosaurus" *sinensis*), and *Sinraptor dongi*, but it needed to be checked and in some cases modified.

It is worthwhile to note that the type specimen of *Sinosaurus triassicus* (Young, 1948) only includes a partial maxilla (three fragments with several teeth in position) and three associated isolated teeth, and therefore did not have enough characters to be included in the phylogenetic analysis. *Shidaisaurus* is a basal tetanuran theropod from the lower Middle Jurassic of the Chuanjie Formation (Upper Lufeng Formation) of the Lufeng Basin, Yunnan Province, China (Wu et al., 2009). However, the front of the skull and mandibles are missing, and the braincase is still covered by sediment. Thus, the phylogenetic analysis did not

include this genus.

The well-preserved lacrimal and lacrimal crest of *Sinosaurus triassicus* (ZLJT01) added three new characters into the matrix.

(1) Lacrimal fenestra: opens ventrally (0); laterally (1).

(2) Lacrimal, series of pneumatic diverticula in the dorsal crest: absent (0); present (1).

(3) Lacrimal, contribution to dorsal head crest (if present): less than (0); or more than a third of surface area of crest in lateral view (1).

In order to place ZLJT01, LDM-L10 and KMV8701 (*Sinosaurus triassicus*) within Theropoda more accurately, a phylogenetic analysis of 58 theropod taxa and 144 characters was undertaken. However, twelve taxa were deleted from previous analysis because most of them did not have well-preserved skulls (80% or more data was missing): *Coelurus*, *Condorraptor*, *Dracovenator*, *Elaphrosaurus*, *Ilokelesia*, *Liliensternus*, *Megaraptor*, *Noasaurus*, *Tugulusaurus*, *Tyrannotitan*, *Segisaurus*, and *Streptospondylus*. Therefore, two Triassic dinosauriform outgroup taxa (*Marasuchus* and *Saturnalia*) were dropped from the Smith et al. (2007) selection. The remaining outgroup taxa for the analysis are *Eoraptor*, *Herrerasaurus*, *Plateosaurus*, and *Silesaurus*.

The character list and taxon-character matrix are provided in supplementary Appendixes S1 and S2, respectively. The parsimony analysis was performed using heuristic search in PAUP \*4.0b10 version. Trees were obtained via stepwise addition; addition sequence are simple; and branches were swapped using tree-bisection-reconnection algorithm. All characters were equally weighted

and treated as unordered. Synapomorphies were evaluated under accelerated transformation (ACCTRAN) and delayed transformation (DELTRAN) options; unambiguous synapomorphies are those that diagnosed a node under both ACCTRAN and DELTRAN optimizations.

### 3.5 Discussion and Conclusions

The parsimony analysis generated 1968 most parsimonious trees (MPTs). The tree length is 383 steps with a consistency index (CI) of 0.446, a rescaled consistency index (RC) of 0.325 and a retention index (RI) of 0.728.

The results of Smith et al.'s (2007) phylogenetic analysis supported the monophyly of several previously recognized major theropod clades including: Coelurosauria, Neoceratosauria, Spinosauroida, and Tetanurae (Fig. 3.1), .

However, in this phylogenetic analysis (Fig. 3.2), the consensus tree suggested that *Sinosaurus* and "Coelophysoidea" each form a clade amongst a paraphyletic group outside Tetanura. *Sinosaurus* forms a polytomy with *Cryolophosaurus*, *Piatnitzkysaurus* and Tetanura within Averostr (Paul, 2002; Ezcurra and Cuny, 2007: a node-based clade containing *Allosaurus fragilis*, *Ceratosaurus nasicornis*, their common ancestor and all its descendants).

Several medium-sized Early Jurassic theropods (including *Cryolophosaurus ellioti*, *Dilophosaurus wetherilli*, and *Sinosaurus triassicus*; Smith et al., 2007a) were separated into different clades in this phylogenetic analysis. *Coelophysis bauri*, *Coelophysis rhodesiensis*, *Dilophosaurus wetherilli*, "*Syntarsus*" *kayentakatae*, and *Zupaysaurus rougieri* form a clade named

"Coelophysoidea". *Coelophysis bauri*, *Coelophysis rhodesiensis*, and *Dilophosaurus wetherilli* occur in the monophyletic Coelophysoidea along with *Zupaysaurus* and *Syntarsus*. In this phylogenetic analysis, *Dilophosaurus wetherilli* emerged as the most basal coelophysoid.

The clade that includes *Sinosaurus* is supported by ten unambiguous synapomorphies:

- (1). Constriction between articulated premaxillae and maxillae (Character 21);
- (2). Premaxilla and maxilla do not contact at alveolar margins (Character 22);
- (3). Depth of the ventral part of the antorbital fossa much greater than the depth of the maxilla below the ventral margin of the antorbital fossa (Character 27);
- (4). Jugal, anterior end does not participate in margin of antorbital fenestra (Character 50);
- (5). Lacrimal contacts frontal (Character 54);
- (6). Lacrimal contacts postorbital (Character 55);
- (7). Lacrimal, ventral ramus is bar- or strut-like, and is roughly the same length anteroposteriorly throughout ventral ramus (Character 59);
- (8). Median fossa in saddle-shaped depression overlapping frontal-parietal contact (Character 66);
- (9). Paroccipital process directed strongly ventrolaterally, with distal end entirely below the level of the foramen magnum (Character 90);

(10). Retroarticular process of the mandible is narrow and rod-like, with the anteroposterior length much greater than mediolateral breadth (Character 139).

Unlike the results of Smith et al. (2007a), the specimens of *Sinosaurus triassicus* (KMV8701 [*Dilophosaurus sinensis*” Hu, 1993], LDM-L10 and ZLJT01) form a distinct clade. In this phylogenetic analysis, *Cryolophosaurus* and *Sinosaurus* were more advanced, and were more closely related to *Averostra* than to *Coelophysis bauri* and *Dilophosaurus wetherilli*.

The number of MPTs (1968) is much higher than the 108 of Smith et al. (2007a), suggesting that the new specimens of *Sinosaurus* introduced new character information that conflicts with other characters present in other theropods. Maybe *Sinosaurus* has a unique mix of some characters typical of basal theropods but others more typical of derived theropods.

Another interesting result of the phylogenetic analysis is that LDM-L10 emerged as the more basal than KMV8701 and ZLJT01. LDM-L10 also emerged as the sister taxon of a clade composed of KMV8701 and ZLJT01. After Young (1948) named *Sinosaurus triassicus* (IVPP V34), Hu (1993) described and named “*Dilophosaurus sinensis*” (KMV8701). Dong (2003) considered “*Dilophosaurus sinensis*” (LDM-L10) to be similar to *Sinosaurus triassicus*. Currie et al. (in progress) compared all these specimens, and referred them to *Sinosaurus triassicus*. They suggest that *Sinosaurus* incorporates IVPP V34, KMV8701, and LDM-L10. IVPP V34 and LDM-L10 can both be referred with little doubt to *Sinosaurus triassicus*, considering their overlapping geographical provenance (see chapter 1: Fig. 1.1) and morphology. Based on the results of the phylogenetic

analysis, KMV8701 and ZLJT01 may represent another species of *Sinosaurus*.

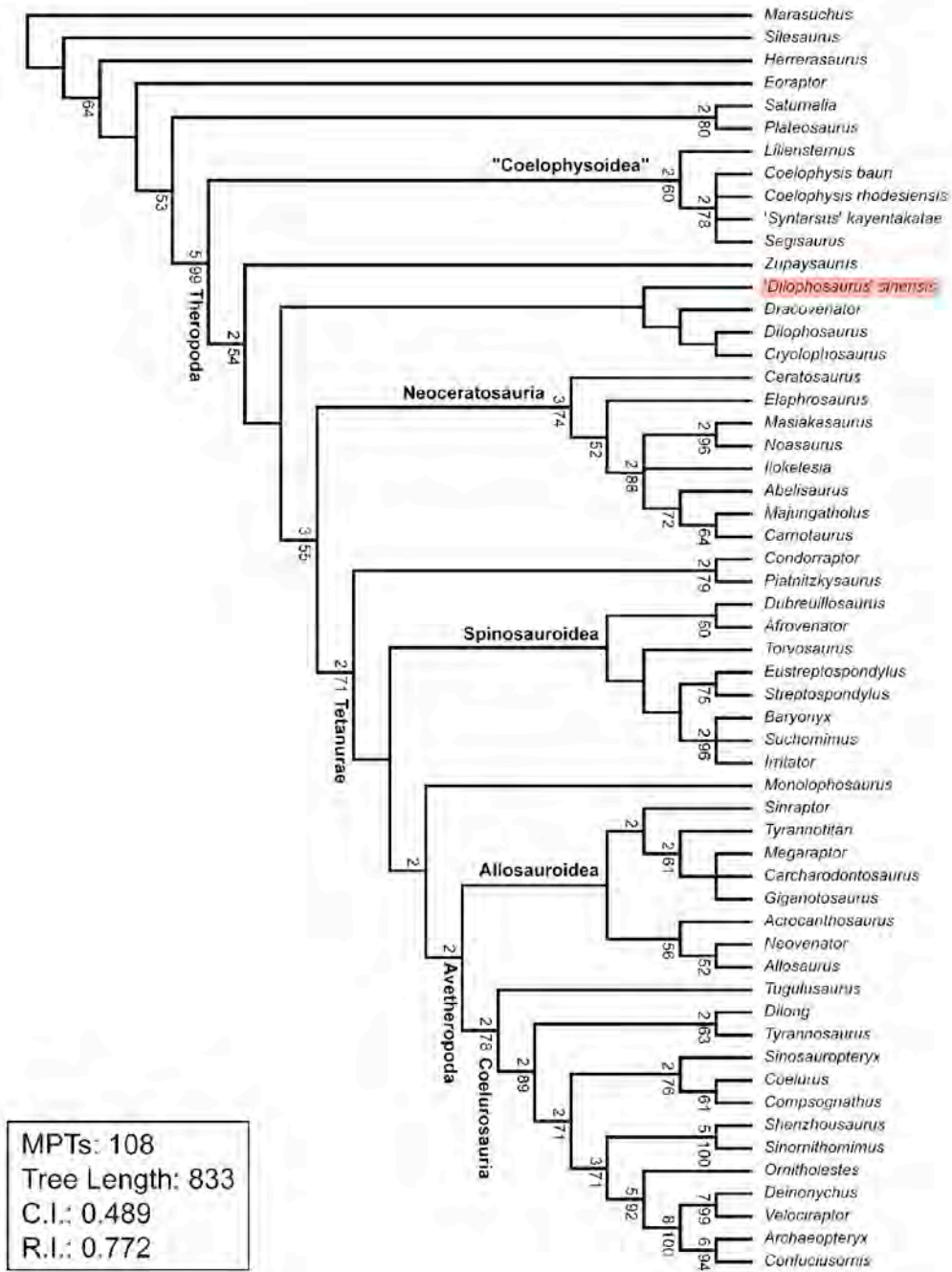
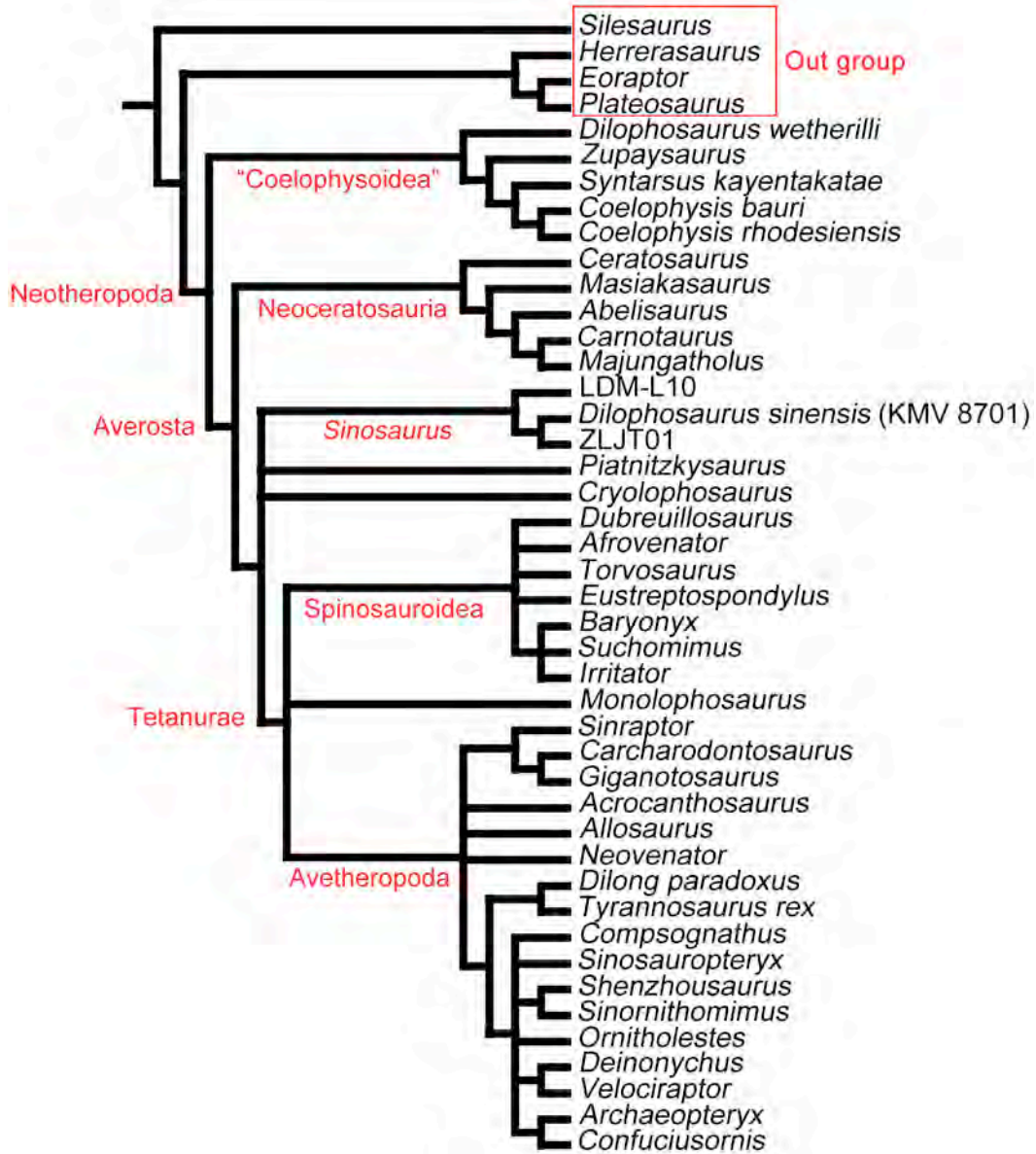


FIGURE 3.1. Strict consensus tree (Smith et al., 2007a)



**FIGURE 3.2.** Strict consensus of 1968 MPTs. All trees have length of 383 steps, CI 0.446, RI 0.728. Several theropod clades are indicated in bold.

### 3.6 Crest evolution and the phylogenetic analysis

Previous studies suggest that most dilophosaurids probably have crests on their skulls. However, the crests of *Dracovenator* (Yates, 2005), "*Syntarsus*" *kayentakatae* (Tykoski, 1998) and *Zupaysaurus* (Arcucci and Coria, 2003) still have been contradictory because the supporting cranial evidence was not strong enough. Only three dilophosaurids have certain crests: *Cryolophosaurus* (Smith et al. 2007a), *Dilophosaurus* (Welles, 1984), and *Sinosaurus* (Currie et al., in progress).

(1). *Cryolophosaurus* has a pair of large, posterodorsally curving transverse crests, formed by dorsal expansions of the lacrimals (Smith et al., 2007a).

(2). *Dilophosaurus* had a pair of hatchet-like crests, one on either side of the skull roof, with each extending from the nasal opening to the orbit (Welles, 1984; Currie, 1999).

(3). The crest of *Sinosaurus* is similar to that of *Dilophosaurus*. However, its crest has distinct pneumatic depressions and openings (including the presence of a series of oval openings on the medial surface of the lacrimal portion of the crest, and an ovoid lacrimal pneumatic aperture near the posterodorsal corner of the antorbital fossa).

In addition, cranial crests in theropods are present in abelisaurids (*Carnotaurus*, Bonaparte et al., 1990), ceratosaurids (*Ceratosaurus*, Madsen and Welles, 2000), megalosauroids (*Monolophosaurus*, Zhao and Currie 1993), oviraptorosaurs (*Oviraptor*, Barsbold, 1986; *Rinchenia*, Osmólska et al., 2004)

and tyrannosauroids (*Guanlong*, Xu et al., 2006 and *Yutyrannus*, Xu et al., 2012).

(1). Abelisaurids. *Carnotaurus* had a pair of robust frontal horns (Bonaparte et al., 1990).

(2). Ceratosaurids. *Ceratosaurus* possessed a prominent horn-like crest formed by the nasals. It also possessed smaller hornlike ridges -- formed by the lacrimals -- in front of each eye, similar to those of *Allosaurus* (Madsen and Welles, 2000).

(3). Megalosauroids. *Monolophosaurus* had an elaborate midline crest, formed by the fusion of the premaxillae, nasals, lacrimals, and frontals. It is noteworthy in that it is pneumatized, with connections to the antorbital fossae (Zhao and Currie, 1993; Brusatte et al., 2010).

(4). Tyrannosauroids. *Guanlong* had a large, fragile and highly pneumatic nasal crest, consisting of a median crest that is about 1.5 mm thick for most of its length with four supporting lateral laminae (Xu et al., 2006). *Yutyrannus* has a pair of highly fenestrated midline crests formed by the premaxillae and nasals (Xu et al., 2012), which are similar to those of the carcharodontosaurian *Concavenator* (Ortega et al., 2010).

(5). Oviraptorosaurs had diverse forms of crests, including the highly pneumatized crest of *Rinchenia mongoliensis* that was formed by the premaxillae, nasals, frontals, and parietals (Osmólska et al., 2004). The more conservative crest of *Citipati sp.* was formed by the premaxillae, nasals, and frontals (Barsbold, 1986).

Holtz (2012) believes that because some coelophysoids (*Dilophosaurus*,

Welles, 1984) and some primitive tetanurines (*Monolophosaurus* Zhao and Currie 1993) have similar development of crests, this may have been a trait common to basal neotheropods. However, crests appeared in almost every branch of theropod, but differ in the sizes, positions, compositions of bones, and whether the crests are pneumatic or not. Taxa with pneumatic crests include *Guanlong*, *Monolophosaurus*, *Oviraptor*, *Rinchenia*, and *Sinosaurus*. Among these theropods, *Sinosaurus* is the most basal form (Fig. 3.2; *Guanlong*, *Oviraptor*, and *Rinchenia* are not included in the tree but are amongst coelurosaurs), and is the earliest form with a pneumatic crest from the Mesozoic. Also, based on the results of the phylogenetic analysis, it is noteworthy that there are no pneumatic crests in coelophysoids. The phylogenetic analysis suggests that a pneumatic crest is probably an advanced character for theropods.

Furthermore, based on the the results of the phylogenetic analysis, the crest may have evolved independently in coelophysoids (including *Dilophosaurus*) and in *Sinosaurus*. If this is true, then the similarities in shape should be superficial. Nevertheless, as they are both similar in size (longer than twice the body length of typical coelophysoids such as *Coelophysis*), it is conceivable that the independent development of the crests is a size-related feature in these animals. Some characters certainly suggest that *Sinosaurus* may have been an offshoot of the evolutionary lineage leading to more advanced theropods.

### **3.7 Paleobiogeographic Implications**

The Lufeng Formation has yielded a diverse Early Jurassic terrestrial

fauna, which includes the nearly complete theropod dinosaur *Sinosaurus*, and almost a hundred skeletons of sauropodomorph dinosaurs. The latter include prosauropod dinosaurs such as *Jingshanosaurus* (Zhang and Yang, 1995), *Lufengosaurus* (Young, 1941; 1951), *Xixiposaurus* (Sekiya, 2010), and *Yunnanosaurus* (Young, 1942), and the earliest sauropod represented in the fossil record by a complete skeleton—*Yizhousaurus sunae* (Chatterjee et al., 2010).

Smith et al. (2007b) suggested closer faunal affinities between the Hanson Formation of Antarctica and the Lufeng Formation of China than between the latter and the Upper Elliot Formation of southern Africa. However, the pattern recovered for basal theropods implies the Hanson Formation fauna is more similar to that of the Kayenta Formation of North America or the Upper Elliot Formation.

The phylogenetic relationships recovered in this chapter suggest that *Sinosaurus* forms a polytomy with *Cryolophosaurus*, *Piatnitzkysaurus* and Tetanura within Averostra. Within this clade, *Cryolophosaurus* is from Antarctica (Hammer and Hickerson, 1994), *Piatnitzkysaurus* is from Argentina (Bonaparte, 1979), and *Sinosaurus* is from southwest China (Fig. 3.3). It seems to suggest that there was global distribution of this grade of theropods before the origin of Tetanura.

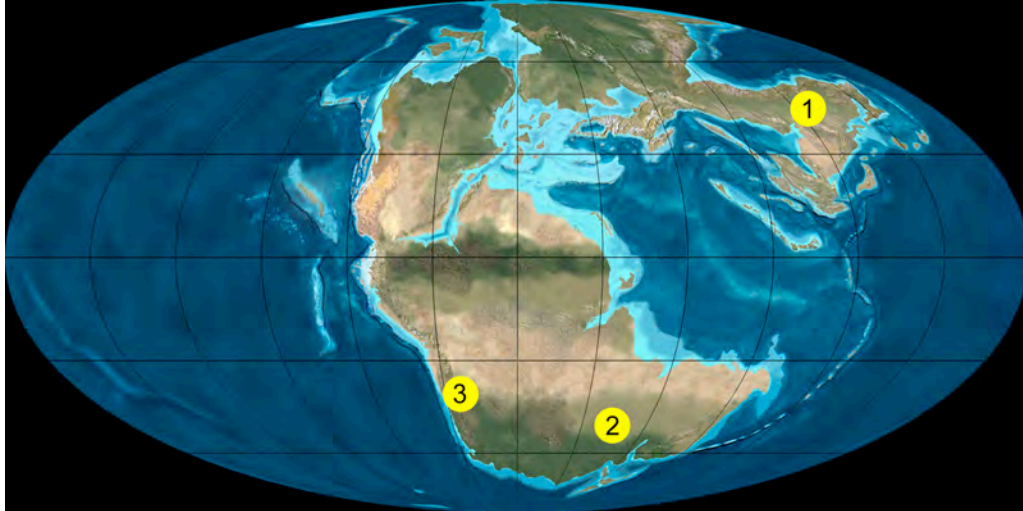


**FIGURE 3.3.** Early Jurassic theropod paleogeographic reconstruction. Labeled faunas: (1) *Sinosaurus*, Lufeng Formation, China; *Cryolophosaurus*, Hanson Formation, Antarctica; (3) *Piatnitzkysaurus*, Canadon Asfalto Formation, Argentina. Paleogeographic map from Blakey (2006: <http://jan.ucc.nau.edu/>).

## References

- Arcucci AB, Coria RA. 2003. A new Triassic carnivorous dinosaur from Argentina. *Ameghiniana* 40: 217–228.
- Allain R. 2002. Discovery of megalosaur (Dinosauria, Theropoda) in the middle Bathonian of Normandy (France) and its implications for the phylogeny of basal Tetanurae. *Journal of Vertebrate Paleontology* 22: 548–563.
- Allain R, Tykoski R, Aquesbi N, Jalil NE, Monbaron M, Russell D, Taquet P. 2007. A basal abelisauroid from the late Early Jurassic of the High Atlas Mountains, Morocco, and the radiation of ceratosaurs. *Journal of Vertebrate Paleontology* 27 (3): 610–624.
- Barsbold R. 1983. Жъщные динозавры мела Монголий (Carnivorous dinosaurs from the Cretaceous of Mongolia). Труды – Совместная Советско–Монгольской Палеотологическая Экспедиция – Joint Soviet–Mongolian Paleontological Expedition, Transactions 19: 1–120.
- Barsbold R. 1986. Raubdinosaurier Oviraptoren. In: Vorob'eva OI (ed.), *Gerpetologičeskie issledovaniâ v Mongol'skoj Narodnoj Respublike. Institut èvolucionnoj morfologii i èkologii životnyh im. A.N. Severcova, Akademiâ nauk SSSR, Moscow.* 210–223.

Bonaparte JF, 1979. Dinosaurs: A Jurassic assemblage from Patagonia. *Science* 205: 1377–1379.

Bonaparte JF, Novas FE, Coria RA. 1990. *Carnotaurus sastrei* Bonaparte, the horned, lightly built carnosaur from the middle Cretaceous of Patagonia. *Contributions in Science, Natural History Museum of Los Angeles County* 416: 1–42.

Brusatte SL, Benson RB, Currie PJ, Zhao, X. 2010. The skull of *Monolophosaurus jiangi* (Dinosauria: Theropoda) and its implications for early theropod phylogeny and evolution. *Zoological Journal of the Linnean Society* 158: 573–607.

Carrano MT, , Sampson SD, Forster CA. 2002. The osteology of *Masiakasaurus knopfleri*, a small abelisauroid (Dinosauria: Theropoda) from the Late Cretaceous of Madagascar. *Journal of Vertebrate Paleontology* 22: 510–534.

Carrano MT, Benson RBJ, Sampson SD. 2012. The phylogeny of Tetanurae (Dinosauria: Theropoda). *Journal of Systematic Palaeontology* 10(2): 211–300.

Charig AJ, Milner AC. 1990. The systematic position of *Baryonyx walkeri*, in the light of Gauthier's reclassification of the Theropoda. In: Carpenter K, Currie

- PJ (eds.), *Dinosaur Systematics: Approaches and Perspectives*. Cambridge University Press, Cambridge. 127–140.
- Clark JA, Norell MA, Makovicky PJ. 2002. Cladistic approaches to the relationships of birds to other theropod dinosaurs. In: Chiappe LM, Witmer LM (eds.), *Mesozoic Birds, Above the Heads of the Dinosaurs*. University of California Press, Berkeley. 31–61.
- Chatterjee S, Wang T, Pan SG, Dong ZM, Wu XC, Upchurch P. 2010. A complete skeleton of a basal sauropod dinosaur from the Early Jurassic of China and the origin of Sauropoda. *Geological Society of America Abstracts with Programs*. 42 (5): 26.
- Colbert EH. 1989. The Triassic dinosaur, *Coelophysis*. *Museum of Northern Arizona, Bulletin*. 57: 1–160.
- Colbert EH. 1990. Variation in *Coelophysis bauri*. In: Carpenter K, Currie PJ (eds.), *Dinosaur Systematics: Approaches and Perspectives*. Cambridge University Press, New York. 81–89.
- Coria RA, Currie PJ. 2002. Braincase of *Giganotosaurus carolinii* (Dinosauria: Theropoda) from the Upper Cretaceous of Argentina. *Journal of Vertebrate Paleontology*, 22(4): 802–811.

- Currie PJ. 1999. Theropods. In: Farlow J, Brett-Surman M (eds.), *The Complete Dinosaur*. Indiana University Press, Bloomington. 216–233.
- Currie PJ, Varricchio DJ. 2004. A new dromaeosaurid from the Horseshoe Canyon Formation (Upper Cretaceous) of Alberta, Canada. In: *Feathered Dragons*. Indiana University Press, Indianapolis. 112–132.
- Currie PJ, Carpenter K. 2000. A new specimen of *Acrocanthosaurus atokensis* (Theropoda, Dinosauria) from the Lower Cretaceous Antlers Formation (Lower Cretaceous, Aptian) of Oklahoma, USA. *Geodiversitas* 22: 207–246.
- Currie PJ, Hurum JH, Sabath K. 2003. Skull structure and evolution in tyrannosaurid dinosaurs. *Acta Palaeontologica Polonica* 48: 227–234.
- Currie PJ, Xing LD, Wu XC, Dong, ZM. In progress. Anatomy and relationships of *Sinosaurus triassicus* (“*Dilophosaurus sinensis*”) from the Lufeng Formation (Lower Jurassic) of Yunnan, China.
- Dong ZM. 2003. Contributions of new dinosaur materials from China to dinosaurology. *Memoir of the Fukui Prefectural Dinosaur Museum* 2: 123–131.

- Downs A. 2000. *Coelophysis bauri* and *Syntarsus rhodesiensis* compared, with comments on the preparation and preservation of fossils from the Ghost Ranch *Coelophysis* quarry: New Mexico Museum of Natural History and Science, Bulletin 17: 27–32.
- Choiniere JN, Clark JM, Forster CA, Xu X. 2010. A basal coelurosaur (Dinosauria: Theropoda) from the Late Jurassic (Oxfordian) of the Shishugou Formation in Wucuiwan, People's Republic of China. *Journal of Vertebrate Paleontology* 30(6): 1773–1796
- Ezcurra MD, Cuny G. 2007. The coelophysoid *Lophostropheus airelensis*, gen. nov.: A review of the systematics of "*Liliensternus*" *airelensis* from the Triassic–Jurassic outcrops of Normandy (France). *Journal of Vertebrate Paleontology* 27(1): 73–86.
- Ezcurra MD, Brusatte SL. 2011. Taxonomic and phylogenetic reassessment of the early neotheropod dinosaur *Camposaurus arizonensis* from the Late Triassic of North America. *Palaeontology* 54: 763–772.
- Forster CA. 1999. Gondwanan dinosaur evolution and biogeographic analysis. *Journal of African Earth Sciences* 28: 169–185.
- Foth C, Rauhut OWM. In press. Macroevolutionary and morphofunctional

patterns in theropod skulls: a morphometric approach. *Acta Palaeontologica Polonica*. doi: <http://dx.doi.org/10.4202/app.2011.0145>

Gauthier JA. 1986. Saurischian monophyly and the origin of birds. In: Padian K. (ed.), *The Origin of Birds and the Evolution of Flight*. *Memoirs of the California Academy of Sciences* 8: 1–47.

Harris JD. 1998. A reanalysis of *Acrocanthosaurus atokensis*, its phylogenetic status, and paleobiogeographic implications, based on a new specimen from Texas. *New Mexico Museum of Natural History and Science Bulletin* 13: 1–75.

Hammer WR, Hickerson WJ. 1994. A crested theropod dinosaur from Antarctica. *Science* 264 (5160): 828–830.

Holtz TR Jr. 1994. The phylogenetic position of the Tyrannosauridae: implications for theropod systematics. *Journal of Paleontology* 68: 1100–1117.

Holtz TR Jr. 2000. A new phylogeny of the carnivorous dinosaurs. *GAIA* 15: 5–61.

Holtz TR, Jr. 2012. Origin of Theropods. In: Brett–Surman MK, Holtz TR Jr, Farlow JO (eds.), *The Complete Dinosaur* (2nd Edition). Indiana University

Press, Bloomington. 346–378.

Hwang SH, Norell MA, Ji Q, Gao KQ. 2004. A large compsognathid from the Early Cretaceous Yixian Formation of China. *Journal of Systematic Paleontology* 2: 13–30.

Hu SJ. 1993. A short report on the occurrence of *Dilophosaurus* from Jinning County, Yunnan Province. *Vertebrata Palasiatica* 31: 65–69.

Langer MC. 2004. Basal Saurischia. In: Weishampel DB, Dodson P, Osmólska H (eds.), *The Dinosauria* (2nd Edition). University of California Press, Berkeley. 25–46.

Madsen JH Jr, Welles SP. 2000. *Ceratosaurus* (Dinosauria, Theropoda) a revised osteology. *Miscellaneous Publication 00–2*, Utah Geological Survey. 1–80.

Martinez RN, Sereno PC, Alcober OA, Colombi CE, Renne PR, Montañez IP, Currie BS. 2011. A Basal Dinosaur from the Dawn of the Dinosaur Era in Southwestern Pangaea. *Science* 331 (6014): 206–210.

Nesbitt SJ, Smith ND, Irmis RB, Turner AH, Downs A, Norell MA. 2009. A complete skeleton of a Late Triassic saurischian and the early evolution of dinosaurs, *Science* 326 (5959): 1530–1533.

- Novas FE, de Valais S, Vickers-Rich P, Rich T. 2005. A large Cretaceous theropod from Patagonia, Argentina, and the evolution of carcharodontosaurids. *Naturwissenschaften* 92: 226–230.
- Ortega F, Escaso F, Sanz JL 2010. A bizarre, humped Carcharodontosauria (Theropoda) from the Lower Cretaceous of Spain. *Nature* 467: 203–206.
- Osmólska H, Currie PJ, Barsbold R. 2004. Oviraptorosauria. In: Weishampel DB, Dodson P, Osmólska H. (eds.), *The Dinosauria* (2nd Edition). California University Press, Berkeley. 165–183.
- Paul GS. 1988. *Predatory Dinosaurs of the World*. Simon & Schuster, New York. 1–464.
- Paul GS. 2002. *Dinosaurs of the Air*. The John Hopkins University Press, Baltimore and London. 1–460.
- Rauhut OWM. 2003. The interrelationships and evolution of basal theropod dinosaurs. *Special Papers in Palaeontology*, 69: 1–213.
- Rowe T. 1989. The early history of theropods. In: Padian K, Chure DJ (eds.), *The age of dinosaurs*, 12th Annual Short Course of the Paleontological Society.

University of Tennessee, Knoxville. 100–112.

Rowe T, Gauthier J. 1990. Ceratosauria. In: Weishampel DB, Dodson P, Osmolska H. (eds.), *The Dinosauria*. University of California Press, Berkeley. 151–168.

Sampson SD, Witmer LM, Forster CA, Krause DW, O'Connor PM, Dodson P, Ravoavy F. 1998. Predatory dinosaur remains from Madagascar: implications for the Cretaceous biogeography of Gondwana. *Science* 280: 1048–1051.

Schachner ER, Lyson T, Dodson P. 2009. Evidence from rib and vertebral morphology for the evolution of the avian respiratory system in non-avian theropod dinosaurs. *Anatomical Record B* 292: 1501–1513.

Sekiya T. 2010. A new prosauropod dinosaur from Lower Jurassic in Lufeng of Yunnan. *Global Geology* 29 (1): 6–15.

Sereno PC. 1999. The evolution of dinosaurs. *Science* 284: 2, 137–2, 132, 147.

Sereno PC, Wilson JA, Larsson HCE, Dutheil DB, Sues H–D. 1994. Early Cretaceous dinosaurs from the Sahara. *Science* 266: 267–271.

Sereno PC, Beck AL, Dutheil DB, Gado B, Larsson HCE, Rauhut OWM, Sadleir RW, Sidor CA, Varricchio DJ, Wilson GP, Wilson JA. 1998. A long-snouted predatory dinosaur from Africa and the evolution of spinosaurids. *Science* 282: 1298–1302.

Sereno PC, Dutheil DB, Iarochene M, Larsson HCE, Lyon GH, Magwene PM, Sidor CA, Varricchio DJ, Wilson JA. 1996. Predatory dinosaurs from the Sahara and Late Cretaceous faunal differentiation. *Science* 272: 986–991.

Sereno PC. 1999. The evolution of dinosaurs. *Science* 284, 2137–2147.

Smith ND, Makovicky PJ, Pol D, Hammer WR, Currie PJ. 2007a. Osteology of *Cryolophosaurus ellioti* (Dinosauria: Theropoda) from the Early Jurassic of Antarctica and implications for early theropod evolution. *Zoological Journal of the Linnean Society* 151: 377–421.

Smith ND, Makovicky PJ, Pol D, Hammer WR, Currie PJ. 2007b. The dinosaurs of the Early Jurassic Hanson Formation of the Central Transantarctic Mountains: Phylogenetic review and synthesis, in *Antarctica: A Keystone in a Changing World—Online Proceedings of the 10th ISAES*, edited by Cooper AK and Raymond CR et al., USGS Open-File Report 2007-1047, Short Research Paper 003, 1–5

- Swofford DL. 2002. PAUP\*: Phylogenetic Analysis Using Parsimony (\* and Other Methods). Version 4.0b10. Sinauer Associates, Sunderland.
- Tykoski RS. 1998. The osteology of *Syntarsus kayentakatae* and its implications for ceratosaurid phylogeny. MSc thesis, University of Texas at Austin. 1–217.
- Tykoski RS. 2005. Anatomy, ontogeny, and phylogeny of coelophysoid theropods. PhD dissertation, University of Texas at Austin. 1–553.
- Weishampel DB, Dodson P, Osmólska H. 2004. The Dinosauria (2nd Edition). University of California Press, Berkeley. 1–861.
- Welles SP. 1984. *Dilophosaurus wetherilli* (Dinosauria, Theropoda): Osteology and comparisons. *Palaeontographica Abteilung A*. 185: 85–180.
- Wu XC, Currie PJ, Dong ZM, Pan S, Wang T. 2009. A new theropod dinosaur from the Middle Jurassic of Lufeng, Yunnan, China. *Acta Geologica Sinica* 83(1): 9–24
- Xu X, Clark JM, Forster CA, Norell MA, Erickson GM, Eberth DA, Jia CK, Zhao Q. 2006. A basal tyrannosauroid dinosaur from the Late Jurassic of China. *Nature* 439: 715–718.

- Xu X, Clark JM, Mo J, Choiniere J, Forster CA, Erickson GM, Hone DWE, Sullivan C, Eberth DA, Nesbitt S, Zhao Q, Hernandez R, Jia CK, Han FL, Guo Y. 2009. A Jurassic ceratosaur from China helps clarify avian digital homologies (supplementary information). *Nature* 459 (7249): 940–944.
- Xu X, You H, Du K, Han F. 2011. An Archaeopteryx–like theropod from China and the origin of Avialae. *Nature* 475: 465–470.
- Xu X, Wang K, Zhang K, Ma Q, Xing LD, Sullivan C, Hu D, Cheng S. 2012. A gigantic feathered dinosaur from the Lower Cretaceous of China. *Nature* 484: 92–95
- Yates AM. 2005. A new theropod dinosaur from the Early Jurassic of South Africa and its implication for the early evolution of theropods. *Palaeontologia Africana* 41: 105–122.
- Young CC. 1941. A complete osteology of *Lufengosaurus huenei* Young (gen. et sp. nov.) from Lufeng, Yunnan, China. *Palaeontologica Sinica, Series C* 7, 1–53.
- Young CC. 1942. *Yunnanosaurus huangi* Young (gen. et sp. nov.), a new Prosauropoda from the red beds at Lufeng, Yunnan." *Bulletin of the Geological Society of China* 22 (1–2): 63–104.

- Young CC. 1948. On two new saurischai from Lufeng, Yunnan. *Bulletin of the Geological Society of China*, 28(1–2): 75–90
- Young CC. 1951. The Lufeng saurischian fauna. *Palaeontologica Sinica, Series C* 13: 1–96.
- Zanno LE. 2010. A taxonomic and phylogenetic review of Therizinosauria. *Journal of Systematic Paleontology* 8: 503–543.
- Zhao XJ, Currie PJ. 1993. A large crested theropod from the Jurassic of Xinjiang, People's Republic of China. *Canadian Journal of Earth Sciences* 30: 2027–2036.
- Zhang Y, Yang Z. 1995. A new complete osteology of Prosauropoda in Lufeng Basin, Yunnan, China. Yunnan Publishing House of Science and Technology, Kunming, China. 1–100.

## CHAPTER 4

### **Tooth loss and alveolar remodeling in *Sinosaurus triassicus* (Dinosauria: Theropoda) from the Lower Jurassic strata of the Lufeng Basin, China**

#### **4.1 Introduction**

Palaeopathology includes the study of disease and other abnormalities in the fossil record. Such investigations can reveal unique insights into the behavior, biology, and development of extinct animals. The main assumption in palaeopathology is that modern processes that dictate an osseous response to trauma can be extrapolated into fossil taxa. Among theropod dinosaurs, injury-related trauma (bites, exostoses, fractures, infection, stress fractures) is the overriding cause of osteopathy; however, congenital abnormalities, and arthritis (gout) have also been documented (Molnar, 2001; Rothschild and Tanke, 2005).

Few records of osseous abnormalities have been published for Chinese dinosaurs. Formal reports include possible bacterial infection in the fibula of the basal ceratopsid *Psittacosaurus* (Lü et al., 2007), osteoarthritis in *Caudipteryx*, *Confuciusornis* and *Microraptor* (Rothschild et al., 2012a), *Monolophosaurus* (Zhao and Currie, 1993), and *Sinraptor* (Currie and Zhao, 1993), healed bite marks in *Sinraptor* (Tanke and Currie, 2000), and a healed fracture in the theropod *Yangchuanosaurus* (Xing et al., 2009). Xing et al. (2009) also mentioned possible palaeopathological phenomena in the sauropods *Fusuisaurus* and *Mamenchisaurus*, although these were not described in detail.

*Sinosaurus triassicus* (= "*Dilophosaurus sinensis*") is an early Jurassic

theropod characterized by twin hatchet-shaped crests similar to its North American relative *Dilophosaurus* (Hu, 1993; Dong, 2003). In 2007, the Lufeng Dinosaurian Museum recovered an incomplete skull, and several postcranial fragments of a new specimen of *Sinosaurus* (ZLJT01) from the Lufeng Basin in Yunnan Province, China. The right maxilla includes an abnormal, closed alveolus, the significance and possible etiology of which are considered in this paper.

ZLJT01 was discovered near Hewanzi Village, Ganchong Village Committees, Konglongshan Township, Lufeng County, Chuxiong Yi Autonomous Prefecture, Yunnan Province, China. The specimen includes parts of both premaxillae, both maxillae, a dentary, the nasal crest, occiput, and fragments of the postcranial skeleton. A detailed description of ZLJT01 and *Sinosaurus* will be presented elsewhere. This paper details the palaeopathological description.

## **4.2 Geological Setting**

The Lower Lufeng Formation of Yunnan Province (People's Republic of China) contains a diverse dinosaur assemblage, including ornithischians, prosauropods, sauropods, and theropods that were preserved in a variety of fluvial, overbank, and lacustrine settings (Luo and Wu, 1994). The age of the Lower Lufeng Formation (Bien, 1941) was originally thought to be Late Triassic (Bien 1940; Young 1951). However, biostratigraphical correlates (both vertebrate and invertebrate) indicate an Early Jurassic (Hattangian–Sinemurian) age (Sheng et al. 1962; Sun and Cui, 1986; Luo and Wu, 1994). Fang et al. (2000) later restricted the name “Lufeng Formation” to what previously was the Lower Lufeng

Formation, further subdividing it into the Shawan (Hettangian) and Zhangjia'ao (Sinemurian) members. However, as noted by Barrett et al. (2005), this nomenclature has not been widely accepted. ZLJT01 (*Sinosaurus*) comes from the lowermost (Shawan member) portion of the Lower Lufeng Formation. Associated fauna include prosauropods (*Anchisaurus*, *Lufengosaurus*, *Yunnanosaurus*) and theropods (*Lukousaurus*, *Sinosaurus*) and the ankylosaur *Bienosaurus*.

### 4.3 Methods

ZLJT01 was prepared manually using pneumatic airscribes and pin vises. This specimen was scanned using a PHILIPS Brilliance 16 CT scanner at Sichuan Forth People's Hospital (Chengdu, China), at 650 $\mu$ m slice thickness, rendering 6 longitudinal, 99 coronal, and 391 transverse slices.

### 4.4 Description

The right maxilla of ZLJT01 is incomplete, lacking most of the posterodorsal process and the distal end of the jugal process (Fig. 4.1A–E). Alveoli maxillary tooth positions one to ten (mx1 to mx10) are preserved in ZLJT01; however, the 10<sup>th</sup> alveolus is broken. Based on other *Sinosaurus* specimens, there were probably 13 (KMV 8701) or 14 (LDM–L10) tooth positions in the complete maxilla. Two broken teeth are preserved in alveoli for mx3 and mx8, and an incompletely erupted tooth crown is present in the alveolus of mx5. The remaining alveoli (with the exception of mx6) lack teeth, undoubtedly as a result of postmortem tooth loss.

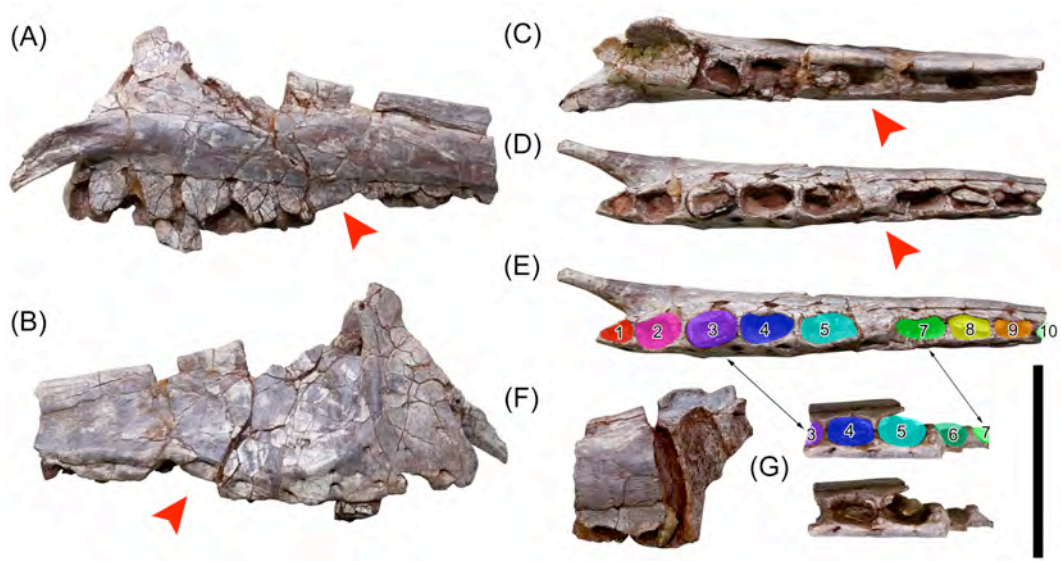


**FIGURE 4.1.** Palaeopathological characters of ZLJT01 (*Sinosauros triassicus*), a right maxilla in A, medial; B, lateral; C, dorsal; D, E, ventral views. Position of the abnormal alveolus mx6 is indicated by an arrowhead. F, G, incomplete, normal left maxilla of ZLJT01 in F, medial and G, ventral aspects showing non-pathologic alveolus mx6. Numerals in E and G refer to alveoli. Scale bar = 10 cm.

In contrast with the other alveoli, the sixth maxillary alveolus is entirely closed by a layer of secondary bone (Figs. 4.1A–E). In medial or lateral aspect, the rim of the alveolus of mx6 is dorsal to the horizontal plane formed by the other alveoli, giving the jaw a distinct notch. The external surface of the new bone is smooth and the interdental plate is indistinct, having either been lost or fused with the adjacent secondary bone. An X-ray of the maxilla (Fig. 4.2) clearly shows the outline of the original alveolus; however, the alveolar space is less radiolucent than the adjacent alveoli, which is indicative of secondary bone filling the alveolar space. This is further evidenced by the near total absence of pyrite growth (‘pyrite rot’) that pervades the other alveolar spaces (Fig. 4.2). No additional evidence of damage or remodeling to the bone surrounding mx6 was observed. Comparison with the incomplete left maxilla, which includes alveoli mx3–7 (Fig. 4.1F, G), shows a normal alveolus for mx6 and indicates tooth loss was unilateral, at least in the preserved parts of the jaw. CT scans (Fig. 4.3B) showed the same results. The fifth maxillary tooth (mx5) is represented by a distinct replacement tooth (Fig. 4.3B). With the exception of the alveolus for mx6, the gaps between the teeth and their alveoli are filled with pyrite; this is seen best in the alveoli for mx3 and mx5. Only a small amount of pyrite appears in the corner of the mx6 alveolus.

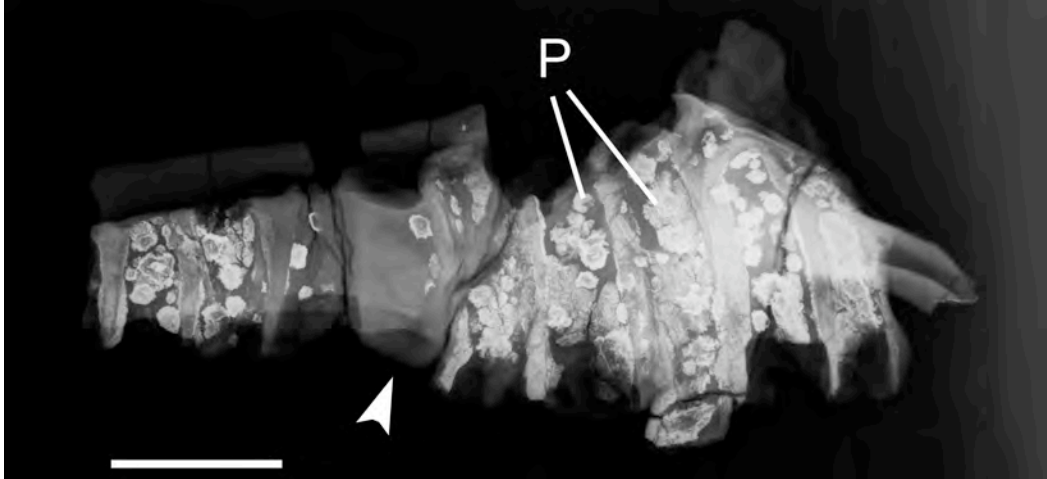


**FIGURE 4.2.** X-ray scan of ZLJT01 (*Sinosaurus triassicus*), a pathological right maxilla in lateral aspect. Anterior is right. Arrowhead indicates pathologic alveolus mx6. Pyrite growths (P) show up as white discs. Note the near absence of pyrite in mx6. Scale bar = 5 cm.

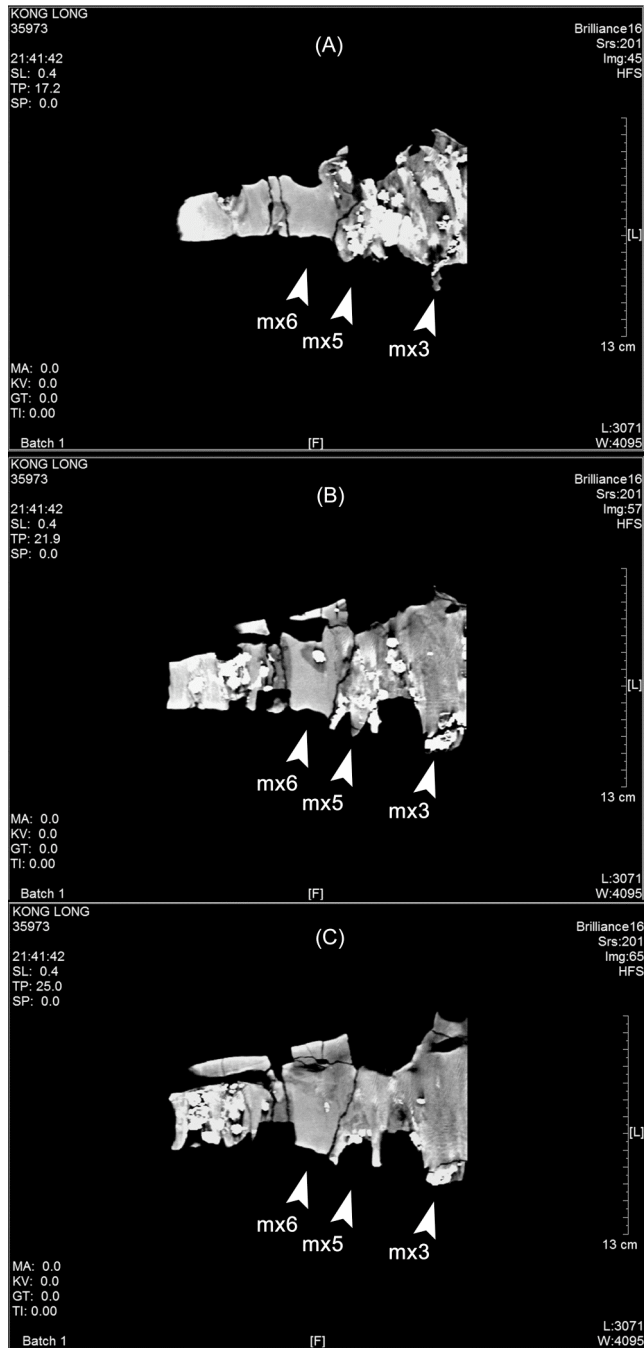


**FIGURE 4.3.** CT scan of the pathological right maxilla (ZLJT01) in lateral aspect. Anterior is right. Arrowheads indicate the positions of the alveoli for mx3, mx5 and mx6. The white discs are pyrite.

#### 4.5 Discussion and Conclusions

Dental abnormalities in theropods are infrequently reported in the literature. Broken teeth (Farlow et al. 1991; Farlow and Brinkman, 1994; Schubert and Ungar, 2005), and congenitally deformed teeth (such as the split carinae of Abler, 1991, Erickson, 1995, Molnar, 2001 and Rothschild and Tanke, 2005) are among the most commonly documented abnormalities. Other potential congenital abnormalities include a ‘twisted’ dentary in a hatchling *Troodon* (Carpenter 1982; Molnar 2001). Bite-marks and related trauma are also relatively common on the jaws and faces of a range of theropod taxa (Tanke and Currie, 2000; Wolff and Varricchio, 2005; Rothschild and Molnar, 2008; Bell and Currie, 2009; Bell, 2010; see also Molnar, 2001 and references therein).

Dental abscesses, such as those reported in an unidentified hadrosaurid jaw (Moodie 1930) and in the captorhinid *Labidosaurus* (Reisz et al. 2011), have yet to be identified in theropods. Abscesses form as a result of deep bacterial infections, resulting in osseous erosions associated with tooth-row groove destruction and tooth loss.

When teeth are lost or removed in vivo, the bony socket remodels over time in mammals so that there is no longer a cavity (Morgan 2011). X-ray and CT scan evidences demonstrates that the osseous infilling of the alveolus in ZLJT01 is typical of alveolar remodeling. This type of healing process following antemortem tooth loss is the first recorded for a dinosaur. Alveolus closure is extremely rare among living and fossil reptiles, having only been observed in the phytosaur *Nicrosaurus kapffi* (Hungerbühler, 2000). Hungerbühler (2000) noted a single

closed alveolus in the right maxilla of *Nicrosaurus kapffi* (Staatliches Museum für Naturkunde Stuttgart SMNS 4379), which may have resulted from injury or failed replacement (Rothschild et al. 2012b). In contrast, alveolar remodeling is relatively common in extant primates, where tooth loss may be a result of feeding behaviour (Miles and Grigson, 1990; Stoner, 1995; Cuozzo and Sauter, 2004, 2006).

*In vivo* tooth loss is a result of pathological and/or traumatic mechanisms. Pathological changes such as periodontal disease (including periodontitis and alveolar osteomyelitis such as abscesses) may be responsible for destruction of the tooth root, the periodontal ligament, and/or the tooth socket itself resulting in avulsion of the affected tooth (Hillson, 2001). This is accompanied by an osseous response to infection, including pus-draining sinuses (fistulae) and rapid bone growth with a characteristic disorganized bone texture. Such evidence of osteomyelitis was not observed in ZLJT01.

Traumatic tooth loss typically occurs as a result of a forceful impact to the tooth crown but may also be initiated by trauma to the alveolar margin or jaw (Lukacs, 2007; Morgan, 2011). Trauma can occur with or without damage to the surrounding bone and soft-tissue (Wright et al. 2007). Although obvious indicators of dental trauma, such as retained tooth fragments and alveolar or jaw fracture were not observed in ZLJT01, it is well known that theropods frequently damaged teeth antemortem, presumably as a result of feeding activity (Shubert and Ungar, 2005). Shed theropod teeth commonly encountered within ornithischian-dominated bonebeds are similarly reflective of antemortem tooth loss due to

feeding behavior (Varricchio and Horner, 1993; Ryan *et al.* 2001; Eberth and Getty, 2005). These are usually tooth crowns shed during the normal process of tooth replacement. However, virtually all show some evidence of damage, such as spalled or chipped enamel and breakage, that occurred before the crowns were shed. Broken tips of teeth are sometimes also found in the bonebeds, and there are also rare examples of broken theropod teeth still embedded in prey bone that demonstrate a clear relationship between feeding and tooth avulsion (Currie and Jacobsen, 1995; Buffetaut *et al.* 2004; Bell and Currie, 2010; Xing *et al.* 2012). Although direct evidence of trauma (retained tooth fragments, healed fractures) was not observed in ZLJT01, traumatic tooth loss does not necessarily involve the surrounding bone (Wright *et al.* 2007). Given the known relationship between theropod feeding behavior and loss of replacement teeth, it is unlikely that tooth loss in ZLJT01 was a result of trauma to the tooth crown alone. It is possible that in this case the loss of the tooth was traumatic enough to have damaged the root of the tooth and the associated replacement (or germ) teeth. The apparent absence of the associated dental plate is likely a result of resorption and remodeling following tooth loss, although traumatic loss to all or part of the dental plate cannot be discredited entirely. A similar condition was observed in a peculiar *Allosaurus* dentary (USNM 2315; holotype of *Labrosaurus ferox*) that lacks the anterior four or five teeth. The alveoli were resorbed, resulting in a concave oral margin in lateral view giving the false impression of an edentulous jaw (Marsh, 1884; Rothschild, 1997). Molnar (2001) suggested a possible traumatic etiology for the lost teeth.

The total closure of the alveolus in ZLJT01 and remodeling of the alveolar space indicate the animal survived for a significant period following tooth loss. In human subjects, remodeling of the alveolar cavity occurs after the third month (Schropp et al. 2003; Morgan, 2011); however, this cannot be postulated to accurately reflect recovery time in any other species, particularly if they are extinct dinosaurs. As noted earlier, reptilian examples of alveolar remodeling are rare, and recovery times have not been studied in extant reptiles. Nevertheless, it is clear that tooth loss in *Sinosaurus* was non-fatal and that ZLJT01 survived probably for months or even years before it died (Fig. 4, 4). This finding adds to the known range of dental pathologies found in theropods and contributes to mounting evidence suggesting theropods were highly resilient to a wide range of trauma and disease (Hanna, 2002; Farke and O'Connor, 2007; Bell, 2010).



**FIGURE 4.4.** Life reconstruction of *Sinosaurus triassicus* with dental abnormality based on ZLJT01. Illustration by Mr. Chenyu Liu.

## References

- Barrett PM, Upchurch P, Wang XL. 2005. Cranial osteology of *Lufengosaurus hueni* Young (Dinosauria: Prosauropoda) from the Lower Jurassic of Yunnan, People's Republic of China. *Journal of Vertebrate Paleontology* 25: 806–822.
- Bell PR. 2010. Palaeopathological changes in a population of *Albertosaurus sarcophagus* from the Upper Cretaceous Horseshoe Canyon Formation of Alberta, Canada. *Canadian Journal of Earth Sciences* 47: 1263–1268.
- Bell PR, Currie PJ. 2010. A tyrannosaur jaw bitten by a confamilial: scavenging or fatal agonism? *Lethaia* 43: 278–281.
- Bien MN. 1941. “Red Beds” of Yunnan. *Bulletin of the Geological Society of China* 21: 159–198.
- Buffetaut E, Martill D, Escuillié, F. 2004. Pterosaurs as part of a spinosaur diet. *Nature* 430: 33.
- Carpenter K. 1982. Baby dinosaurs from the Late Cretaceous Lance and Hell Creek formations and a description of a new species of theropod. *Contributions to Geology* 20: 123–134.

- Cuozzo FP, Sauther M L. 2004. Tooth loss, survival, and resource use in wild ring-tailed lemurs (*Lemur catta*): implications for inferring conspecific care in fossil hominids. *Journal of Human Evolution* 46: 623–631.
- Cuozzo FP, Sauther ML. 2006. Severe wear and tooth loss in wild ring-tailed lemurs (*Lemur catta*): a function of feeding ecology, dental structure, and individual life history. *Journal of Human Evolution* 51: 490–505.
- Currie PJ, Jacobsen AR. 1995: An azhdarchid pterosaur eaten by a velociraptorine theropod. *Canadian Journal of Earth Sciences* 32: 922–925.
- Dong ZM. 2003. Contributions of new dinosaur materials from China to dinosaurology. *Memoir of the Fukui Prefectural Dinosaur Museum* 2: 123–131.
- Eberth DA, Getty M. 2005. Ceratopsian bonebeds. In: Currie PJ, Koppelhus EB. (eds.), *Dinosaur Provincial Park: a Spectacular Ancient Ecosystem Revealed*. Indiana University Press, Bloomington. 501–536.
- Erickson GM. 1995. Split carinae on tyrannosaurid teeth and implications of their development. *Journal of Vertebrate Paleontology* 15: 268–274.
- Fang XS, Pang QJ, Lu LW, Zhang ZX, Pan SG, Wang YM, Li XK, Cheng ZW.

2000. Lower, Middle, and Upper Jurassic subdivision in the Lufeng region, Yunnan Province. In Proceedings of the Third National Stratigraphical Congress of China. Geological Publishing House, Beijing. 208–214.
- Farke AA, O'Connor PM. 2007. Pathology in *Majungasaurus crenatissimus* (Theropoda: Abelisauridae) from the Late Cretaceous of Madagascar. *Journal of Vertebrate Paleontology* 27 (suppl. to Number 2): 180–184.
- Farlow JO, Brinkman DL. 1994. Wear surfaces on the teeth of tyrannosaurs. In Rosenberg GD, Wolberg DL. (eds.), *Dino Fest. The Paleontological Society Special Publication* 7. 165–175.
- Farlow JO, Brinkman DL, Abler WL, Currie PJ. 1991. Size, shape, and serration density of theropod dinosaur lateral teeth. *Modern Geology* 16: 161–198.
- Hanna RR. 2002. Multiple injury and infection in a sub-adult theropod dinosaur *Allosaurus fragilis* with comparisons to allosaur pathology in the Cleveland–Lloyd Dinosaur Quarry collection. *Journal of Vertebrate Paleontology* 22: 76–90.
- Hillson S. 2001. Recording dental caries in archaeological remains. *International Journal of Osteoarchaeology* 11: 249–289.

- Hu SJ. 1993. A new Theropoda (*Dilophosaurus sinensis* sp. nov.) from Yunnan, China. *Vertebrata Palasiatica* 31: 65–69.
- Hungerbühler A. 2000. Heterodonty in the European phytosaur *Nicrosaurus kapffi* and its implications for the taxonomic utility and functional morphology of phytosaur dentitions. *Journal of Vertebrate Paleontology* 20: 31–48.
- Lü JC, Kobayashi Y, Lee YN, Ji Q. 2007. A new *Psittacosaurus* (Dinosauria: Ceratopsia) specimen from the Yixian Formation of western Liaoning, China: the first pathological psittacosaurid. *Cretaceous Research* 28: 272–276.
- Lukacs JR. 2007. Dental trauma and antemortem tooth loss in prehistoric Canary Islanders: prevalence and contributing factors. *International Journal of Osteoarchaeology* 17: 157–173.
- Luo ZX, Wu XC. 1994. The small tetrapods of the Lower Lufeng Formation, Yunnan, China. In: Fraser NC, Sues HD. (eds.), *In the Shadow of the Dinosaurs: Early Mesozoic Tetrapods*. Cambridge University Press, Cambridge. 251–270.
- Marsh O. 1884. Principal characters of American Jurassic dinosaurs, the order Theropoda. *American Journal of Science* 27: 411–416.

- Miles AE, Grigson C. 1990. Colyer's Variations and Diseases of the Teeth of Animals. Cambridge University Press, Cambridge. 1–692.
- Molnar RE. 2001. Theropod paleopathology: a literature survey. In: Tanke DH, Carpenter K. (eds.), Mesozoic Vertebrate Life. Indiana University Press, Bloomington. 337–363.
- Moodie RL. 1930. Dental abscesses in a dinosaur millions of years old, and the oldest yet known. Pacific Dental Gazette 38: 435–440.
- Morgan J. 2011. Observable stages and scheduling for alveolar remodeling following antemortem tooth loss. Unpublished PhD Dissertation, Johannes Gutenberg–Universität, Mainz, 1–204.
- Reisz R, Scott DM, Pynn BR, Modesto SP. 2011. Osteomyelitis in a Paleozoic reptile: ancient evidence for bacterial infection and its evolutionary significance. Naturwissenschaften 98: 551–555.
- Rothschild BM. 1997. Dinosaurian paleopathology. In: Farlow JO, Brett–Surman MK. (eds.), The Complete Dinosaur. Indiana University Press, Bloomington. 426–448.

- Rothschild BM, Molnar RE. 2008. Tyrannosaurid pathologies as clues to nature and nature in the Cretaceous. In: Larson P, Carpenter K. (eds.), *Tyrannosaurus rex*, the Tyrant King. Indiana University Press, Bloomington. 287–306.
- Rothschild B, Tanke DH. 2005. Theropod paleopathology, state-of-the-art review. In: Carpenter K. (ed.): The Carnivorous Dinosaurs. Indiana University Press, Bloomington. 351–365.
- Rothschild B, Zheng XT, Martin L. 2012a. Osteoarthritis in the early avian radiation: Earliest recognition of the disease in birds. *Cretaceous Research* 35: 178–180.
- Rothschild BM, Schultze H-P, Peligrini R. 2012b. *Herpetological Osteopathology: Annotated Bibliography of Amphibians and Reptiles*. Springer-Verlag, Heidelberg, Germany. 1–461.
- Rowe T. 1989. A new species of the theropod dinosaur *Syntarsus* from the Early Jurassic Kayenta Formation of Arizona. *Journal of Vertebrate Paleontology* 9: 125–136.
- Ryan MJ, Russell AP, Eberth DA, Currie PJ. 2001. The taphonomy of a *Centrosaurus* (Ornithischia: Ceratopsidae) bonebed from the Dinosaur

Park Formation (upper Campanian), Alberta, Canada, with comments on cranial ontogeny. *Palaios* 16: 482–506.

Schropp L, Wenzel A, Kostopoulos L, Karring T. 2003. Bone healing and soft tissue contour changes following single-tooth extraction: a clinical and radiographic 12-month prospective study. *International Journal of Periodontics and Restorative Dentistry* 23: 313–323.

Schubert BW, Ungar PS. 2005. Wear facets and enamel spalling in tyrannosaurid dinosaurs. *Acta Palaeontologica Polonica* 50: 93–99.

Sheng SF, Chang LQ, Cai SY, Xiao RW. 1962. The problem of the age and correlation of the red beds and the coal series of Yunnan and Szechuan. *Acta Geologica Sinica* 42: 31–56.

Stoner KE. 1995. Dental pathology in *Pongo satyrus borneensis*. *American Journal of Physical Anthropology* 98: 307–321.

Sun AL, Cui KH. 1986. A brief introduction to the Lower Lufeng saurischian fauna (Lower Jurassic: Lufeng, Yunnan, People's Republic of China). In: Padian K. (ed.), *The Beginning of the Age of Dinosaurs: Faunal Change Across the Triassic–Jurassic Boundary*. Cambridge University Press, Cambridge. 275–278.

- Tanke DH, Currie PJ. 2000. Head-biting behavior in theropod dinosaurs: paleopathological evidence. *Gaia* 15: 167–184.
- Varricchio D, Horner JR. 1993. Hadrosaurid and lambeosaurid bonebeds from the Upper Cretaceous Two Medicine Formation of Montana: taphonomic and biologic implications. *Canadian Journal of Earth Sciences* 29: 997–1006.
- Welles SP. 1984. *Dilophosaurus wetherilli* (Dinosauria, Theropoda) osteology and comparisons. *Palaeontographica Abteilung A* 185: 85–180.
- Wolff EDS, Varricchio D. 2005. Zoological paleopathology and the case of the tyrannosaurus jaw: integrating phylogeny and the study of ancient disease. *Geological Society of America Abstracts with Programs* 37: 88.
- Wright G, Bell A, McGlashan, G, Vincent C, Wellbury RR. 2007. Dentoalveolar trauma in Glasgow: an audit of mechanism and injury. *Dental Traumatology* 23: 226–231.
- Xing LD, Dong H, Peng GZ, Shu CK, Hu XD, Jiang H. 2009. A scapular fracture in *Yangchuanosaurus hepingensis* (Dinosauria: Theropoda). *Geological Bulletin of China* 28: 1390–1395.

Xing LD, Bell PR, Currie PJ, Shibata M, Tseng K, Dong ZM. 2012. A sauropod rib with an embedded theropod tooth: direct evidence for feeding behaviour in the Jehol group, China. *Lethaia*. DOI: 10.1111/j.1502-3931.2012.00310.x.

Young CC. 1951. The Lufeng saurischian fauna in China. *Palaeontologia Sinica*, New Series C 13: 1-96.

## CHAPTER 5

### Model-based identification of mechanical characters in the crest of

### *Sinosaurus* (Dinosauria: Theropoda)

#### 5.1 Introduction

Finite element analysis can biomechanically test the function of unusual features in extinct vertebrates, to assess their possible utility for behavior. For example, suitability for combat has been tested for the caudal clubs of ankylosaurian (Arbour and Snively, 2009) and sauropod dinosaurs (Xing et al., 2009), and the domes of pachycephalosaurs (Snively and Cox, 2008; Snively and Theodor, 2011).

Elaborate cranial ornamentations of theropod dinosaurs were highly diverse and widely distributed phylogenetically. Various hypotheses have been advanced for their functions. However, all the hypotheses are based on reasonable imagination or analogies with modern animals, and lack biomechanical testing. Therefore, finite element analysis was employed on two specimens of *Sinosaurus* with a distinct type of crest. This approach grounds the debate within a quantitative biomechanical framework.

#### 5.2 Hypotheses of crest function in *Dilophosaurus* and *Sinosaurus*

Cranial ornamentations in theropods are present in abelisaurids (*Carnotaurus*, Bonaparte et al., 1990), allosauroids (*Allosaurus*, Madsen, 1976; *Mapusaurus*, Coria and Currie, 2006), coelophysoids (*Dilophosaurus*, Welles,

1984), megalosauroids (*Monolophosaurus*, Zhao and Currie 1993), tyrannosauroids (*Guanlong*, Xu et al., 2006), and oviraptorosaurs (*Oviraptor*, Barsbold, 1986). The variability of the crest within each genus have been attributed to ontogenetic stage, sexual differences, or individual variation (Currie and Eberth, 2010), and possible functions include intraspecific combat, sexual recognition, sound production, and the establishment of dominance within a group.

All species with double-hatchet crests are assigned to Early Jurassic theropod, including *Dilophosaurus* (Welles, 1984), *Sinosaurus* (Young, 1948), "*Syntarsus*" *kayentakatae* (Rowe, 1989), and probably *Zupaysaurus* (Arcucci and Coria, 2003). The crests of *Dilophosaurus* and *Sinosaurus* are the largest and most remarkable. Furthermore, they are so similar in morphology (Currie et al., in progress), that a comparatively complete *Sinosaurus triassicus* was immediately assigned to *Dilophosaurus* as a new species when it was discovered (Hu, 1993).

There are various hypotheses on the functions of the crests of *Dilophosaurus* and *Sinosaurus*. In skeletal morphology, the crests of *Dilophosaurus* and *Sinosaurus* were probably were too thin and fragile to have served as weapons for intraspecific combat (Tykoski and Rowe 2004). Dong (2003) considered that the crest of *Sinosaurus* may have kept the abdominal wall of a carcass open while the theropod devoured it. Tykoski and Rowe (2004) felt the crests were likely used for display purposes only. Gay (2005) considered the differences among various specimens of *Dilophosaurus* lie in individual variation and ontogeny alone, but not sexual dimorphism. Hone and Cuthill (2011)

proposed that the cranial crests of *Dilophosaurus* were involved in mutual sexual selection, and inferred that they were most likely used for either sexual or social display. Padian and Horner (2011) pointed out that neither sexual dimorphism nor ontogenetic maturity can yet be examined statistically for these "bizarre structures" in theropods. Even the large sample of Ghost Ranch *Coelophysis* has yet to be properly utilized for such studies (Padian and Horner, 2011).

### 5.3 Materials

The paired crests in *Dilophosaurus* and *Sinosaurus* are formed by the nasals anteriorly, and the lacrimals posteriorly (Currie et al., in progress). The left crest of ZLJT01 (Fig. 5.1) only preserves the axe-shaped posterior section, which is formed by the lacrimal; although incomplete, it is well preserved. The partial crest is 110 mm in length, and rises to a height of 73 mm above the postorbital contact of the lacrimal. The back of the crest extends posterolaterally above the rim of the orbit.

The crest of LDM-L10 (Fig. 5.1) is 440 mm long, but the nasal extends in front of the crest along the margin of the external naris for a short distance. In dorsal view, the crests remain separate for their entire anteroposterior lengths, and diverge posteriorly. The right crest of LDM-L10 is damaged, but most of the upper margin of the left crest is well preserved. The crest of LDM-L10 is pierced by several possible openings; each was probably covered by skin in the living animal. The bone can be thin (less than 4 mm) between ridges that are perpendicular to the convex upper margin of the crest.



**FIGURE 5.1.** *Sinosaurus triassicus* (LDM-L10) skull, and *Sinosaurus triassicus* (ZLJT01) lacrimal crest in lateral views. Scale bar=10 cm

## **5.4 Methods**

### **5.4.1 Modeling approach**

*Sinosaurus* crests are formed of bone, which is considered as a continuous medium; continuum mechanics and finite element modeling (FEM) were adapted as the analytical/mathematical foundation to study their deformation under external loads. Such analyses follows previous FE quantitative study developed to understand bone deformations in humans and other animals (Pesce Delfino et al. 1981; Krajcinovic et al. 1987; Kabel et al. 1999; Fernandez et al. 2004; Rayfield 2007 and references therein).

More precisely, FE modeling of the *Sinosaurus* crest can be divided into two major parts -- the geometrical model and the material model. Geometric modeling uses a finite volumetric element mesh to fill in the outer shape of the crest, reflecting its structural features and the connectivity of multiple local parts. Material modeling defines stress–strain behaviours of material (bone) under different stretch–compression situations. For more comprehensive theoretical and practical details about continuum mechanics and its application in FE modelling, see Holzapfel (2000) and Bonet and Wood (2008).

### **5.4.2 Geometrical Modeling**

Constructing an FE model of a fossil consists of three steps, 1) Image scanning, 2) geometry reconstruction, and 3) FE mesh generation. The geometrical data can be acquired by magnetic resonance imaging (MRI), computed tomography (CT) or laser scanner. For bone, CT is the most common

option to obtain external and internal structural images. Image segmentation is used to produce a data cloud to indirectly obtain a fossil shape or its internal structures. Then, the data cloud is processed by a few common algorithms to construct a FE model.

The crest of *Sinosaurus* (ZLJT01) was scanned using computed tomography (CT) to provide information on its internal structure, and to derive three-dimensional models for use in volume estimates. ZLJT01 was scanned at the University of Alberta Hospital Alberta Cardiovascular and Stroke Research Centre (ABACUS), on a Siemens Somatom Sensation 64 CT scanner, with imaging resolution  $0.2969 \text{ mm} \times 0.2969 \text{ mm} \times 0.6 \text{ mm}$ . The entire set of these grey scale CT images was then loaded into medical imaging processing software, called ITK-snaps, for automatic segmentation. This segmented data cloud subsequently was used to build the FE model. The mesh consists of 18343 nodes and a total 72091 linear basis elements, including 673 hexahedral elements (8 nodes) and 71418 tetrahedral elements.

The construction of the finite element model of the crest of *Sinosaurus* LDM-L10 required its 3D geometric data. Because the specimen was deemed too fragile to transport, a cast of LDM-L10 was CT scanned for 3D reconstruction. The machine employed was a Non-contact Grating-Type Structured Light 3D Scanning System (JiRui II, see Table 5.1; [JiRui Xintian Technology Co., Ltd., Beijing]). The high-precision 3D data of the skull of LDM-L10 were saved in IGES format for use in FE software.

**Table 5.1.** JiRui II Technical Data

Type	JRXS
Unit scan scope (mm <sup>2</sup> )	150×100~200×150
Precision of measurement (mm)	0.01~0.02
Unit measurement points	About 1, 330, 000 points
Average pixel pitch (mm)	0.1~0.15
Scan speed for single surface	<10S
Connection manner	Automatically connected

### 5.4.3 Material Modeling

The *Sinosaurus* crest can be treated as homogenous isotropic linear material that is close to the properties of modern bone. In studies of modern animal bones, the values of those material constants come from material sample testing (for instance, uniaxial stretch/compression). However, such testing is almost impossible for dinosaur studies because fossilized bone is too brittle, and material properties were estimated based on extant analogs (assigned the material properties of bovine haversian bone, Rayfield et al., 2001). The crest is modeled as undergoing linear deformation under a single external loadcase, assuming that fatigue would be irrelevant given intermittent bouts of combat.

Under these assumptions, the stress–strain relation of the bony material is mathematically described as a St. Venant–Kirchhoff material model, approximating linear elastic behavior. As a starting point, the bone was assigned the Young's modulus ( $E$ )=10 Gpa, and Poisson's ratio ( $\nu$ )=0.4. The choice of parameter values follows the previous study by Rayfield (2005) on an *Allosaurus* cranium. The same assumption (Rayfield, 2005) is made that the *Sinosaurus* crest possesses similar material stiffness to that of cranial bone of another large carnivorous dinosaur. The model deformation here is a quasi–static deformation without accounting for the gravitational force; in other words, the investigation only is interested in its structural equilibrium state under different loads.

### 5.4.4 Computational Experiments

The aim of the computational experiments is to capture a general feature of

crest deformation under various external loading conditions. The current sample limits the analyses from CT scans to the posterior part of *Sinosaurus* crest; therefore, the results may lack a more comprehensive insight of overall structural features, especially the roles of cavities on the crest, and possibly lose useful information. To simulate mechanical behavior of the complete structure, a full conceptual crest model was built based on the geometry and major features (including fenestrae) of the *Sinosaurus* crest.

A simple two-step strategy was used to study the crest based on those available samples and data. The incomplete crest ZLJT01 was modeled and its mechanical characteristics were investigated under different external loads. Based on these results, an idealized complete crest model based on LDM-L10 was built on the original data of LDM-L10, but rescaled to fit the actual length, height and width of ZLJT01. This complete model was treated as an idealized model of the actual full *Sinosaurus* crest. A series of external loads were applied to outline potential patterns of deformation.

The complete crest model was scaled to ensure that its height and length matched the measurements of a full *Sinosaurus* crest model. For comparison, a counterexample model of the crest was constructed without cavities.

Local structural features of the skull where the crest connects to it must be considered. The full crest model was mounted on a skull with major cranial cavities, including a nasal and an antorbital fenestra. Other regions of the skull were considered as a solid body, and their deformation was not assessed in the following computational experiments. The areas at the bottom of the conceptual

skull model were simply fixed in their spatial locations.

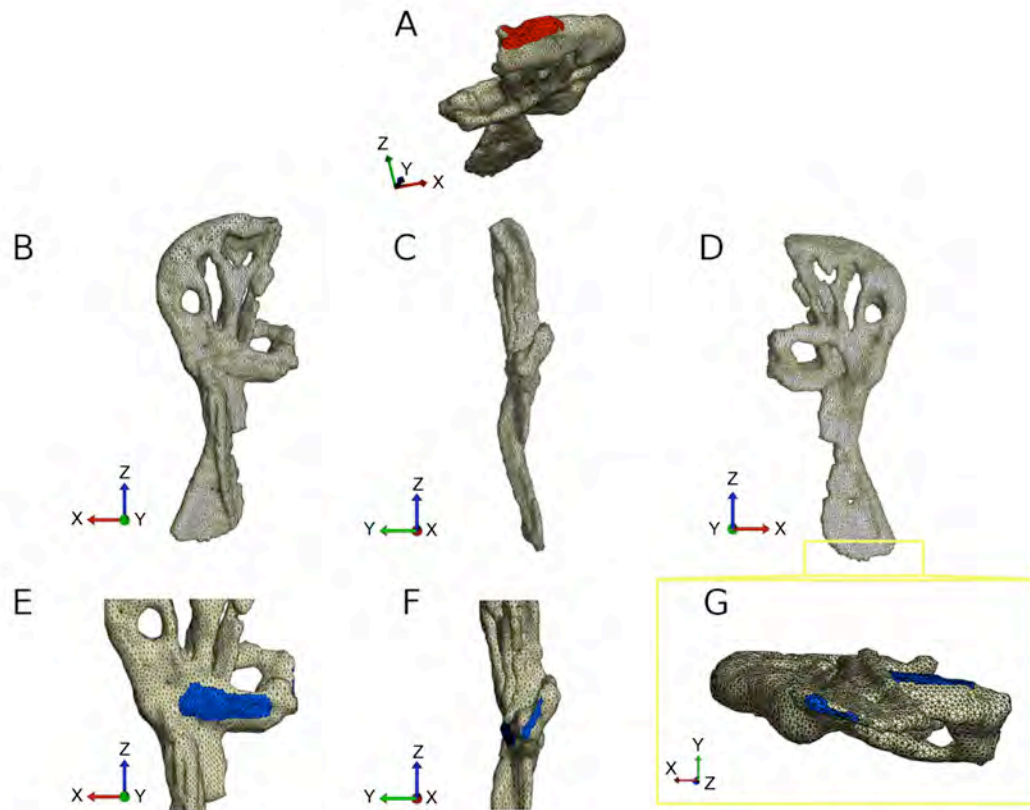
Febio 1.4 (<http://mrl.sci.utah.edu/febio-overview>) was used to solve the deformation of the crest model. It has been extensively used to compare biomechanical problems, and has been extensively applied in orthopedic research, such as the cartilage contact problem in normal human hips (Harris *et al.*, 2011). This open-source software is developed and maintained by Musculoskeletal Research Laboratories (MRL) at University of Utah.

## **5.5 Simulations and Results**

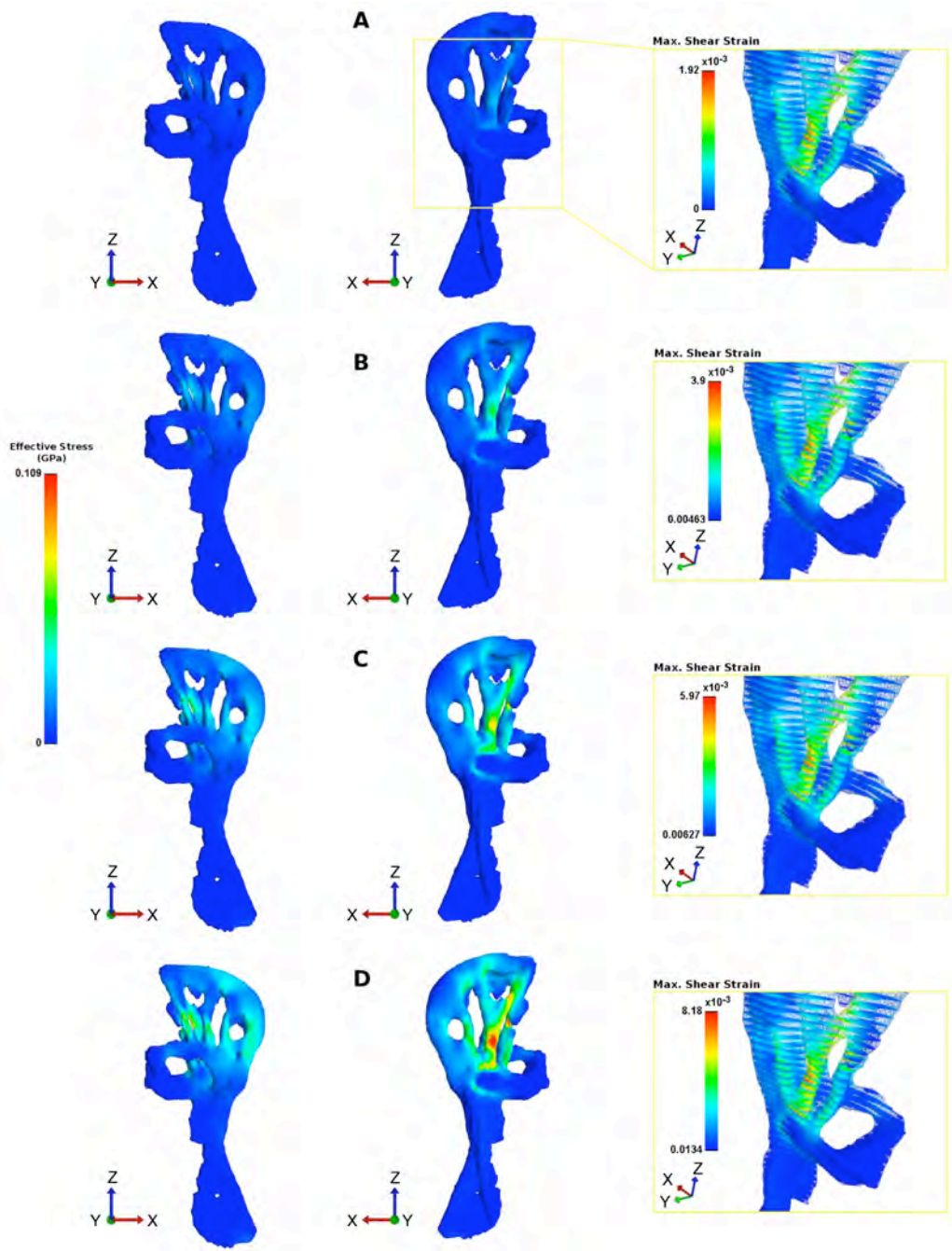
### **5.5.1 Sample Model**

Fig. 5.2 shows an overall view of the sample model that was built directly through CT image data. A directional external load (traction vector) along the Z-axis was directly applied on the top contact area (Fig. 5.2A), with four levels of magnitude (1000N, 2000N, 3000N and 4000N). This contact area was approximately 438.82 mm<sup>2</sup>; the loading pressure was about 2.2788MPa, 4.558MPa, 6.837MPa and 9.115MPa to 1000N, 2000N, 3000N and 4000N, respectively.

Fig. 5.2 (E), (F) and (G) depicts another set of boundary conditions, on which those spatial locations of selected areas are fixed, and where they are supposed to connect with the anterior crests and main parts of the skull. The results corresponding to different levels of loads are demonstrated in Fig. 5.3.



**FIGURE 5.2.** A, B, C, D show overall views of the FE crest model. C is anterior and B and D are left lateral and right lateral views, respectively. A indicates the loading areas coloured as red; the blue area in E, F and G represents the spatially fixed boundary. Red, green and blue arrows represent x, y and z directions.



**FIGURE 5.3.** Deformations of the crest model corresponding to 1000N (A), 2000N (B), 3000N (C) and 4000N (D) loading.

In general, effective stress (von Mises stress) and maximum shear strains on both left and right sides increased with the raising of external loading. The colour distributions (Fig. 3) on both sides show different configurations. The overall colours on the lateral side show a larger area with warmer colour compared with the left medial side. The hot area, which indicates a large stress, mostly concentrates in the middle part of the crest model. The top region of the crest has a cooler area in stress distribution maps; however, it has a large total displacement. In the cases of 1000N, 2000N, 3000N and 4000N loading, the maximum total displacement is 0.6427mm, 1.331mm, 2.068mm and 2.859mm comparing average displacement 0.1193mm, 0.2478mm, 0.3863mm and 0.536mm, respectively. These are displacements of the entire structure; displacement is much lower between localized regions, but strain is high. In summary, the top of the crest performs like a large rigid body with motion towards the lateral side, whereas the lower middle part provides a supporting structure for the entire deformation processing.

Note that the material failure is caused by, in most cases, shear strain in a linear context. The shear strains in four testing cases exhibit similar patterns, in which the bony part around the cavities of the crest possessed an area with higher magnitude of shear strain, compared to other regions. The maximum shear strains increased from 0.0028 to 0.01181 with raising the loading from 1000N to 4000N. Bone breaks at 0.2–0.6% strain, and failure is likely to have occurred under higher loadings.

### 5.5.2 Full Scale Model

Three loading areas had been selected (the front, middle and back) to perform the sensitivity analyses with the different loading scenarios. Three directional loadings, including  $(1, 0, -1)$ ,  $(0, 0, -1)$  and  $(-1, 0, -1)$ , had been applied on these selected (front, middle and back) areas, respectively, with magnitudes of 0.009115 GPa and 0.01823 GPa. These vectors are defined in accordance with the coordinate system used here, that x, y and z axes are the anterior–posterior, medial–lateral and superior–inferior directions, respectively (Fig. 5.4). The case of applying force from  $(1, 0, -1)$  direction on the front area attempts to recreate the force directly applied on the anterior part of crest.

Assuming that *Sinosaurus* would lower the skull to a certain degree when loading the crest, a  $45^\circ$  direction was chosen for loading orientation. The vertical loading from  $(0, 0, -1)$  on the middle selected area reproduces the case of the weight load directly applied on top of the skull (crest), and the back loading testing, a force direction  $(-1, 0, -1)$ , is an attempt to investigate the deformation of the posterior part of the crest in a case of loading from the back.

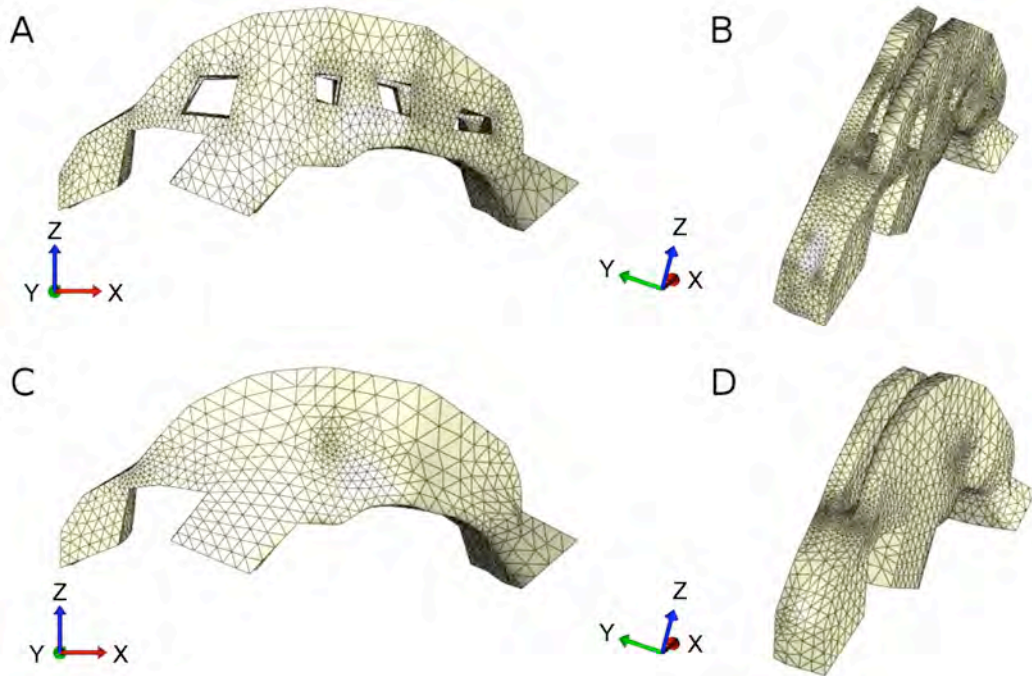


**FIGURE 5.4.** Subfigures A and B show the conceptual full scale crest model of the *Sinosaurus* crests; C and D demonstrate a solid body model used for comparisons. The x axis is in the anterior–posterior direction, where + x is anterior. Subfigures A and C therefore show the lateral direction of two full crest models. Red, green and blue arrows represent x, y and z directions.

Throughout all three loading areas tested (Fig. 5.5), the stresses on the full crest model with cavities shows a consistent colour distribution, with higher stress concentrated on areas around the cavities. The increasing loading pressure produces a slightly higher stress represented by warmer colour; average effective stresses were 0.0177 Gpa, 0.01086 Gpa and 0.01838 Gpa in the front, middle and back loading testing under the pressure of 0.01823 Gpa. The counterexample of the full crest model (Fig. 6), however, showed a cooler colour distribution that indicates a smaller stress than in the full crest model with cavities. The average effective stresses of the same three loads reached 0.01236 GPa, 0.005705 GPa and 0.0135 GPa. In short, in all three different loading tests, the stress patterns on the crest model without cavities shows less concentration compared with the crest model with cavities.

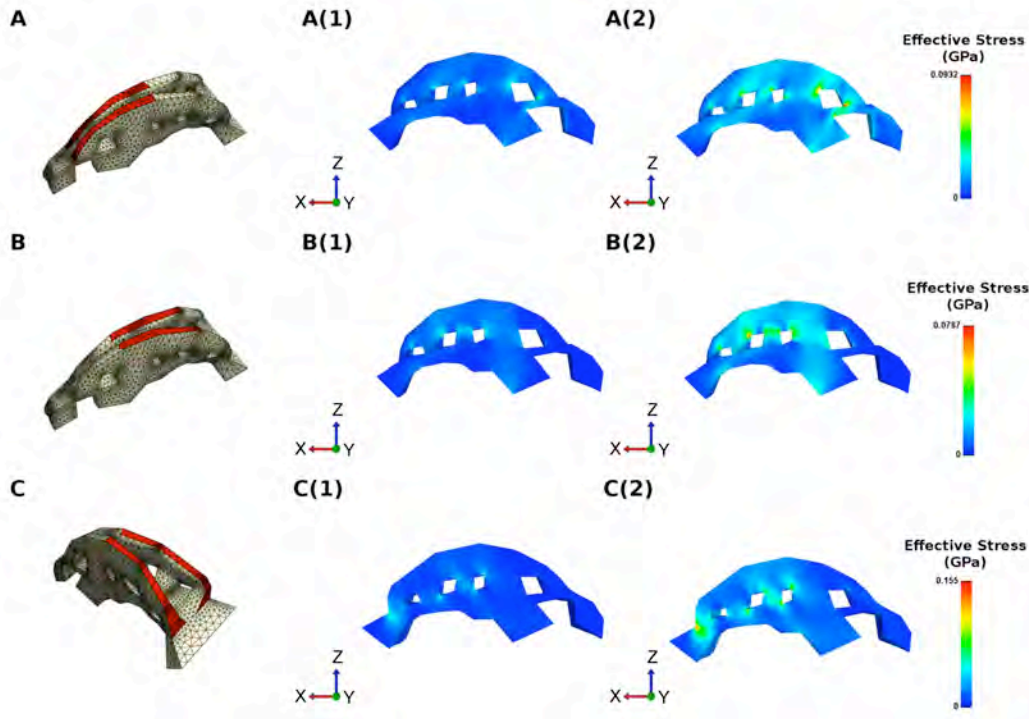


**FIGURE 5.5.** A, B and C depict the front, middle and back loading areas on the full crest model with cavities; the middle and third columns depict the effective stress distribution corresponding to the loading magnitude of 0.009115 GPa and 0.01823 GPa.

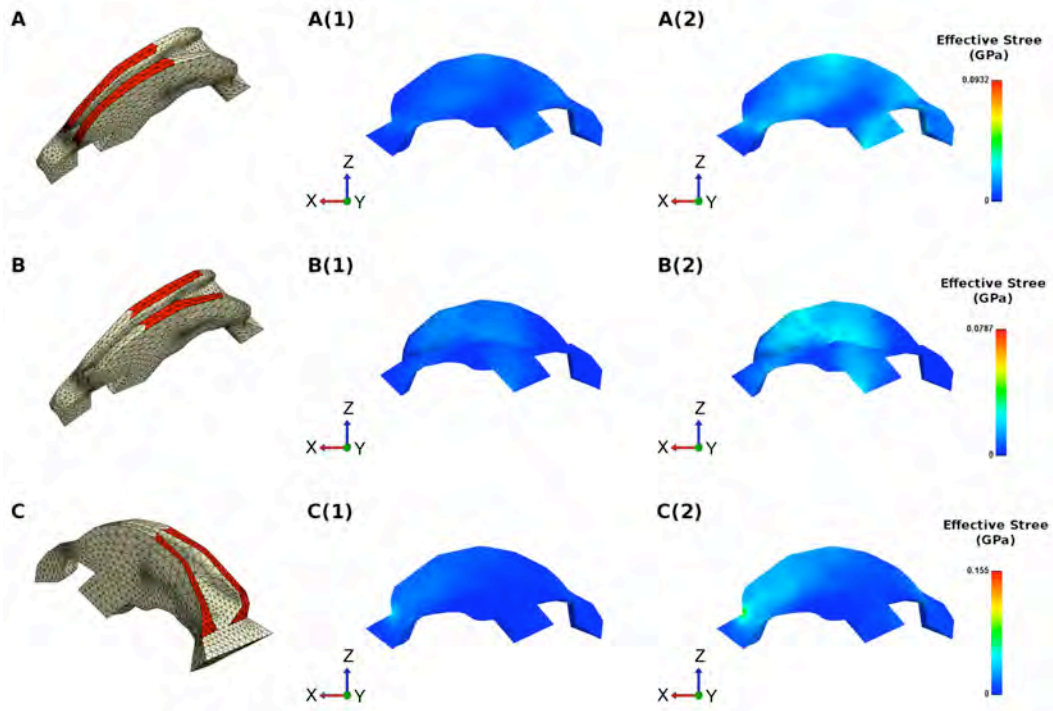


**FIGURE 5.6.** Case study of different loading areas on the counterexample model without crest cavities. The second and third columns shows the stress distribution under the loads with magnitudes of 0.006415 GPa and 0.01283 GPa.

The increased magnitude of loading stimulated the magnitudes of effective stress but does not fundamentally change stress patterns in either model. The model with cavities under smaller pressure (0.009115 GPa) showed a similar pattern as observed in the case of 0.01823 GPa. The peak stress was certainly reduced. The peak stress of 0.1325 GPa, 0.1039 GPa and 0.1788 GPa were reduced to 0.06702 GPa, 0.05183 GPa and 0.08881 GPa, respectively, in the case of directional pressure of 0.009115 GPa.

The stress is driven by the deformation in which the superior part was bent towards the right or left direction. This is similar to the case of the fossil sample model. In the front loading test of the full crest model with cavities, the peak total displacement of the crest is 0.4292 mm and 0.872 mm, corresponding to the pressures 0.009115 GPa and 0.01823 GPa, whereas the back area loading bends the left posterior crest towards the lateral left direction with the peak total displacements of 0.6071 mm and 1.2515 mm in the case of 0.009115 GPa and 0.01823 GPa, respectively. The crest in general deforms toward the lateral (left and right) directions under middle area load, with the peak displacements of 0.3582 mm (0.009115 GPa) and 0.7412 mm (0.01823 GPa). Under the same conditions, the deformations of the crest model without cavities produced similar results, with the peak total displacements of 0.9935 mm, 0.7775 mm and 1.177 mm.

## **5.6 Discussion**

A model-based study has been presented here to investigate possible

mechanical characteristics of the *Sinosaurus* crest under superior surface loading conditions, including different applied directions and stress magnitudes. The load testing on a fossil sample model reproduced a deformation pattern corresponding to three linearly increased vertical loads, each applied to the same limited selected area. The effective stress distributions show that the stresses were slightly higher on the areas that form the cavities. In general, the superior part of crest was moving towards the lateral (right) direction; however, the lower part was bending more along superior–inferior directions. Importantly, the shear strain (shear stress) shows slightly higher values on this area than in other regions throughout all case studies with such models. Note that the computational experiments did not introduce any of the fracturing conditions for this bony material, because no clear evidence or study can be directly adapted. Shear strain may be seen as a representation of bone fracture, a higher shear strain may create a higher chance of material failure. Peak strains were high enough in the model for the bone to fail, especially under 2000–4000 N loads. Questions arise of a more comprehensive role of the cavities in the bone and stress on those areas, and (most importantly) whether a more complete model would result in strains below failure levels.

The sample crest model here merely represents a partial and incomplete part of the original full crest. The anterior surface of the modeled crest connected to the anterior part of original crest, and restricted the movement of the material points around this region, unlike the freely moveable conditions in this study. In other words, the boundary conditions and the model were insufficient to represent the real situation from the perspective of mechanical analysis. Furthermore, the

loading only applied on the initially selected top areas along with a fixed direction (z axis). In a real situation, the loading may have come from other directions. Consequently, a fixed directional load may not provide a deeper insight of deformation patterns under various loading conditions.

The conceptual full crest model was built to reflect the major features of the crest geometry and structure (including cavities), and a counterexample model was constructed to provide information about what a crest does when it has cavities in it. Complex loads were applied to three selected areas with varying directional loads (traction vectors). This objective of this computational experiment was to reproduce a possible deformation pattern under a true scenario, or a close mathematical approximation.

The computational results from these case studies clearly showed that the effective stresses on the areas around the cavities were slightly higher than other regions; and the results from counterexample exhibits a dramatically different pattern, in which stress distributions were more average. It seems that the columnar-like parts have to sustain more energy than remaining regions, implying higher chances of bone fracture within struts.

Limitations to the full crest models obviously exist. The models lack full interior and structural details of the skull, the generated stress distributions may not be valid in these areas, and as a consequence, the potential influence on the rest of the skull remains unknown. Furthermore, the deformations produced by the superior directional loads cannot reveal the stress patterns produced by medial-lateral loading. Therefore, the results shown here can be considered valid under

the conditions of vertical loads on superior regions of the crests. Furthermore, the material parameters used here are only based on assumption, and a further investigation of sensitivity to parameter value is also highly recommended.

In addition, the superior surface contacts on *Sinosaurus* may not truly reflect other possible applications. More precisely, the loading conditions applied in computational experiments lack the consideration of effect of shear stress between the dermis and bone. In reality, the integument covered the surface of crest would have also sealed the cavities. Those soft tissues can be largely deformed (strain greater than 5%) and absorb more energy than bone. Simulations of soft tissue/bone shear under impacts are amenable to methods used to examine dog vessel deformation under the shear stress of blood flow (Kamiya and Togawa 1980).

In summary, the experimental deformations in the incomplete *Sinosaurus triassicus* (ZLJT01) crest suggest that loads on the superior surface of the crest can yield slightly higher shear stress around areas surrounding the cavities in the crest. Similar results were observed on the cavities of the full-scale *Sinosaurus triassicus* (LDM-L10) crests, and the areas around the cavities have significant higher effective stresses that imply a higher chance of material failure. Therefore, the structure of a *Sinosaurus triassicus* crest may limit the ability of the crest from taking external loads because increased shear strain and effective stress around the cavities would result in fractures. These experimental results support the suggestion that *Sinosaurus triassicus* crests probably cannot serve as weapons for intraspecific combat. Similar hypotheses (based on skeleton morphology) were

also brought forward by Tykoski and Rowe (2004) for *Dilophosaurus wetherilli*.

Moreover, because *Sinosaurus triassicus* crests were hollow and pneumatic, and probably had connections with the nasal cavities, they may have functioned as resonating chambers for the alteration and amplification of sounds produced in the throat; this feature is similar with the Middle Jurassic *Monolophosaurus* from China (Currie, 1999).

### **5.7. Future Research**

Despite the existing limitations, this study gives insightful understanding of the structural characteristics of a crest. Results indicate that the *Sinosaurus* crest did not function to support vertical loading on the superior surface of the crest. This bony structure, especially those regions around the cavities, sustained high tension, which implies a high potential of material failure. In other words, such structures cannot provide benefits for any activities involving direct superior surface contacts. However, the results do not preclude the use of *Sinosaurus* crests under other mechanical structural purposes.

In future, research of this nature will focus on constructing a full crest model from true fossil data with fine interior and structural details and features. Direct contact simulation within the skull, including the crest, and the addition of soft tissue and other bones, can also extend the model of the crest. Skull deformation can also be tested under different circumstances. Importantly, the shear stress on this crest structure, especially its soft tissue layer, needs to be investigated through a common engineering (fluid–solid interaction) approach.

## References

- Arbour VM, Snively E. 2009. Finite element analyses of ankylosaurid dinosaur tail club impacts. *The Anatomical Record* 292: 1412–1426.
- Arbour VM. 2009. Estimating impact forces of tail club strikes by ankylosaurid dinosaurs. *PLoS ONE* e6738.
- Bonet J, Wood RD. 2008. Nonlinear continuum mechanics for finite element analysis. *Communications in Numerical Methods in Engineering* 24(11): 1567–1568.
- Bonaparte JF, Novas FE, Coria RA. 1990. *Carnotaurus sastrei* Bonaparte, the horned, lightly built carnosaur from the middle Cretaceous of Patagonia. *Contributions in Science, Natural History Museum of Los Angeles County* 416: 1–42.
- Clark JM, Norell MA, Barsbold R. 2001. Two new oviraptorids (Theropoda: Oviraptorosauria), Upper Cretaceous Djadokhta Formation, Ukhaa Tolgod, Mongolia. *Journal of Vertebrate Paleontology* 21(2): 209–213
- Coria RA, Currie PJ. 2006. A new carcharodontosaurid (Dinosauria, Theropoda) from the Upper Cretaceous of Argentina. *Geodiversitas* 28 (1): 71–118.

- Cotton JR, Winwood K, Zioupos P, Taylor M. 2005, Damage rate is a predictor of fatigue life and creep strain rate in tensile fatigue of human cortical bone samples. *Journal of Biomechanical Engineering* 127: 213–219.
- Currie PJ, Eberth DA. 2010. On gregarious behavior in *Albertosaurus*. *Canadian Journal of Earth Sciences* 47: 1277–1289.
- Currie PJ, Xing LD, Wu XC, Dong, ZM. In progress. Anatomy and relationships of *Sinosaurus triassicus* (“*Dilophosaurus sinensis*”) from the Lufeng Formation (Lower Jurassic) of Yunnan, China.
- Dong ZM. 2003. Contributions of new dinosaur materials from China to dinosaurology. *Memoir of the Fukui Prefectural Dinosaur Museum* 2: 123–131.
- Fernandez JW, Mithraratne P, Thrupp SF, Tawhai MH, Hunter PJ. 2004. Anatomically based geometric modelling of the musculo–skeletal system and other organs. *Biomechanics and Modeling in Mechanobiology* 2(3): 139–155.
- Gay R. 2005. Sexual dimorphism in the early Jurassic theropod dinosaur *Dilophosaurus* and a comparison with other related forms. In: Carpenter K, editor. *The carnivorous dinosaurs*. Indiana University Press, Bloomington. 277–28.

Harris MD, Anderson AE, Henak CR, Ellis BJ, Peters CL, Weiss JA. 2011, Finite element prediction of cartilage contact stresses in normal human hips. *Journal of Orthopaedic Research*, doi: 10.1002/jor.22040.

Holzappel GA. 2000. *Nonlinear Solid Mechanics. A Continuum Approach for Engineering*. John Wiley & Sons, Inc. Chichester. 1–455.

Hone D, Naish D, Cuthill I. 2011. Does mutual sexual selection explain the evolution of head crests in pterosaurs and dinosaurs? *Lethaia* doi: 10.1111/j.1502–3931.2011.00300.x

Kabel J, Van Rietbergen B, Odgaard A, Huiskes R. 1999. Constitutive relationships of fabric, density, and elastic properties in cancellous bone architecture. *Bone*, 25(4): 481–486.

Kamiya A, Togawa T. 1980. Adaptive regulation of wall shear stress to flow change in the canine carotid artery. *American Journal of Physiology–Heart and Circulatory Physiology*, 239(1): 14–21.

Krajcinovic D, Trafimow J, Sumarac D. 1987. Simple constitutive model for a cortical bone. *Journal of Biomechanics* 20(8): 779–784.

Madsen JH Jr. 1976, *Allosaurus fragilis*: a revised osteology. Utah Geological and Mineralogical. Survey Bulletin 109: 1–163.

Padian P, Horner JR. 2011. The evolution of ‘bizarre structures’ in dinosaurs: biomechanics, sexual selection, social selection or species recognition?.  
Journal of Zoology 283: 3–17.

Pesce Delfino V, De Marzo C, Prete A, Stucci N. 1981. Biomechanical simulation model of the developmental morphology of the human skull. Further observations on the model construction. Bollettino Della Societa Italiana Di Biologia Sperimentale 57(20): 2011–2017.

Rayfield EJ, Norman DB, Horner CC, Horner JR, Smith PM, Thomason JJ, Upchurch P. 2001. Cranial design and function in a large theropod dinosaur.  
Nature 409(6823): 1033–1037.

Rayfield, EJ. 2005. Using finite–element analysis to investigate suture morphology: a case study using large carnivorous dinosaurs. The Anatomical Record Part A Discoveries in molecular cellular and evolutionary biology, 283(2): 349–365.

Snively E, Theodor JM, 2011 Common functional correlates of head–strike behavior in the pachycephalosaur *Stegoceras validum* (Ornithischia,

- Dinosauria) and combative artiodactyls. PLoS ONE 6(6): e21422.
- Snively E, Cox A. 2008. Structural mechanics of pachycephalosaur crania permitted head-butting behavior. *Palaeontologica Electronica* 11(1); 3A: 17.
- Tykoski RS, Rowe T. 2004. Ceratosauria. In: Weishampel DB, Dodson P, Osmolska H, editors. *The Dinosauria*. Berkeley (CA): University of California Press. 47–70.
- Welles SP. 1984: *Dilophosaurus wetherilli* (Dinosauria, Theropoda). Osteology and comparisons. *Palaeontographica A* 185: 85–180.
- Xing LD, Ye Y, Shu CK, Peng GZ, You HL. 2009. Structure, orientation and finite element analysis of the tail club of *Mamenchisaurus hochuanensis*. *Acta Geologica Sinica (English edition)*, 83(6): 1031–1040.
- Zhao XJ, Currie PJ. 1993. A large crested theropod from the Jurassic of Xinjiang, People's Republic of China. *Canadian Journal of Earth Sciences* 30: 2027–2036.

## CHAPTER 6

### The fourth *Sinosaurus triassicus* from the Lufeng Basin of China, and reflections on the paleoecology of *Sinosaurus*

#### 6.1 Introduction

In 2006, a Japanese paleontologist (Dr. Sekiya Toru) discovered the fourth dilophosaurid specimen (ZLJ0003) from the Lufeng Formation at Konglong Hill, Dawa Village Committees, Jinshan Township, Lufeng County, Yunnan, China.

Konglong Hill was the source of a number of *Lufengosaurus* specimens (Young, 1941, 1947), but ZLJ0003 represents the front of a skull and a nearly complete postcranial skeleton of *Sinosaurus triassicus*. This skull was not completely prepared, but was incorporated as part of a composite skull and put on display (Fig. 6.1). The postcranial skeleton was mounted with the skull of LDM-L10, and then put on display in the China Science and Technology Museum, Beijing, in 2009.

For security reasons, the postcranial skeleton of ZLJ0003 cannot be moved and measured; the author negotiated for an exemption from these security measures for years, but in vain. Furthermore, when the incomplete skull was assembled, the right and left maxillae were mistakenly reversed. This resulted in the medial surfaces of the maxillae being exposed on the lateral surfaces of the composite skull, whereas the lateral surfaces of the maxillae are turned inward on the composite skull and are partially covered by the iron supports of the mounted

skeleton (Fig. 6.1). Even so, this specimen (ZLJ0003) still provides interesting and new morphologic information about *Sinosaurus triassicus*.



**FIGURE 6.1.** *Sinosaurus triassicus* (ZLJ0003) skull display in the World Dinosaur Valley Park, Yunnan Province, China. Scale bar = 10 cm.

## 6.2 Maxilla

Both maxillae are preserved in ZLJ0003; the right maxilla is 35 cm long (Figs. 6.2A, 6.3) and the left is 33.5 cm long. The anteromedial portion of the left maxilla was seriously deformed, due to post-depositional conditions (Figs. 6.2B, 6.4). Only the medial anterior portion of the right maxilla is preserved. In overall form, this maxilla is similar to that of *Sinosaurus triassicus* (LDM-L10, Currie et al., in progress, Fig. 6.5). Because of the lack of fine preparation, the margin of the antorbital fossa is indistinct, and the fossil seems to be lacking any opening on the maxilla anterior to the antorbital fenestra within the anterior region of the antorbital fossa.

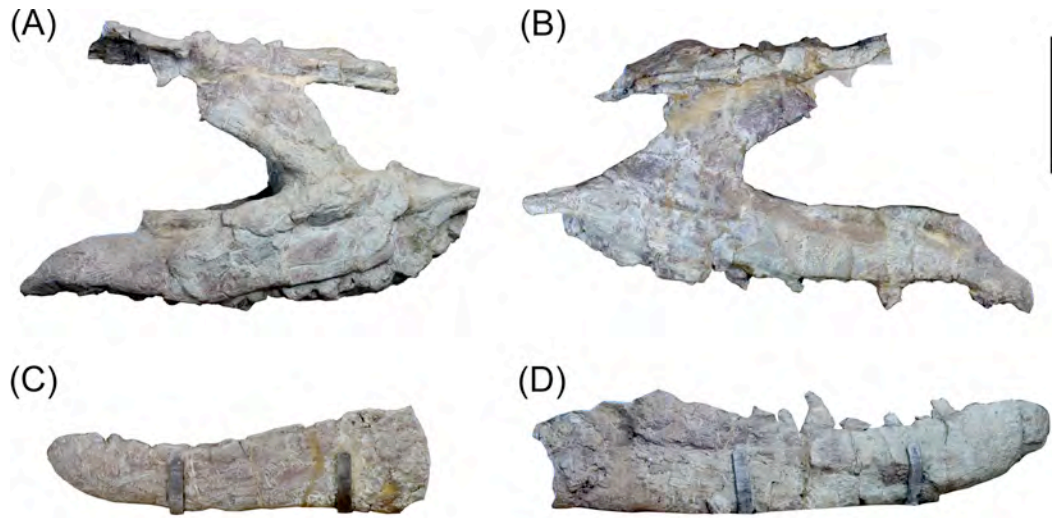


**FIGURE 6.2.** *Sinosaurus triassicus* (ZLJ0003). Left maxilla (A) and right maxilla (B) in medial views; left (C) and right (D) dentaries in lateral views. Scale bar = 10 cm.

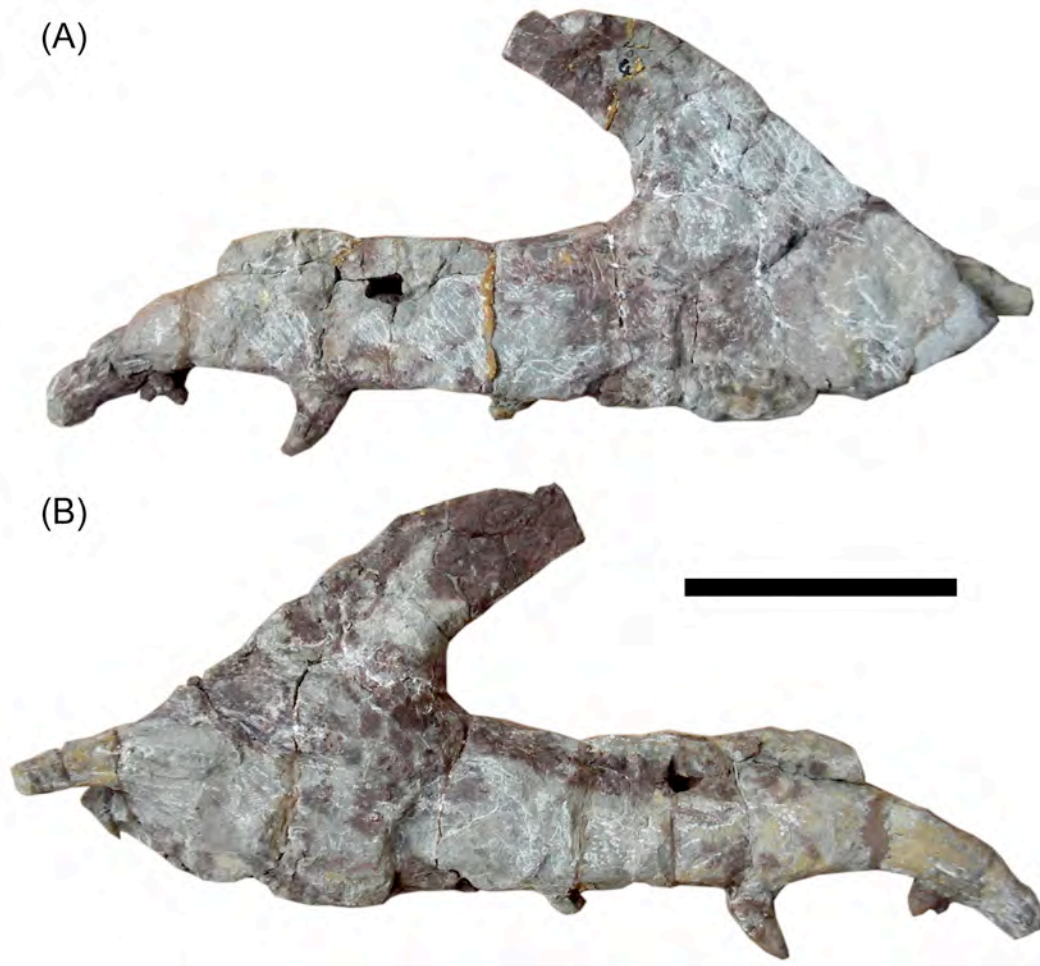


**FIGURE 6.3.** *Sinosaurus triassicus* (ZLJ0003) Right maxilla in lateral (A) and medial (B) views. Scale bar = 10 cm.



**FIGURE 6.4.** *Sinosaurus triassicus* (ZLJ0003). Left maxilla in medial view, plus portion of the base of the nasal-lacrima crest. Scale bar = 10 cm.



**FIGURE 6.5.** Right maxilla of *Sinosaurus triassicus* (ZLJ0003) shown overlapping one of the skulls of *Sinosaurus triassicus* (LDM-L10). Scale bar = 10 cm.

In ZLJ0003, the anterior margin of the maxilla is inclined posteriorly at a relatively lower angle from the horizontal than in LDM–L10 and other *Sinosaurus* specimens. ZLJ0003 is more similar to *Dilophosaurus wetherilli* (UCMP 37303; Welles, 1984) in this respect, which is an interesting characteristic. Because the anterior margin of the maxilla is at a lower angle, the teeth are inclined anteriorly. This has been cited as an adaptation for piscivory in *Spinosaurus* (Dal Sasso et al., 2005). The anteromedial process of the maxilla is distinct, 4.6 cm long, but is poorly prepared, without any discernible suture and slot. The left maxilla probably preserves a jugal suture, but it is deformed and bent downwards.

The alveoli are weathered, but there seem to have been 13 maxillary tooth positions in ZLJ0003 (Fig. 6). This is the same number as in KMV 8701, LDM–L10 and ZLJT01.



**FIGURE 6.6.** *Sinosaurus triassicus* (ZLJ0003). Left maxilla in ventral view (A).

The red circles indicate alveoli (B). Scale bar = 10 cm.

### 6.3 The crest base

The paired crests in *Dilophosaurus* and *Sinosaurus* are formed by the nasals anteriorly, and the lacrimals posteriorly (Currie et al., in progress). ZLJ0003 has partially preserved nasals and lacrimals. The damaged surfaces are rough, with bony prominences of variable sizes, which were interpreted as representing incomplete teeth when excavated. By comparison with the damaged right crest of LDM-L10, these bony prominences can be interpreted as the base of the crest of ZLJ0003. In dorsal view (Fig. 7), these bony prominences are discontinuous, with irregular intervals, which implies that the crest of ZLJ0003 possessed a number of mediolateral depressions (or openings). However, the thin walls of the depressions were lost, and only the bases of the thicker support struts were preserved.



**FIGURE 6.7.** Naso-lacrimal crests of *Sinosaurus triassicus* (ZLJ0003) in dorsal view (A). The region between the yellow lines is formed by the resin reconstruction done by the local museum (B). Scale bar = 10 cm.

#### **6.4 Lower jaws**

The lower jaws are crushed and only the largely fragmentary left and right dentaries are preserved (Figs. 6.2C, D, 6.8, 6.9). The left dentary is 32.1 cm long, with a maximum depth of 8.6 cm (Figs. 6.2C, 6.8); the right dentary is 42.3 cm long, with a maximum depth of 9.1 cm (Figs. 6.2D, 6.9).

The Meckelian groove is shallow as in all theropods except troodontids (Currie, 1987). A Meckelian foramen is on the lingual surface of the bone at the anterior end of the Meckelian groove. In ZLJ0003, the Meckelian groove is distinct but shallower than in ZLJT01, which could be the result of incomplete preparation. Likewise, the foramen for the inferior branch of the alveolar nerve is unexposed because of incomplete preparation. Some anterior portions of the surangular and angular are probably preserved, but do not present any valuable characteristics. The margins of the external mandibular fenestra are not visible. The dentary appears to have 13 alveolar positions, which is the same as in KMV 8701 (Hu, 1993) and ZLJT01.



**FIGURE 6.8.** *Sinosaurus triassicus* (ZLJ0003). Left dentary in lateral (A) and medial (B) views. Scale bar = 10 cm.



**FIGURE 6.9.** *Sinosaurus triassicus* (ZLJ0003). Right dentary in lateral (A) and medial (B) views. Scale bar = 10 cm.

## 6.5 Discussion

Because of the lack of sufficient characteristics, specimen ZLJ0003 was not included in the analysis of phylogenetic systematics of *Sinosaurus triassicus* (Chapter 3). However, the size, base of the crest and the number of alveoli, all suggest that the specimen represents *Sinosaurus*. Furthermore, ZLJ0003 was excavated from a site close to the *Sinosaurus triassicus* specimens IVPP V34 and LDM–L10 (distance approximately one kilometer).

*Sinosaurus* was at the top trophic level of the Lufeng food chain. As such, it was the most common large theropod in the Lufeng Formation, accounting for 56% of theropod specimens recovered (Table 6.1). However, this figure is less than that of a similar sized predator, *Allosaurus fragilis* in proportion to Morrison Formation theropods (70 to 75% according to Foster, 2007).

**TABLE 6.1** Numbers of recovered specimens of Theropoda (and a carnivorous crocodylomorph) from the Lufeng Formation.

Carnivorous species	Numbers
<i>Sinosaurus triassicus</i> (Young, 1948; Hu, 1993)	5
<i>Megapnosaurus</i> sp. (Irmis, 2004)	1
<i>Eshanosaurus deguchiiianus</i> (Xu, 2001)	1
<i>Lukousaurus yini</i> (Young, 1948)*	1
An unnamed small-sized Coelophysoidea	1

\**Lukousaurus* is likely a crocodylomorph (Irmis, 2004)

The Lufeng Formation is interpreted as having been deposited on a piedmont plain, lake or fluvial environment (Luo and Wu, 1995). The lower part of the Lufeng Formation is considered to represent shallow lacustrine sediments (Tan, 1997).

Palynological research indicates that the Lufeng Basin was dominated by gymnosperms, with abundant ferns. The forests were luxuriant, dominated by conifers, mixed with nearby cedars. Lygodiaceae and Lycopodiaceae ferns were present on the coniferous forest floor, or at the edges of the woods (Wei et al., 2001).

The Lufeng Basin is a rich source of vertebrate fossils that contains abundant dinosaur remains (see Chapter 1). Numerous fossils of other vertebrate taxa are also found in the basin, including Amphibia (*Labyrinthodontia* indet., Sun, 1962), Pseudosuchia (*Dibothrosuchus elaphros* and *Strigosuchus licinus*, Simmons, 1965), Phytosauria (*Pachysuchus imperfectus*, Young, 1951), Protosuchia (*Dianosuchus chanchiawaensis*, Young, 1982), Lacertilia (*Fulengia youngi*, Carroll and Galton, 1977), Mammaliaformes, (*Hadrocodium*, Luo et al., 2001), and Therapsida (*Lufengia delicate*, Chow and Hu, 1959, and *Dianzhongia longirostrata*, Cui, 1981). The theropods included large (4–6 m) *Sinosaurus*, and smaller (1–2m) *Lukousaurus* as well as an unnamed coelophysoid that would have occupied different ecological niches.

Some ichnites seem to indicate that dilophosaurids might swim and feed on fish, of which the most famous fossil evidence is the St. George Dinosaur Discovery Site (Milner et al., 2006). Except for an unpublished *Lepidotes* (Dong

Z.M., pers. comm.), fish fossils have never been recovered from the Lower Jurassic Lufeng Basin so far (Chen and Chui, 1989). However, bivalves (*Sibireconcha–Unio* association) are known (Zhang, 1995), indicating that the local aquatic environment was probably productive. Therefore, it is conceivable that *Sinosaurus* might have fed on fish.

More direct evidence is the association of fossils of *Sinosaurus* and the prosauropod *Yunnanosaurus* in the Lufeng Basin. Not only was the latter discovered in association with almost all *Sinosaurus* sites, but also one specimen of *Sinosaurus* (KMV 8701) was found in the same quarry with a specimen of *Yunnanosaurus* (Dong, 2003). Unfortunately, no quarry map was done when the local museum excavating the fossils, and the only evidence is a single photograph showing the quarry (Fig. 6.10). According to the witnesses, the skull of the *Sinosaurus* was found close to the tail of the *Yunnanosaurus*. This evidence suggests that *Sinosaurus* may have hunted, or at least scavenged, the prosauropod.



**FIGURE 6.10.** *Sinosaurus triassicus* (KMV 8701) and *Yunnanosaurus* found in the same quarry (Dong, 2003).

The right occipital condyle of *Sinosaurus* specimen LDM-L10 was recovered with a theropod tooth inserted into it (Fig. 6.11). The crown base length and crown base width of the embedded tooth are 11 mm and 4.5 mm, respectively. The crown base ratio (CBR) is 0.41, which is close to the CBR value of teeth of other *Sinosaurus* specimens (0.46, see Chapter 1.3.3). As *Sinosaurus* is the only large theropod known from the area, the most likely explanation is that it was feeding on other members of its own species, representing evidence for theropod cannibalism. More detailed information will probably be available with further preparation of the occiput of LDM-L10.

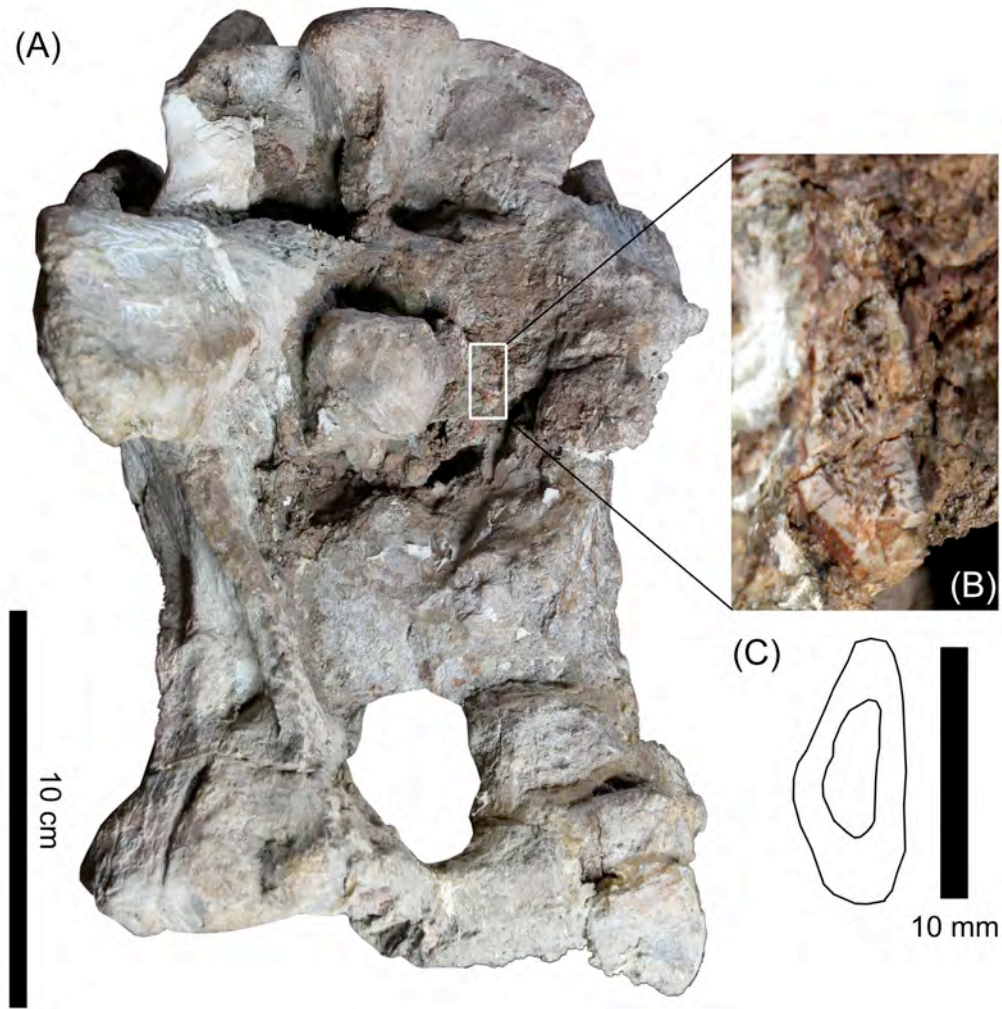


**FIGURE 6.11.** Braincase of *Sinosaurus triassicus* (LDM-L10) in occipital view (A); close-up of cross-section of tooth (B) and outline drawing (C).

Currently, the best evidence of theropod cannibalism is associated with *Majungasaurus* from the Late Cretaceous of Madagascar (Rogers et al., 2007), and *Tyrannosaurus* from the Late Cretaceous of North America (Longrich et al., 2010). More controversial evidence for cannibalism relates to the Late Triassic *Coelophysis* (Nesbitt et al., 2006) and the Late Cretaceous *Deinonychus* (Roach et al., 2007). As for *Majungasaurus*, it is unknown if *Sinosaurus* actively hunted their own kind or only scavenged their carcasses. In the extant Komodo Dragon (*Varanus komodoensis*), cannibalism occurs over violently contested prey carcasses, with the winner finally feeding on the dead body of its congener (Auffenberg, 1981; Roach et al., 2007). Similar behavior may have led to cannibalism in *Majungasaurus* and other theropods.

## References

- Auffenberg W. 1981. The Behavioral Ecology of the Komodo Monitor.  
University Presses of Florida. Gainesville. 1–406.
- Carroll RL, Galton PM. 1977. Modern lizard from the Upper Triassic of China.  
*Nature*, 266, 5599: 252–255.
- Chen YR, Chui GH. 1989. Review of Yunnan fish fossils. *Sichuan Journal of Zoology* 8(1): 27–29.
- Chow MC, Hu CZ. 1959. A new genus of tritylodontid from Lufeng, Yunnan.  
*Vertebrata Palasiatica* 1(1): 7–10.
- Cui GH. 1981. A new genus of tritylodontid. *Vertebrata Palasiatica* 14(1): 7–10.
- Currie PJ. 1987. Bird-like characteristics of the jaws and teeth of troodontid theropods (Dinosauria: Saurischia). *Journal of Vertebrate Paleontology* 7: 72–81.
- Currie PJ, Xing LD, Wu XC, Dong, ZM. In progress. Anatomy and relationships of *Sinosaurus triassicus* (“*Dilophosaurus sinensis*”) from the Lufeng Formation (Lower Jurassic) of Yunnan, China.

- Dal Sasso C, Maganuco S, Buffetaut E, Mendez MA. 2005. New information on the skull of the enigmatic theropod *Spinosaurus*, with remarks on its sizes and affinities. *Journal of Vertebrate Paleontology* 25 (4): 888–896.
- Dong ZM. 2003. Contributions of new dinosaur materials from China to dinosaurology. *Memoir of the Fukui Prefectural Dinosaur Museum* 2: 123–131.
- Foster J. 2007. *Allosaurus fragilis*. *Jurassic West: The Dinosaurs of the Morrison Formation and Their World*. Indiana University Press, Bloomington. 170–176.
- Irmis RB. 2004. First report of *Megapnosaurus* (Theropoda: Coelophysoidea) from China. *PaleoBios* 24 (3): 11–18.
- Longrich NR, Horner JR, Erickson GM, Currie PJ. 2010. Cannibalism in *Tyrannosaurus rex*. *PLoS ONE* 5(10): e13419.
- Luo ZX, Wu XC. 1995. Correlation of vertebrate assemblage of the Lower Lufeng Formation, Yunnan, China. In: Sun AL, Wang Y, editors. 6th Symposium on Mesozoic Terrestrial Ecosystems and Biotas: China Ocean Press. 83–88.
- Luo ZX, Crompton AW, Sun AL. 2001. A new mammaliaform from the Early

Jurassic and evolution of mammalian characteristics. *Science* 292 (5521): 1535–1540.

Milner ARC, Lockley MG, Kirkland JI, 2006. A large collection of well-preserved theropod dinosaur swim tracks from the Lower Jurassic Moenave Formation, St. George. In: Harris JD, Lucas SG, Spielmann JA et al. (eds), *The Triassic–Jurassic Terrestrial Transition*. *Bulletin of the New Mexico Museum of Natural History and Science* 37: 315–328

Nesbitt SJ, Turner AH, Erickson GM, Norell MA. 2006. Prey choice and cannibalistic behaviour in the theropod *Coelophysis*. *Biology Letters* 2 (4): 611–614.

Roach BT, Brinkman DT. 2007. A reevaluation of cooperative pack hunting and gregariousness in *Deinonychus antirrhopus* and other non-avian theropod dinosaurs. *Bulletin of the Peabody Museum of Natural History* 48 (1): 103–138

Rogers RR, Krause DW, Curry Rogers K. 2007. Cannibalism in the Madagascan dinosaur *Majungatholus atopus*. *Nature* 422 (6931): 515–518.

Simmons DT. 1965. The non-therapsid reptiles of the Lufeng Basin, Yunnan, China. *Fieldiana: Geology* 15(1): 1–96.

- Sun AL. 1962. The discovery of new segments of vertebrae at Lufeng. *Vertebrata Palasiatica* 6(2): 109–110.
- Tan XH. 1997. Stratigraphy and Depositional Environments of the Lufeng Basin. *Yunnan Geological Science and Technology Information* 1: 21–22.
- Wei M, Hu S, Zhang V. 2001. The diet of prosauropods and sauropods from Lufeng, Yunnan Province, China. In: Deng T, Wang Y. (eds.), *Proceedings of the Eighth Annual Meeting of the Chinese Society of Vertebrate Paleontology*. China Ocean Press. Beijing. 21–27.
- Welles SP. 1984. *Dilophosaurus wetherilli* (Dinosauria, Theropoda): Osteology and comparisons. *Palaeontographica Abteilung A* 185: 85–180.
- Xu X, Zhao X, Clark JM. 2001. A new therizinosaur from the Lower Jurassic Lower Lufeng Formation of Yunnan, China. *Journal of Vertebrate Paleontology*, 21(3): 477–483.
- Young CC. 1941. A complete osteology of *Lufengosaurus huenei* Young (gen. et sp. nov) from Lufeng, Yunnan, China. *Palaeontologia Sinica, New Series C* 7: 1–53.

- Young CC. 1947. On *Lufengosaurus magnus* Young (sp. nov.) and additional finds of *Lufengosaurus huenei* Young. *Palaeontologia Sinica*, New Series C 12: 1–53.
- Young CC. 1948. On two new Saurischia from Lufeng, Yunnan. *Bulletin of the Geological Society of China* 28(1–2): 75–90
- Young CC. 1951. The Lufeng saurischian faunas. *Collected Papers on Chinese Paleontology* 134, Series III, 13: 1–96.
- Young CC. 1982. A new fossil reptile from Lufeng, Yunnan. *Collected Papers of C.C. Young*. 36–37.
- Zhang YZ, 1995. *Stratigraphy (Lithostratic) of Yunnan Province*. Wuhan: China University of Geosciences Press. 1–366.

## Conclusion

Dilophosaurids represent the first large dinosaurian predators. They were also the first dinosaurian top (apex) predators in their environments after the extinction of the large predatory crurotarsalians that "ruled" the Triassic. Early Jurassic dilophosaurids of the Lufeng Basin have remained poorly known, even though they were first described in 1948, and at least five different *Sinosaurus triassicus* (=“*Dilophosaurus sinensis*”) specimens have been recovered. However, the Hewanzi specimen described in this thesis is the only well prepared one.

A detailed anatomical description and a phylogenetic analysis of the Lufeng theropod taxa allow a critical assessment for the first time. Morphology of the braincase of the Hewanzi specimen indicates that it possesses advanced characteristics, such as pneumatic recesses, that are more developed than in *Dilophosaurus*, and are even comparable with the Late Jurassic *Sinraptor*. A new phylogenetic analysis shows that *Sinosaurus triassicus* (=“*Dilophosaurus sinensis*”) is not the most basal dilophosaurid as was previously concluded by Smith et al. (2007a). In contrast, *Sinosaurus* and the Antarctic *Cryolophosaurus* emerge as more derived theropods; they were recovered as more closely related to *Averostra* than to *Coelophysis bauri* and *Dilophosaurus wetherilli*. Furthermore, based on the results of the phylogenetic analysis, it appears that the crest probably evolved independently in coelophysoids (including *Dilophosaurus*) and in *Sinosaurus*.

Pathologic or traumatic loss of teeth often results in the resorption and

remodeling of the affected alveoli in mammals; however, instances of alveolar remodeling in reptiles are extremely rare. A remodeled alveolus in the maxilla of *Sinosaurus* is the first confirmed example of such dental pathology in a dinosaur (Marsh [1884]'s research is insufficient to assess alveolar healing).

The functions of the crests in *Dilophosaurus* and *Sinosaurus* remain uncertain. One thought is that they may have played a mechanical role during combat, or that they provided a bony foundation for supporting external structures. However, these hypothetical purposes have no clear verification or direct evidence. A finite element analysis suggests that the structural features of the crest limited its abilities to support external pressures and/or loads and that higher shear strains and effective stress would have led to fracturing. Therefore, the hypothesis that the crest was used during combat can be shown to be false, and that it is unlikely to have supported any significant external structures.

The Konglong Hill specimen, another incomplete theropod skeleton from the Lower Jurassic Lufeng Formation, can also be assigned to *Sinosaurus triassicus*. The base of the crest on the nasal and lacrimal of the Konglong Hill specimen shows that the crest was broken but present as in other specimens of *Sinosaurus*. Other problems with this specimen include its reconstruction with the insides of some bones facing outward. The diet and paleoecology of *Sinosaurus* potentially may have included cannibalism.

## **Bibliography**

Marsh O. 1884. Principal characters of American Jurassic dinosaurs, the order Theropoda. *American Journal of Science* 27: 411–416.

**Appendix 1** List of characters and character–states used in the phylogenetic analysis. Original citations and/or modifications are provided in parentheses. The abbreviation “TWGM” is used to denote characters derived or modified from the Theropod Working Group Matrix.

**1.** Orbit round in lateral or dorsolateral view (0); or dorsoventrally elongate (1; Smith et al., 2007a).

ZLJT01: ?

LDM–L10: ?

KMV8701: 1

**2.** Skull length relative to femur length:  $> 0.5$  (0);  $\leq 0.5$  (1; Benton et al., 2000).

ZLJT01: ?

LDM–L10: ?

KMV8701: ?

**3.** Maxillary tooth row: extends posteriorly to approximately half the length of the orbit (0); ends at the anterior rim of the orbit (1); ends anterior to the vertical antorbital strut of the lacrimal (2; Gauthier, 1986).

ZLJT01: ?

LDM-L10: ?

KMV8701: 2

**4.** Infratemporal fenestra: smaller than or subequal in size to orbit (0); strongly enlarged, more than 1.5 times the size of the orbit (1; Bonaparte, 1991).

ZLJT01: ?

LDM-L10: ?

KMV8701: 1

**5.** Premaxilla, height: length ratio below external naris: 0.5–1.25 (0), < 0.5 (1), or > 1.25 (2) (modified from Carrano et al., 2002 and Rauhut, 2003)

ZLJT01: ?

LDM-L10: ?

KMV8701: 2

**6.** Premaxillary body in front of external nares: shorter than body below the nares and angle between anterior margin and alveolar margin more than 75 degrees (0); longer than body below the nares and angle less than 70 degrees (1; Rauhut, 2003).

ZLJT01: ?

LDM-L10: ?

KMV8701: 0

**7.** Premaxillary body, ventral process at the posterior end: absent (0); present (1; Rauhut, 2003).

ZLJT01: ?

LDM-L10: ?

KMV8701: 0/1

**8.** Premaxillary tooth count: three (0); four (1); five (2); more than five (3); premaxillary teeth absent (4; Rauhut, 2003).

ZLJT01: ?

LDM-L10: ?

KMV8701: 0/1

**9.** Premaxillary tooth row ends: ventral (0); anterior (1) to naris (Sereno, 1999).

ZLJT01: ?

LDM-L10: ?

KMV8701: 0

**10.** Premaxilla, subnarial process: wide; plate-like, broadly contacting the nasals and excluding the maxilla from the external nares (0); strongly reduced in width, but still contacting the nasals (1); strongly reduced process does not contact the nasals, and the maxilla forms part of the posteroventral border of the external nares (2; modified from Gauthier, 1986; Rauhut, 2003).

ZLJT01: ?

LDM-L10: ?

KMV8701: 1/2

**11.** Premaxilla, maxillary/palatal process: large flange (0); blunt triangle (1; Sampson et al., 1998).

ZLJT01: ?

LDM-L10: ?

KMV8701: ?

**12.** Premaxillary body, foramen on the medial side below the narial margin: absent (0); present (1; modified from Sereno et al., 2004; Yates, 2005).

ZLJT01: ?

LDM-L10: ?

KMV8701: ?

**13.** Premaxilla, slot-shaped foramen on the lateral face at the base of the nasal process: absent (0); present (1; Yates, 2005).

ZLJT01: ?

LDM-L10: ?

KMV8701: ?

**14.** Premaxilla, length of the nasal process: posterior tip level with the posterior tip of the posterolateral premaxillary process (0); posterior tip extends posterior to the posterior tip of the posterolateral premaxillary process (1; Yates, 2005).

ZLJT01: ?

LDM-L10: ?

KMV8701: ?

**15.** Premaxillary posterodorsal process contributes to a blade-like nasal crest: no (0); yes (1).

ZLJT01: ?

LDM-L10: ?

KMV8701: 1

**16.** Premaxilla–nasal suture on internarial bar: V–shaped (0); W–shaped (1; Sereno et al., 2004).

ZLJT01: ?

LDM–L10: ?

KMV8701: ?

**17.** Premaxillary tooth denticles: present (0); absent (1; Rauhut, 2003).

ZLJT01: ?

LDM–L10: ?

KMV8701: ?

**18.** Premaxillary tooth cross–section: elliptical (0); subcircular (1); D–shaped in cross–section (modified from Carrano et al., 2002; Smith et al., 2007a; Tykoski & Rowe, 2004; Yates, 2005).

ZLJT01: ?

LDM–L10: ?

KMV8701: 0/1

**19.** Premaxillary teeth, labiolingual symmetry: symmetrical (0); asymmetrical (1); (Bakker et al., 1988).

ZLJT01: ?

LDM–L10: ?

KMV8701: ?

**20.** Narial fossa, anteroventral: absent or shallow (0); expanded, well–developed fossa on the premaxilla in the anteroventral corner of the naris (1; modified from Sereno, 1999; Langer & Benton, 2006).

ZLJT01: ?

LDM–L10: ?

KMV8701: 1

**21.** Constriction between articulated premaxilla and maxilla: absent (0); present (1). (Rauhut, 2003).

ZLJT01: 1

LDM–L10: 1

KMV8701: 1

**22.** Premaxilla and maxilla in contact at alveolar margins (0), or alveolar margins do not contact (1; Tykoski, 2005).

ZLJT01: 1

LDM-L10: 1

KMV8701: 1

**23.** Maxillary orientation towards each other in dorsal view: acutely angled (0); subparallel (1; Harris, 1998).

ZLJT01: ?

LDM-L10: 1

KMV8701: 1

**24.** Maxilla, ascending process: confluent with anterior rim of maxillary body and gently sloping posterodorsally (0); offset from anterior rim of maxillary body, with anterior projection of maxillary body shorter than high (1); offset from anterior rim of maxillary body, with anterior projection of maxillary body as long as high or longer (2; Sereno et al., 1996).

ZLJT01: 1

LDM-L10: 1

KMV8701: 1

**25.** Maxillary antorbital fossa: deep, and with sharp margins (0); shallow, margins formed by low ridges, a sharp rim may be present only in front of the

promaxillary foramen (1; Sues, 1997).

ZLJT01: 1

LDM-L10: 1

KMV8701: 1

**26.** Maxillary antorbital fossa in front of the internal antorbital fenestra: 25 percent or less of the length of the external antorbital fenestra (0); more than 40 percent of the length of the external antorbital fenestra (1; Sereno et al., 1996).

ZLJT01: 0

LDM-L10: 0

KMV8701: 0

**27.** Antorbital fossa, depth of the ventral region: less than or subequal to the depth of the maxilla below the ventral margin of the antorbital fossa (0); or much greater than the depth of the maxilla below the ventral margin of the antorbital fossa (1; Yates, 2005).

ZLJT01: 1

LDM-L10: 1

KMV8701: 1

**28.** Maxilla, horizontal ridge: absent (0); present (1; Rowe & Gauthier, 1990).

ZLJT01: 0

LDM-L10: 0

KMV8701: 0

**29.** Maxillary fenestra: absent (0); present (1; Gauthier, 1986).

ZLJT01: 0

LDM-L10:

KMV8701: 0

**30.** Maxillary fenestra situated at anterior border of antorbital fossa (0); or situated posterior to anterior border of fossa (1; Smith et al., 2007a).

ZLJT01: ?

LDM-L10: ?

KMV8701: ?

**31.** Maxillary anterior ramus, pneumatic excavation/antrum: absent (0); present (1; Sereno et al., 1994).

ZLJT01: ?

LDM-L10: ?

KMV8701: ?

**32.** Maxilla, promaxillary fenestra: absent (0); present (1; Carpenter, 1992).

ZLJT01: 1

LDM-L10: 1

KMV8701: 1

**33.** Maxilla, palatal process: ridged flange (0); reduced, simple process (1); long, and plate-shaped (2; modified from Sereno et al., 1998; Carrano et al., 2002).

ZLJT01: ?

LDM-L10: ?

KMV8701: ?

**34.** Secondary palate formed by premaxilla only (0); or by premaxilla, maxilla, and vomer (1; Smith et al., 2007a).

ZLJT01: ?

LDM-L10: ?

KMV8701: ?

**35.** Maxillary tooth count: 12–18 (0);  $\geq 20$  (1);  $< 12$  (2; modified from Carrano et al., 2002; Tykoski, 2005).

ZLJT01: 0 (13 maxillary tooth)

LDM–L10: 0

KMV8701: 0

**36.** Maxillary and dentary teeth: serrated (0); some or all without serrations (1; modified from Chiappe et al., 1996; Rauhut, 2003; Smith et al., 2007a).

ZLJT01: 0

LDM–L10: 0

KMV8701: 0

**37.** Medial surface of parodontal plates: smooth (0); striated (1; Sampson et al., 1998).

ZLJT01: ?

LDM–L10: ?

KMV8701: ?

**38.** Nasals, pneumatic foramen: absent (0); present (1; Rauhut, 2003).

ZLJT01: ?

LDM-L10: 1

KMV8701: 1

**39.** Dorsal extent of antorbital fossa: dorsal rim of antorbital fossa below nasal suture, or formed by this suture (0); antorbital fossa extending onto the lateroventral side of the nasals (1; Sereno et al., 1994).

ZLJT01: ?

LDM-L10: 1

KMV8701: 1

**40.** Nasals: unfused (0); partially or fully fused (1) in adults (Sereno, 1999).

ZLJT01: ?

LDM-L10: 0

KMV8701: 0

**41.** Nasal, lateral surface of anterior end along the posterior margin of the external naris: flat (0); concave fossa (1); lateral convex hood covering posterior part of external naris (2; modified from Tykoski, 1998, 2005; Carrano et al., 2002).

ZLJT01: ?

LDM-L10: 1

KMV8701: 1

**42.** Nasals: flat or gently convex, lacking crest (0); expanded into sagittal or parasagittal crests (1).

ZLJT01: ?

LDM-L10: 1

KMV8701: 1

**43.** Nasal crest (when present): midline sagittal crest (0); parasagittal crests (1).

ZLJT01: ?

LDM-L10: 1

KMV8701: 1

**44.** Nasal crest construction: formed from the nasals only (0); lacrimal contributes to posterior margin of crest (1).

ZLJT01: ?

LDM-L10: 1

KMV8701: 1

**45.** Nasal, posterolateral process envelops part of the anterior ramus of the lacrimal: no (0); yes (1; modified from Yates, 2003b; Langer & Benton, 2006).

ZLJT01: ?

LDM-L10: ?

KMV8701: ?

**46.** Jugal, sublacrimal region: tapering (0); triradiate anterior end (1); strongly expanded anteriorly, overlapping most of the ventral portion of the lacrimal (2; Rauhut, 2003).

ZLJT01: ?

LDM-L10: 2

KMV8701: 2

**47.** Jugal pneumatization: absent (0); pneumatized by a foramen in the posterior rim of the jugal part of the antorbital fossa (1; Sereno et al., 1996).

ZLJT01: ?

LDM-L10: 0

KMV8701: 0

**48.** Jugal, foramen present on medial surface ventral to postorbital bar: absent (0)

or present (1; Smith et al., 2007a).

ZLJT01: ?

LDM-L10: ?

KMV8701: ?

**49.** Jugal, lateral ridge longitudinally traversing the anterior and posterior processes of the jugal: present (0), absent (1; modified from Sereno & Novas 1993; Tykoski 1998).

ZLJT01: ?

LDM-L10: ?

KMV8701: ?

**50.** Jugal, anterior end participates in internal antorbital fenestra: yes (0); no (1; modified from Holtz, 1994; Rauhut, 2003).

ZLJT01: ?

LDM-L10: 1

KMV8701: 1

**51.** Lacrimal fenestra: absent (0); present (1; Molnar et al., 1990).

ZLJT01: 1

LDM-L10: 0

KMV8701: ?

**52.** Lacrimal ‘horn’: absent (0); dorsal crest above orbit (1; Russell & Dong, 1993).

ZLJT01: 1

LDM-L10: 1

KMV8701: 1

**53.** Lacrimal, posterodorsal process: absent (0); present, lacrimal ‘T’-shaped in lateral view (1; Currie, 1995).

ZLJT01: 0

LDM-L10: 0

KMV8701: 0

**54.** Configuration of lacrimal and frontal: lacrimal separated from frontal by prefrontal (0); lacrimal contacts frontal (1; Rauhut, 2003).

ZLJT01: 1

LDM-L10: 1

KMV8701: 1

**55.** Contact between lacrimal and postorbital: absent (0); present (1; Sampson et al., 1998).

ZLJT01: 1

LDM-L10: 1

KMV8701: 1

**56.** Lacrimal anterior ramus length:  $> 65\%$  ventral ramus length (0),  $\leq 65\%$  ventral ramus length (1); lacrimal anterior ramus strongly reduced and almost non-existent (2); (Serenio et al., 1998).

ZLJT01: 0

LDM-L10: 0

KMV8701: 0

**57.** Lacrimal, suborbital process: absent (0); present (1; Sampson et al., 1998).

ZLJT01: 0

LDM-L10: 0

KMV8701: 0

**58.** Lacrimal, lateral blade (sensu Britt, 1991) overhangs antorbital fenestra: yes (0); no (1; modified from Britt, 1991; Allain, 2002).

ZLJT01: 0

LDM-L10: 0

KMV8701: 0

**59.** Lacrimal, ventral ramus: broadly triangular, articular end nearly twice as wide anteroposteriorly as lacrimal body at juncture between anterior and ventral ramus (0); bar- or strut-like, roughly same width anteroposteriorly throughout ventral ramus (1).

ZLJT01: 1

LDM-L10: 1

KMV8701: 1

**60.** Lacrimal, orientation of the long axis of the ventral process: strongly sloping anterodorsally (0); erect or nearly vertical (1); strongly sloping posterodorsally (2; Yates, 2006).

ZLJT01: 1

LDM-L10: 1

KMV8701: 1

**61.** Prefrontal: exposed dorsally on the anterior rim of the orbit in lateral view and with a slender ventral process along the medioposterior rim of the lacrimal (0); excluded from the anterior rim of the orbit in lateral view, being displaced posteriorly and/or medially; ventral process absent, but dorsal exposure similar to that of lacrimal (1); excluded from the anterior rim of the orbit in lateral view, being displaced posteriorly and/or medially; ventral process absent, and greatly reduced in size (2); absent (3; modified from Rauhut, 2003; Smith et al., 2007a).

ZLJT01: ?

LDM–L10: ?

KMV8701: ?

**62.** Frontals, anterior edge of associated frontals: rectangular anteriorly (0); triangular, wedge-shaped anteriorly (1; Holtz, 1994).

ZLJT01: 1

LDM–L10: 1

KMV8701: 1

**63.** Frontals, relative length of associated frontals: longer than wide (0); as wide as long, or wider (1; Allain, 2002).

ZLJT01: 1

LDM-L10: 1

KMV8701: 1

**64.** Frontal contribution to midline nasal crest: no (0); yes (1).

ZLJT01: 0

LDM-L10: 0

KMV8701: 0

**65.** Frontals and parietals: separate (0); fused (1) in adults (Forster, 1999).

ZLJT01: 0

LDM-L10: 0

KMV8701: 0

**66.** Frontal-parietal contact, median fossa in saddle-shaped depression: absent (0); present (1; Sampson et al., 1998).

ZLJT01: 1

LDM-L10: 1

KMV8701: 1

**67.** Frontal, supratemporal fossa extends onto posterodorsal surface (0); restricted by overhanging frontoparietal shelf (1; Coria & Currie, 2002).

ZLJT01: 0

LDM–L10: 0

KMV8701: 0

**68.** Supratemporal fenestrae: face dorsally (0); face anterodorsally (1; Coria & Currie, 2002).

ZLJT01: ?

LDM–L10: 0

KMV8701: 0

**69.** Postorbital jugal process, distinct anterior spur indicating the lower delimitation of the eyeball present: no (0); yes (1; Rauhut, 2003).

ZLJT01: ?

LDM–L10: 0

KMV8701: 0

**70.** Postorbital in lateral view with straight anterior (frontal) process (0); or frontal process curves anterodorsally and dorsal border of temporal bar is dorsally

concave (1; Smith et al., 2007a).

ZLJT01: 0

LDM-L10: 0

KMV8701: 0

**71.** Postorbital, cross-section of the ventral process: triangular (0); U-shaped (1; Sereno et al., 1994, 1996).

ZLJT01: ?

LDM-L10: ?

KMV8701: ?

**72.** Postorbital, ventral extent substantially above ventral margin of orbit: yes (0); no (1); no and postorbital process of jugal reduced or absent (2; Allain, 2002).

ZLJT01: ?

LDM-L10: 0

KMV8701: 0

**73.** Postorbital, long axis: dorsoventral (0); anteroventral–posterodorsal (1; Novas, 1989).

ZLJT01: ?

LDM-L10: 0

KMV8701: 0

**74.** Postorbital, stepped-down ventrolateral fossa: absent (0); present (1; Sampson et al., 1998).

ZLJT01: ?

LDM-L10: 0

KMV8701: 0

**75.** Supratemporal fenestrae: separated by a horizontal plate formed by the parietals (0); contact each other posteriorly, but separated anteriorly by an anteriorly widening triangular plate formed by the parietals (1); confluent over the parietals; parietals form a sagittal crest (2; Molnar et al., 1990).

ZLJT01: 0

LDM-L10: 0

KMV8701: 0

**76.** Nuchal wedge and parietal alae: small (0); hypertrophied and elevated (1; Forster, 1999).

ZLJT01: 0

LDM-L10: 0

KMV8701: 0

**77.** Parietals, tongue-like process of parietals overlapping the supraoccipital knob:  
absent (0); present (1; Coria & Currie, 2002).

ZLJT01: 1

LDM-L10: 1

KMV8701: 1

**78.** Squamosal contribution to broad, arching nuchal crest: absent (0); present (1;  
modified from Novas, 1989; Sampson et al., 1998).

ZLJT01: ?

LDM-L10: 0

KMV8701: 0

**79.** Supratemporal fenestra bounded laterally and posteriorly by the squamosal  
(0); or supratemporal fenestra extended as a fossa on to the dorsal surface of the  
squamosal (1; Smith et al., 2007a).

ZLJT01: ?

LDM–L10: 0

KMV8701: 0

**80.** Squamosal, posterolateral shelf overhanging quadrate head: absent (0); present (1; Smith et al., 2007a).

ZLJT01: ?

LDM–L10: 0

KMV8701: 0

**81.** Squamosal, quadratojugal process: tapering (0); broad, and somewhat expanded (1; Rauhut, 2003).

ZLJT01: ?

LDM–L10: 1

KMV8701: 1

**82.** Squamosal–quadratojugal contact: at tips (0); absent (1); broad (2; modified from Carrano et al., 2002, 2005; Rauhut, 2003).

ZLJT01: ?

LDM–L10: 0

KMV8701: 0

**83.** Quadratojugal, anteroposterior breadth of dorsal process: narrow (0); broad (1).

ZLJT01: ?

LDM-L10: 0

KMV8701: 0

**84.** Quadratojugal: hook-shaped, without posterior process (0); with broad, short posterior process that wraps around the lateroventral edge of the quadrate (1; Rauhut, 2003).

ZLJT01: ?

LDM-L10: 0

KMV8701: 0

**85.** Quadratojugal fused to quadrate in adults: no (0); yes (1; Holtz, 1994, 2000).

ZLJT01: ?

LDM-L10: 1

KMV8701: 1

**86.** Quadratojugal-Quadrate suture, exposed laterally and with a sharp lateral

flange running anterodorsally on the quadratojugal: no (0); yes (1).

ZLJT01: ?

LDM-L10: 1

KMV8701: 1

**87.** Quadrate pneumatization: absent (0); present (1; Rauhut, 2003).

ZLJT01: ?

LDM-L10: ?

KMV8701: ?

**88.** Quadrate, lateral border of shaft straight (0); or with lateral tab that touches squamosal and quadratojugal above an enlarged quadrate foramen (1; Smith et al., 2007a).

ZLJT01: ?

LDM-L10: 0

KMV8701: 0

**89.** Quadrate foramen: developed as a distinct opening between the quadrate and quadratojugal (0); almost entirely enclosed in the quadrate (1); absent (2; modified from Carrano et al., 2002; Rauhut, 2003; Tykoski, 2005).

ZLJT01: ?

LDM–L10: ?

KMV8701: ?

**90.** Paroccipital processes: directed laterally, or slightly ventrolaterally (0); directed strongly ventrolaterally, with distal end entirely below the level of the foramen magnum (1); (modified from Rauhut, 1997; Rauhut, 2003; Smith et al., 2007a).

ZLJT01: 1

LDM–L10: 1

KMV8701: 1

**91.** Paroccipital processes, ventral rim of the bases: above or level with the dorsal border of the occipital condyle (0); situated at mid–height of occipital condyle or lower (1; Rauhut, 2003).

ZLJT01: 1

LDM–L10: 1

KMV8701: 1

**92.** Paroccipital process elongate and slender, with dorsal and ventral edges nearly

parallel (0); or process short, deep with convex distal end (1; Smith et al., 2007a).

ZLJT01: ?

LDM-L10: 0

KMV8701: 0

**93.** Paroccipital process with straight dorsal edge (0); or with dorsal edge twisted rostromedially at distal end (1; Currie 1995).

ZLJT01: 0

LDM-L10: 0

KMV8701: 0

**94.** Posterior tympanic recess: absent (0); present as opening on anterior surface of paroccipital process (1); or extends into opisthotic posterodorsal to fenestra ovalis, confluent with this fenestra (2; Smith et al., 2007a).

ZLJT01: 0

LDM-L10: ?

KMV8701: ?

**95.** Supraoccipital, depth of median supraoccipital ridge: < (0); ≥ (1) depth of occipital condyle (Carrano et al., 2002).

ZLJT01: 1

LDM–L10: ?

KMV8701: ?

*Sinraptor*: 1 (revise)

**96.** Supraoccipital participation in the dorsal margin of the foramen magnum:  
large (0); reduced or absent (1; Allain, 2002).

ZLJT01: 1

LDM–L10: ?

KMV8701: ?

**97.** Supraoccipital, width of dorsal expansion: less than twice the width (0); or  
more than twice the width (1) of the foramen magnum (Coria & Currie, 2002).

ZLJT01: 0

LDM–L10: ?

KMV8701: 1

**98.** Occipital condyle, neck invaded by ventrolateral pair of pneumatic cavities  
that join medially: no (0); yes (1; Coria & Currie, 2002).

ZLJT01: 1

LDM-L10: ?

KMV8701: ?

**99.** Occipital condyle, angle with basal tubera: perpendicular or almost perpendicular (0); acute (1; Coria & Currie, 2002).

ZLJT01: 1

LDM-L10: ?

KMV8701: ?

**100.** Basal tubera: equally formed by basioccipital and basisphenoid and not subdivided (0); subdivided by a lateral longitudinal groove into a medial part entirely formed by the basioccipital, and a lateral part, entirely formed by the basisphenoid (1; Rauhut, 2003).

ZLJT01: 0

LDM-L10: ?

KMV8701: ?

**101.** Basioccipital participates in basal tubera: yes (0); no (1; modified from Currie & Carpenter, 2000; Allain, 2002).

ZLJT01: 0

LDM-L10: ?

KMV8701: ?

**102.** Basal tubera width:  $\geq$  (0);  $<$  (1) occipital condyle width (Holtz, 2000).

ZLJT01: 0

LDM-L10: ?

KMV8701: ?

**103.** Basisphenoid between basal tubera and basipterygoid processes:

approximately as wide as long, or wider (0); significantly elongated, at least 1.5 times longer than wide (1; Rauhut, 2003).

ZLJT01: 1

LDM-L10: ?

KMV8701: ?

**104.** Basisphenoid recess: absent or poorly developed (0); present between basisphenoid and basioccipital (1); present entirely within basisphenoid (2; modified from Rauhut, 2003; Smith et al., 2007a).

ZLJT01: 1

LDM-L10: ?

KMV8701: ?

**105.** Basisphenoid recess, posterior opening single (0); or divided into two small, circular foramina by a thin bar of bone (1; Smith et al., 2007a).

ZLJT01: 1

LDM-L10: ?

KMV8701: ?

**106.** Pneumatic openings associated with internal carotid artery: no (0); yes (1; modified from Allain, 2002; Coria & Currie, 2006).

ZLJT01: 1

LDM-L10: ?

KMV8701: ?

**107.** Anterior tympanic recess in the braincase: absent (0); present (1; Makovicky & Sues, 1998).

ZLJT01: 0

LDM-L10: ?

KMV8701: ?

**108.** Cranial nerve V exit foramen: single (0); fully split (1; Currie & Zhao, 1993).

ZLJT01: 0

LDM-L10: ?

KMV8701: ?

**109.** Trigeminal nerve (CN V) exit: in front or below the level of nuchal crest (0); behind the level of nuchal crest (1; Coria & Currie, 2002).

ZLJT01: 0

LDM-L10: ?

KMV8701: ?

**110.** Prootic, foramen for exit of facial nerve (CN VII): round or slightly anteroposteriorly elongate (0); dorsoventrally elongate (1).

ZLJT01: 1

LDM-L10: ?

KMV8701: ?

**111.** Interorbital region: unossified (0); ossified (1; modified from Russell & Dong, 1993; Novas, 1997).

ZLJT01: ?

LDM-L10: ?

KMV8701: ?

**112.** Middle ear region exposed in occipital view: no (0); yes (1; Coria & Currie, 2002).

ZLJT01: 0

LDM-L10: ?

KMV8701: ?

**113.** Median ridge separating exit of sixth cranial nerves: present (0); absent (1; Coria & Currie, 2002).

ZLJT01: ?

LDM-L10: ?

KMV8701: ?

**114.** Palatine, shape in ventral view: plate-like trapezoidal or subrectangular (0); tetraradiate (1); jugal process strongly reduced or absent (2; Harris, 1998).

ZLJT01: ?

LDM-L10: ?

KMV8701: ?

**115.** Palatine, jugal process: tapered (0); expanded (1; Sereno et al., 1994).

ZLJT01: ?

LDM-L10: ?

KMV8701: ?

**116.** Palatine and ectopterygoid separated by pterygoid (0); or contact (1; Currie 1995).

ZLJT01: ?

LDM-L10: ?

KMV8701: ?

**117.** Ectopterygoid, dorsal recess absent (0); or present (1; Smith et al., 2007a).

ZLJT01: ?

LDM-L10: ?

KMV8701: ?

**118.** Ectopterygoid: slender, without ventral fossa (0); expanded, with a deep

ventral depression medially (1); as above, but with a deep groove excavated into the body of the ectopterygoid from the medial side (2); excavated by a foramen leading from the medial side laterally into the body of the ectopterygoid (3; Gauthier, 1986).

ZLJT01: ?

LDM-L10: ?

KMV8701: ?

**119.** Contact between pterygoid and palatine: continuous (0); discontinuous in the mid-region, resulting in a subsidiary palatal fenestra (1; Ostrom, 1969).

ZLJT01: ?

LDM-L10: ?

KMV8701: ?

**120.** Palatal teeth: present (0); absent (1; Rauhut, 2003).

ZLJT01: ?

LDM-L10: 1

KMV8701: 1

**121.** Surangular articulation for dentary: small notch (0); large socket (1; Carrano

et al., 2002).

ZLJT01: ?

LDM-L10: 0

KMV8701: ?

**122.** Dentary, posterior end: strongly forked (0); straight or only slightly concave (1; Barsbold et al., 1990).

ZLJT01: ?

LDM-L10: 0

KMV8701: ?

**123.** Dentary, posteroventral process: far posterior (0), ventral (1) to posterodorsal process (Sereno, 1999).

ZLJT01: ?

LDM-L10: 0

KMV8701: 0

**124.** Anterior end of external mandibular fenestra: posterior (0); ventral (1) to last dentary tooth (Sereno, 1999).

ZLJT01: ?

LDM-L10: 0

KMV8701: 0

**125.** Dentary anterior end: unexpanded (0), dorsally raised over the distance of the first three to four alveoli (1); square-shaped (2; modified from Sereno 1999, Novas et al., 2005).

ZLJT01: 0

LDM-L10: 0

KMV8701: 0

**126.** Jaws occlude for their full length (0); or diverge anteriorly due to kink and downward deflection in dentary buccal margin (1; modified from Perez-Moreno et al., 1994; Smith et al., 2007a).

ZLJT01: 0

LDM-L10: 0

KMV8701: 0

**127.** Dentary teeth: large, less than 25 (0); moderate number of small teeth (25–30; 1); teeth relatively small and numerous (>30; 2; modified from Russell & Dong, 1993; Carrano et al., 2002; Smith et al., 2007a).

ZLJT01: 0

LDM–L10: 0

KMV8701: 0

**128.** Dentary, enlarged, fang–like teeth in the anterior part: absent (0); present (1; Gauthier, 1986).

ZLJT01: 0

LDM–L10: 0

KMV8701: 0

**129.** Splenial: exposed as a broad triangle between dentary and angular on lateral surface of mandible (0); or not widely exposed on lateral surface of mandible (1; Smith et al., 2007a).

ZLJT01: ?

LDM–L10: 1

KMV8701: 1

**130.** Splenial, foramen in the ventral part: absent (0); present (1; Rauhut, 2003).

ZLJT01: ?

LDM-L10: ?

KMV8701: ?

**131.** Splenial, posterior end: straight or slightly curved (0); distinctly forked (1; Sereno et al., 1996).

ZLJT01: ?

LDM-L10: 0

KMV8701: 0

**132.** Surangular, anterior portion: less than half the height of the mandible above the mandibular fenestra (0); more than half the height of the mandible at the level of the mandibular fenestra (1; Gauthier, 1986).

ZLJT01: ?

LDM-L10: 1

KMV8701: 1

**133.** Surangular, horizontal shelf on the lateral surface anteroventral to the mandibular condyle: absent or only a faint ridge (0), prominent and extending laterally (1; Holtz 1998).

ZLJT01: ?

LDM–L10: 1

KMV8701: 1

**134.** Surangular, laterally inclined flange along dorsal edge for articulation with lateral process of lateral quadrate condyle: absent (0); or present (1; Smith et al., 2007a).

ZLJT01: ?

LDM–L10: 0

KMV8701: 0

**135.** Surangular, lateral groove along posterior end just dorsal to articulation with posterior splint of angular: no (0); yes (1).

ZLJT01: ?

LDM–L10: 0

KMV8701: 0

**136.** Surangular, well–developed anterior wall to lateral glenoid, resulting in a lateral glenoid fossa that is at least weakly U–shaped in lateral aspect: no (0); yes (1).

ZLJT01: ?

LDM–L10: 1

KMV8701: 1

**137.** Angular exposed almost to end of mandible in lateral view, reaches or almost reaches articular (0); or excluded from posterior end of articular, suture turns ventrally and meets ventral border of mandible rostral to glenoid (1; Smith et al., 2007a).

ZLJT01: ?

LDM–L10: ?

KMV8701: 1

**138.** Articular, pendant medial process: no (0); yes (1; Sereno et al., 1994).

ZLJT01: ?

LDM–L10: 1

KMV8701: 1

**139.** Articular, retroarticular process of the mandible: narrow and rod-like, anteroposterior length much greater than mediolateral breadth (0); broadened, as wide mediolaterally as long anteroposteriorly or wider, often with groove posteriorly for the attachment of the m. depressor mandibulae (1; modified from Sereno et al., 1996; Harris, 1998).

ZLJT01: ?

LDM–L10: 0

KMV8701: 0

**140.** Articular, attachment for the m. depressor mandibulae on retroarticular process of mandible: facing dorsally (0); facing posterodorsally (1; Sereno et al., 1996).

ZLJT01: ?

LDM–L10: 0

KMV8701: 0

*Sinraptor*: 0 (revise)

**141.** Articular, erect, tab-like dorsal processes, one immediately posterior to the opening of the chorda tympanic foramen and the other on the anterolateral margin of the posterodorsal fossa of the retroarticular process: no (0); yes (1; Yates, 2005).

ZLJT01: ?

LDM–L10: 0

KMV8701: 0

**142.** Lacrimal fenestra: opening ventral (0); lateral (1; TWiG).

ZLJT01: 0

LDM-L10: ?

KMV8701: 1

**143.** Lacrimal, a series of pneumatic diverticula into dorsal crest: absent (0); present (1; TWiG).

ZLJT01: 1

LDM-L10: 0

KMV8701: 1

**144.** Lacrimal, contribution to dorsal head crest (if present): less than (0); or more than a third of surface area of crest in lateral view (1; TWiG).

ZLJT01: ?

LDM-L10: 1

KMV8701: 1

**Appendix 2.** Taxon–character state data matrix used in the phylogenetic analysis. “0, 1, 2, 3, 4” = character states; “?” = unknown; “{}” = uncertainty (register as: multistate codings separated by backslashes in NDE software ); “–” = inapplicable.

<b>Taxa</b>	<b>1</b>	<b>2</b>	<b>3</b>	<b>4</b>	<b>5</b>	<b>6</b>	<b>7</b>	<b>8</b>	<b>9</b>	<b>10</b>	<b>11</b>	<b>12</b>	<b>13</b>	<b>14</b>
<i>Silesaurus</i>	?	0	2	?	1	0	0	1	0	0	-	?	?	?
<i>Herrerasaurus</i>	0	0	0	0	0	0	?	1	0	0	0	0	0	0
<i>Eoraptor</i>	0	0	0	0	0	0	?	1	0	0	?	0	0	?
<i>Plateosaurus</i>	0	1	0	0	0	0	0	3	0	1	0	0	0	0
<i>Coelophysis bauri</i>	0	0	0	0	1	1	1	1	1	2	0	1	0	1
<i>Coelophysis rhodesiensis</i>	0	0	0	0	1	1	1	1	1	2	0	1	0	1
<i>Syntarsus kayentakatae</i>	0	0	0	0	1	1	1	1	1	2	0	?	0	1
<i>Zupaysaurus</i>	0	?	1	0	?	?	?	?	?	1/2	?	?	?	?
<i>Dilophosaurus sinensis</i> (KMV 8701)	1	?	2	1	2	0	0/1	0/1	0	1/2	?	?	?	?
ZLJT01	?	?	?	?	?	?	?	?	?	?	?	?	?	?
LDM-L10	?	?	?	?	?	?	?	?	?	?	?	?	?	?
<i>Dilophosaurus wetherilli</i>	1	0	1	?	1	1	1	1	1	1/2	0	1	1	1
<i>Cryolophosaurus</i>	1	0	1/2	?	?	?	?	?	?	?	?	?	?	?
<i>Ceratosaurus</i>	1	0	1	1	2	0	0	0	0	2	1	1	0	0
<i>Abelisaurus</i>	1	0	?	1	2	0	0	1	0	?	?	?	?	?
<i>Carnotaurus</i>	1	0	1	1	2	0	0	1	0	?	?	?	0	0
<i>Majungatholus</i>	1	0	1	1	2	0	0	1	0	2	1	1	0	0

<i>Masiakasaurus</i>	?	0	?	?	?	?	?	?	?	?	?	?	?	?
<i>Piatnitzkysaurus</i>	?	?	?	?	?	?	?	?	?	1/2	?	?	?	?
<i>Dubreuillosaurus</i>	1	?	2	0	0	1	0	1	0	1/2	0	?	0	?
<i>Afrovenator</i>	1	?	2	0	?	?	?	?	?	1/2	?	?	?	?
<i>Torvosaurus</i>	1	?	?	?	0	1	0	0	0	1/2	0	1	0	0
<i>Eustreptospondylus</i>	1	0	2	0	0	1	?	1	0	2	0	?	0	?
<i>Baryonyx</i>	1	0	?	?	0	1	0	3	1	2	0	?	0	1
<i>Suchomimus</i>	?	0	2	0	0	1	0	3	1	1+2	0	?	0	1
<i>Irritator</i>	1	?	2	0	?	?	?	?	1	2	?	?	?	?
<i>Monolophosaurus</i>	1	?	2	0	0	0	0	1	0	1/2	?	?	0	0
<i>Sinraptor</i>	1	0	2	1	0	0	1	1	0	1	0	1	0	0
<i>Carcharodontosaurus</i>	1	0	2	?	?	?	?	?	?	?	?	?	?	?
<i>Giganotosaurus</i>	1	0	2	?	?	?	?	1	?	?	?	?	?	?
<i>Acrocanthosaurus</i>	1	0	2	0	0	0	0	1	1	1	?	?	0	0
<i>Allosaurus</i>	1	0	2	0	0	0	0	2	0	1	0	1	0	0
<i>Neovenator</i>	?	0	?	?	0	0	0	2	0	2	0	1	0	0
<i>Dilong paradoxus</i>	0	0	2	0	2	0	0	1	0	1	?	?	?	?
<i>Tyrannosaurus rex</i>	1	0	2	0	2	0	0	1	0	1	0	?	0	0
<i>Compsognathus</i>	0	0	1/2	0	0	?	1	1	?	2	?	?	?	?
<i>Sinosauropteryx</i>	0	0	2	0	0	0	0	1/2	0	1	?	?	?	?
<i>Shenzhousaurus</i>	?	?	?	?	0	0	0	4	-	1	?	?	?	0
<i>Sinornithomimus</i>	0	0	?	?	0	0	0	4	-	1	0	?	0	0
<i>Ornitholestes</i>	0	?	2	0	0	0	0	1	0	1	?	?	?	0
<i>Deinonychus</i>	0	?	2	0	0	0	0	1	0	?	?	?	0	0
<i>Velociraptor</i>	0	0	2	0	0	0	0	0/1	0	1	0	?	0	0
<i>Archaeopteryx</i>	0	0	2	0	?	1	0	0/1/2 /3	0/1	2	?	?	?	1

<i>Confuciusornis</i>	0	0	-	0	0	1	0	4	-	2	?	?	0	1
-----------------------	---	---	---	---	---	---	---	---	---	---	---	---	---	---

Taxa	15	16	17	18	19	20	21	22	23	24	25	26	27	28
<i>Marasuchus</i>	?	?	?	?	?	?	?	?	?	?	?	?	?	?
<i>Silesaurus</i>	?	?	?	?	?	0	0	0	0	0	?	0	?	0
<i>Herrerasaurus</i>	0	0	0	0	0	1	0	0	1	0	0	0	0	0
<i>Eoraptor</i>	0	0	0	0	0	1	0	1	0	1	0	0	0	1
<i>Saturnalia</i>	?	?	?	?	?	?	?	?	?	?	?	?	?	?
<i>Plateosaurus</i>	0	0	?	0	0	1	0	0	0	2	0	0	0	0
<i>Coelophysis bauri</i>	0	1	1	1	0	1	1	1	0	0	1	0	1	1
<i>Coelophysis rhodesiensis</i>	0	1	1	1	0	1	1	1	0	0	1	0	1	1
<i>Syntarsus kayentakatae</i>	0	?	1	1	0	1	1	1	0	1	1	0	1	1
<i>Zupaysaurus</i>	?	1	?	?	?	?	?	?	0	0	1	0	1	1
<i>Dilophosaurus sinensis</i> (KMV 8701)	1	?	?	0/1	?	1	1	1	1	1	1	0	1	0
ZLJT01	?	?	?	?	?	?	1	1	?	1	1	0	1	0
LDM-L10	?	?	?	?	?	?	1	1	1	1	1	0	1	0
<i>Dilophosaurus wetherilli</i>	1	1	0	1	0	1	1	1	?	0	1	0	1	0
<i>Cryolophosaurus</i>	?	?	?	?	?	?	?	?	?	?	?	?	?	?
<i>Ceratosaurus</i>	0	1	0	0	1	1	0	0	0	1	1	0	0	0
<i>Abelisaurus</i>	?	?	?	?	?	?	0	0	0	1	1	0	?	0
<i>Carnotaurus</i>	0	1	0	0	1	1	0	0	0	1	1	0	0	0
<i>Majungatholus</i>	0	1	0	0	1	1	0	0	0	1	1	0	0	0

<i>Masiakasaurus</i>	?	?	?	?	1	?	?	?	?	1	1	0	0	1
<i>Piatnitzkysaurus</i>	?	?	?	?	?	?	?	?	?	1	1	0	0	0
<i>Dubreuillosaurus</i>	?	?	0	0	1	1	0	0	?	2	1	0	0	0
<i>Afrovenator</i>	?	?	?	?	?	?	?	0	?	2	1	0	0	0
<i>Torvosaurus</i>	?	1	0	0	0	1	0	0	?	2	1	?	0	0
<i>Eustreptospondylus</i>	?	?	0	0	1	1	0	?	?	2	1	0	0	0
<i>Baryonyx</i>	?	0	?	1	0	?	1	0	?	2	0	0	0	0
<i>Suchomimus</i>	?	0	0	1	0	?	1	0	1	2	0	0	?	0
<i>Irritator</i>	?	?	?	?	?	?	?	?	1	2	0	0	0	0
<i>Monolophosaurus</i>	1	1	?	0	?	1	0	0	1	2	1	0	0	0
<i>Sinraptor</i>	0	1	0	0	1	1	0	0	1	0	1	0	0	0
<i>Carcharodontosaurus</i>	?	1	?	?	1	?	?	?	?	1	1	0	0	0
<i>Giganotosaurus</i>	?	?	0	0	?	?	0	0	?	1	1	0	0	0
<i>Acrocantnosaurus</i>	0	1	0	0	1	1	0	0	1	0	1	0	0	0
<i>Allosaurus</i>	0	1	0	0	1	1	0	0	1	2	1	0	0	0
<i>Neovenator</i>	0	?	?	0	?	1	0	0	?	2	1	0	0	0
<i>Dilong paradoxus</i>	?	?	0	2	1	?	0	0	1	0	1	0	0	0
<i>Tyrannosaurus rex</i>	0	?	0	2	1	1	0	0	1	0	1	1	0	0
<i>Compsognathus</i>	?	?	1	?	1	?	?	?	?	0	1	1	0	0
<i>Sinosauroptryx</i>	?	?	1	?	1	?	?	?	?	0	?	?	0	?
<i>Shenzhousaurus</i>	?	?	?	-	?	?	0	0	?	0	1	1	0	0
<i>Sinornithomimus</i>	0	?	?	-	?	1	?	0	1	0	?	?	0	?
<i>Ornitholestes</i>	0	?	1	2	1	1	0	0	?	0	1	1	0	1
<i>Deinonychus</i>	?	?	?	?	1	1	0	0	?	?	1	?	0	0
<i>Velociraptor</i>	0	?	?	0	1	1	0	0	1	0	1	1	0	0
<i>Archaeopteryx</i>	0	?	1	?	1	?	0	0	?	0	?	1	0	?
<i>Confuciusornis</i>	0	-	-	-	-	?	0	0	0	0	-	-	0	0

<b>Taxa</b>	<b>29</b>	<b>30</b>	<b>31</b>	<b>32</b>	<b>33</b>	<b>34</b>	<b>35</b>	<b>36</b>	<b>37</b>	<b>38</b>	<b>39</b>	<b>40</b>	<b>41</b>	<b>42</b>
<i>Silesaurus</i>	?	?	0	?	0	0	2	0	?	?	?	?	0	0
<i>Herrerasaurus</i>	0	?	0	0	0	0	0	0	0	0	0	0	0	0
<i>Eoraptor</i>	0	?	0	0	?	0	0	0	?	0	0	0	0	0
<i>Plateosaurus</i>	0	0	0	0	0	0	1	0	?	0	0	0	1	0
<i>Coelophysis bauri</i>	0	?	0	0	0	0	1	0	0	0	0	0	1	0
<i>Coelophysis rhodesiensis</i>	0	?	0	0	0	0	1	0	0	0	0	0	1	0
<i>Syntarsus kayentakatae</i>	0	?	0	1	0	0	1	0	?	0	0	0	1	1
<i>Zupaysaurus</i>	0	?	?	1	?	0	1	0	?	0	0	0	?	1
<i>Dilophosaurus sinensis</i> (KMV 8701)	0	?	?	1	?	?	0	0	?	1	1	0	1	1
ZLJT01	0	?	?	1	?	?	0	0	?	?	?	?	?	?
LDM-L10	0	?	?	1	?	?	0	0	?	1	1	0	1	1
<i>Dilophosaurus wetherilli</i>	0	?	0	1	0	0	0	0	0	0	1	0	?	1
<i>Cryolophosaurus</i>	?	?	?	?	?	?	?	0	?	0	1	0	?	1
<i>Ceratosaurus</i>	0	0	0	1	0	0	0	0	0	1	0	1	2	1
<i>Abelisaurus</i>	0	?	0	1	?	?	0	?	1	1	?	1	2	0
<i>Carnotaurus</i>	0	0	0	1	?	0	0	0	1	1	0	1	2	0
<i>Majungatholus</i>	0	0	0	1	0	0	0	0	1	1	0	1	2	0
<i>Masiakasaurus</i>	0	?	0	1	1	?	2	?	0	?	?	?	?	?
<i>Piatnitzkysaurus</i>	0	0	1	1	0	0	0	0	0	?	?	?	?	?
<i>Dubreuillosaurus</i>	0	0	?	1	0	0	0	0	0	?	?	?	?	?

<i>Afrovenator</i>	?	0	1	1	0	0	0	0	0	?	?	?	?	?
<i>Torvosaurus</i>	0	?	1	1	0	0	0	0	0	?	?	?	?	?
<i>Eustreptospondylus</i>	?	0	1	1	0	0	0	0	0	?	?	?	?	?
<i>Baryonyx</i>	?	?	?	?	2	1	?	1	0	?	0	1	?	?
<i>Suchomimus</i>	0	0	1	?	2	1	1	1	?	?	0	?	?	?
<i>Irritator</i>	0	0	?	?	2	?	?	1	?	?	0	1	1	1
<i>Monolophosaurus</i>	0	0	?	1	0	0	0	?	?	1	1	?	1	1
<i>Sinraptor</i>	1	0	1	1	0	0	0	0	0	1	1	0	1	0
<i>Carcharodontosaurus</i>	?	0	1	?	?	0	0	0	?	1	1	0	1	0
<i>Giganotosaurus</i>	0	?	1	1	?	?	0	0	0	?	1	0	?	0
<i>Acrocanthosaurus</i>	1	0	1	1	?	0	0	0	?	1	1	0	1	0
<i>Allosaurus</i>	1	0	1	1	0	0	0	0	0	1	1	0	1	0
<i>Neovenator</i>	1	0	1	?	0	0	0	0	0	?	1	0	1	0
<i>Dilong paradoxus</i>	1	0	1	1	?	?	0	0	?	1	0	1	1	1
<i>Tyrannosaurus rex</i>	1	0	1	1	0	1	0	0	0	0	0	1	1	0
<i>Compsognathus</i>	1	?	?	?	?	?	?	1	?	?	?	?	?	0
<i>Sinosauropteryx</i>	1	?	?	?	?	?	0	1	?	?	?	0	1	0
<i>Shenzhousaurus</i>	1	0	?	?	?	1	-	1	?	0	0	0	1	0
<i>Sinornithomimus</i>	?	0	?	1	0	?	-	?	?	0	0	0	1	0
<i>Ornitholestes</i>	1	1	1	1	?	?	0	0	?	?	0	0	1	0
<i>Deinonychus</i>	1	1	1	1	0	?	0	1	0	0	0/1	0	1	?
<i>Velociraptor</i>	1	1	1	1	0	1	0	1	-	0	0	0	1	0
<i>Archaeopteryx</i>	1	1	1	?	?	?	0	1	?	0	?	?	?	0
<i>Confuciusornis</i>	0	?	?	?	?	?	-	-	-	0	0	?	?	0

Taxa	43	44	45	46	47	48	49	50	51	52	53	54	55	56
------	----	----	----	----	----	----	----	----	----	----	----	----	----	----

<i>Silesaurus</i>	-	-	?	?	?	?	0	?	?	?	?	?	0	?
<i>Herrerasaurus</i>	-	-	0	2	0	0	0	0	0	0	0	0	0	0
<i>Eoraptor</i>	-	-	1	0	0	?	0	1	0	0	0	?	0	0
<i>Plateosaurus</i>	-	-	1	0	0	0	?	0	0	0	0	0	0	0
<i>Coelophysis bauri</i>	-	-	1	0	0	?	0	1	0	0	0	0	0	0
<i>Coelophysis rhodesiensis</i>	-	-	1	0	0	?	0	1	0	0	0	0	0	0
<i>Syntarsus kayentakatae</i>	1	0	?	1	0	?	0	1	0	0	0	0	0	0
<i>Zupaysaurus</i>	1	0	?	2	0	?	1	0	1	?	0	0	0	0
<i>Dilophosaurus sinensis</i> (KMV 8701)	1	1	?	2	0	?	?	1	?	1	0	1	1	0
ZLJT01	?	?	?	?	?	?	?	?	1	1	0	1	1	0
LDM-L10	1	1	?	2	0	?	?	1	0	1	0	1	1	0
<i>Dilophosaurus wetherilli</i>	1	1	?	2	0	?	1	0	?	?	0	?	0	?
<i>Cryolophosaurus</i>	1	1	?	2	0	?	1	?	1	1	0	0	0	0
<i>Ceratosaurus</i>	0	0	?	?	0	0	1	1	1	1	0	0	0	1
<i>Abelisaurus</i>	-	-	?	?	?	?	?	?	0	0	1	1	1	?
<i>Carnotaurus</i>	-	-	1	2	0	0	1	0	0	0	1	1	1	2
<i>Majungatholus</i>	-	-	?	2	0	0	1	0	0	0	1	1	1	2
<i>Masiakasaurus</i>	?	?	?	?	?	?	?	?	?	?	?	?	?	?
<i>Piatnitzkysaurus</i>	?	?	?	?	?	?	?	?	?	?	?	0	?	?
<i>Dubreuillosaurus</i>	?	?	?	2	1	0	?	?	?	?	0	0	0	0
<i>Afrovenator</i>	?	?	?	?	1	?	1	?	1	1	0	?	0	0
<i>Torvosaurus</i>	?	?	?	2	0	0	1	?	1	0	0	?	?	0
<i>Eustreptospondylus</i>	?	?	?	?	?	?	?	?	1	0	0	0	0	?

<i>Baryonyx</i>	0	0	?	2	?	?	0	?	1	1	0	0	0	0
<i>Suchomimus</i>	?	?	?	?	?	?	?	?	?	?	0	0	0	?
<i>Irritator</i>	0	0	?	2	0	?	0	?	1	1	0	0	0	0
<i>Monolophosaurus</i>	0	1	?	2	1	?	1	0	0	1	0	0	0	0
<i>Sinraptor</i>	-	-	1	2	1	1	1	0	1	1	0	0	0	1
<i>Carcharodontosaurus</i>	-	-	?	2	1	?	1	0	1	1	0	?	1	1
<i>Giganotosaurus</i>	-	-	?	2	?	?	?	?	1	1	0	0	1	1
<i>Acrocanthosaurus</i>	-	-	?	2	1	1	1	0	1	1	0	0	1	1
<i>Allosaurus</i>	-	-	1	2	1	0	1	1	1	1	0	0	0	1
<i>Neovenator</i>	-	-	?	?	?	?	?	?	?	?	?	?	?	?
<i>Dilong paradoxus</i>	1	1	?	2	1	?	1	0	1	1	0	0	0	1
<i>Tyrannosaurus rex</i>	-	-	1	2	1	1	1	0	1	1	0	1	1	1
<i>Compsognathus</i>	-	-	?	?	0	?	1	?	?	0	0	0	0	?
<i>Sinosauropteryx</i>	-	-	?	?	?	?	1	?	?	0	0	?	?	?
<i>Shenzhousaurus</i>	-	-	?	?	1	-	?	?	0	0	0	?	?	?
<i>Sinornithomimus</i>	-	-	?	0	?	?	1	?	0	0	0	?	?	1
<i>Ornitholestes</i>	-	-	?	?	?	?	1	0	1	0	0	?	0	1
<i>Deinonychus</i>	?	?	?	0	1	0	1	0	0	0	1	?	?	1
<i>Velociraptor</i>	-	-	?	0	1	0	1	0	0	0	1	1	0	1
<i>Archaeopteryx</i>	-	-	?	?	1	0	1	0	0	0	1	1	?	?
<i>Confuciusornis</i>	-	-	?	0	1	?	1	?	?	0	1	1	0	?

<b>Taxa</b>	<b>57</b>	<b>58</b>	<b>59</b>	<b>60</b>	<b>61</b>	<b>62</b>	<b>63</b>	<b>64</b>	<b>65</b>	<b>66</b>	<b>67</b>	<b>68</b>	<b>69</b>	<b>70</b>
<i>Silesaurus</i>	?	?	?	?	?	?	0	?	?	?	?	?	?	?
<i>Herrerasaurus</i>	0	0	0	0	0	0	0	0	0	0	0	0	0	0
<i>Eoraptor</i>	0	0	0	0	0	0	0	0	0	0	?	0	?	0

<i>Plateosaurus</i>	0	0	1	0	0	0	0	0	0	0	0	0	0	0
<i>Coelophysis bauri</i>	0	0	0	1	0	1	0	0	0	0	0	0	0	0
<i>Coelophysis rhodesiensis</i>	0	0	0	1	0	1	0	0	0	0	0	0	0	0
<i>Syntarsus kayentakatae</i>	0	0	0	1	0	1	0	0	0	0	0	0	0	0
<i>Zupaysaurus</i>	0	0	0	1	0	1	0	0	0	0	0	0	0	?
<i>Dilophosaurus sinensis</i> (KMV 8701)	0	0	1	1	?	1	1	0	0	1	0	0	0	0
ZLJT01	0	0	1	1	?	1	1	0	0	1	0	?	?	0
LDM-L10	0	0	1	1	?	1	1	0	0	1	0	0	0	0
<i>Dilophosaurus wetherilli</i>	0	?	0	1	0	1	?	?	0	0	0	?	0	0
<i>Cryolophosaurus</i>	0	0	0	1	0	1	0	0	0	0	0	0	0	0
<i>Ceratosaurus</i>	0	0	0	1	0	1	1	0	0	0	0	0	0	0
<i>Abelisaurus</i>	1	0	1	1	2/3	0	1	0	1	0	0	0	1	?
<i>Carnotaurus</i>	1	0	1	1	3	0	1	0	1	1	0	0	1	?
<i>Majungatholus</i>	1	0	1	1	3	0	1	0	1	1	0	0	1	?
<i>Masiakasaurus</i>	?	?	?	?	?	?	?	?	?	?	?	?	?	?
<i>Piatnitzkysaurus</i>	?	?	?	?	?	1	0	0	0	?	0	?	?	?
<i>Dubreuillosaurus</i>	0	1	?	1	1	1	0	0	?	0	0	0	0	0
<i>Afrovenator</i>	0	0/1	0	1	?	?	?	?	?	?	?	?	0	0
<i>Torvosaurus</i>	0	1	0	1	?	?	?	?	?	?	?	?	0	0
<i>Eustreptospondylus</i>	0	1	?	1	1	0	0	?	?	?	?	?	0	0
<i>Baryonyx</i>	0	1	0	2	0	-	0	1	0	0	?	?	0	0
<i>Suchomimus</i>	?	?	?	?	0	?	?	?	0	0	?	?	?	?
<i>Irritator</i>	0	1	0	2	0	0	?	?	0	0	0	0	0	0

<i>Monolophosaurus</i>	0	0	0	1	1	-	1	1	0	0	0	0	0	0
<i>Sinraptor</i>	0	0	1	1	1	?	1	0	0	0	0	1	1	0
<i>Carcharodontosaurus</i>	?	?	1	1	1	?	1	?	?	?	1	1	1	0
<i>Giganotosaurus</i>	0	?	?	1	1	?	1	0	?	?	1	1	1	0
<i>Acrocanthosaurus</i>	1	0	1	1	1	?	1	0	0	0	0	0	0	0
<i>Allosaurus</i>	0	0	1	1	1	0	1	0	0	0	0	0	0	0
<i>Neovenator</i>	?	?	?	?	?	?	?	?	?	?	?	?	?	?
<i>Dilong paradoxus</i>	0	?	0	?	1/2	0	0	0	0	0	0	0	0	?
<i>Tyrannosaurus rex</i>	0	0	1	1	2	0	1	0	0	0	0	0	1	0
<i>Compsognathus</i>	?	?	?	1	?	?	?	0	?	?	?	?	0	?
<i>Sinosauropteryx</i>	?	?	?	1	1	?	?	?	?	?	?	?	?	?
<i>Shenzhousaurus</i>	?	?	?	1	-	?	?	0	0	0	0	?	?	0
<i>Sinornithomimus</i>	0	0	1	1	?	?	1	0	0	0	0	0	0	?
<i>Ornitholestes</i>	0	?	0	1	2	?	?	0	0	0	?	0	0	0
<i>Deinonychus</i>	0	0	1	1	2	?	?	?	?	?	?	?	0	1
<i>Velociraptor</i>	0	0	1	1	3	0	1	0	0	0	0	0	0	1
<i>Archaeopteryx</i>	?	?	?	1	3	?	1	0	?	?	0	?	0	?
<i>Confuciusornis</i>	?	?	1	1	3	0	1	0	0	0	?	?	0	1

<b>Taxa</b>	<b>71</b>	<b>72</b>	<b>73</b>	<b>74</b>	<b>75</b>	<b>76</b>	<b>77</b>	<b>78</b>	<b>79</b>	<b>80</b>	<b>81</b>	<b>82</b>	<b>83</b>	<b>84</b>
<i>Silesaurus</i>	?	?	?	?	?	?	?	?	?	?	?	?	?	?
<i>Herrerasaurus</i>	?	0	0	0	0	0	0	0	0	0	1	0	0	0
<i>Eoraptor</i>	?	0	0	0	?	0	?	0	0	0	?	0	0	0
<i>Plateosaurus</i>	0	0	0	0	0	0	0	0	0	0	0	0	0	0
<i>Coelophysis bauri</i>	?	0	0	0	0	0	?	0	0	0	0	1	0	0
<i>Coelophysis</i>	0	0	0	0	0	0	0	0	0	?	0	1	0	0

<i>rhodesiensis</i>														
<i>Syntarsus kayentakatae</i>	0	0	0	0	0	0	0	0	0	0	0	0	0	0
<i>Zupaysaurus</i>	0	0	0	0	0	0	0	0	0	0	1	2	0	0
<i>Dilophosaurus sinensis</i> (KMV 8701)	?	0	0	0	0	0	1	0	0	0	1	0	0	0
ZLJT01	?	?	?	?	0	0	1	?	?	?	?	?	?	?
LDM-L10	?	0	0	0	0	0	1	0	0	0	1	0	0	0
<i>Dilophosaurus wetherilli</i>	0	0	0	0	0	0	?	0	?	0	1	?	0	0
<i>Cryolophosaurus</i>	0	0	0	0	0	0	1	0	0	0	1	2	1	0
<i>Ceratosaurus</i>	0	0	0	0	1	0	1	0	0	0	1	1	0	0
<i>Abelisaurus</i>	0	0	1	?	1	1	1	1	?	0	1	1	?	0
<i>Carnotaurus</i>	0	0	1	1	1	1	1	1	0	0	1	1	-	0
<i>Majungatholus</i>	0	0	1	1	1	1	?	1	0	0	1	1	-	0
<i>Masiakasaurus</i>	?	0	0	?	?	?	?	?	?	?	?	?	?	?
<i>Piatnitzkysaurus</i>	?	?	?	?	?	?	?	?	?	?	?	?	?	?
<i>Dubreuillosaurus</i>	1	1	0	0	0	0	?	0	0	0	1	2	0	0
<i>Afrovenator</i>	1	1	0	0	?	?	?	?	0	0	?	1	?	?
<i>Torvosaurus</i>	1	1	0	0	?	?	?	?	?	?	?	?	?	?
<i>Eustreptospondylus</i>	1	1	0	0	?	?	?	?	0	0	1	?	?	?
<i>Baryonyx</i>	0	?	?	0	?	0	1	?	?	?	?	?	?	?
<i>Suchomimus</i>	0	?	?	?	0	0	?	?	?	?	?	?	?	0
<i>Irritator</i>	?	?	0	0	0	0	1	0	?	?	1	2	0	0
<i>Monolophosaurus</i>	0	1	0	0	?	0	1	0	0	0	1	2	1	0
<i>Sinraptor</i>	0	0	0	0	0	0	1	0	0	0	1	2	1	0
<i>Carcharodontosaurus</i>	?	0	1	?	0	0	1	?	?	?	?	?	?	?

<i>Giganotosaurus</i>	0	0	1	0	0	0	1	?	?	?	?	?	?	?
<i>Acrocanthosaurus</i>	?	0	0	0	0	0	1	0	0	0	1	2	1	0
<i>Allosaurus</i>	0	0	0	0	0	0	1	0	0	0	1	2	1	0
<i>Neovenator</i>	?	?	?	?	?	?	?	?	?	?	?	?	?	?
<i>Dilong paradoxus</i>	0/1	?	0	0	2	0	0	0	0	?	1	2	1	0
<i>Tyrannosaurus rex</i>	0	1	1	0	2	0	0	0	0	0	1	2	1	0
<i>Compsognathus</i>	?	2	?	?	0	?	?	?	?	?	?	?	?	?
<i>Sinosauropteryx</i>	?	?	0	?	?	?	?	?	0	?	0	2	?	?
<i>Shenzhousaurus</i>	?	?	?	?	0	0	?	0	1	0	0	?	?	-
<i>Sinornithomimus</i>	0	2	0	0	0	0	0	0	1	?	0	2	1	0
<i>Ornitholestes</i>	0	0	0	0	2	0	?	0	0	0	0	2	0	1
<i>Deinonychus</i>	0	0	0	0	?	?	?	0	0	1	0	0	0	1
<i>Velociraptor</i>	0	0	0	0	2	0	0	0	0	1	0/1	0	0	1
<i>Archaeopteryx</i>	?	2	0	?	2	?	?	?	0	0	?	0/1	0	1
<i>Confuciusornis</i>	?	?	0	0	?	0	?	0	0	0	0	0/1	0	?

<b>Taxa</b>	<b>85</b>	<b>86</b>	<b>87</b>	<b>88</b>	<b>89</b>	<b>90</b>	<b>91</b>	<b>92</b>	<b>93</b>	<b>94</b>	<b>95</b>	<b>96</b>	<b>97</b>	<b>98</b>
<i>Silesaurus</i>	?	?	0	0	?	0	0	0	0	0	0	0	0	0
<i>Herrerasaurus</i>	0	0	0	0	1	0	0	0	0	?	0	0	0	0
<i>Eoraptor</i>	0	0	?	0	1	?	?	0	0	?	0	?	0	?
<i>Plateosaurus</i>	0	0	0	0	1	0	0	0	0	0	0	0	0	0
<i>Coelophysis bauri</i>	0	?	0	0	?	0	0	0	0	?	0	1	0	?
<i>Coelophysis rhodesiensis</i>	0	0	0	?	1	0	0	0	0	0	0	1	0	0
<i>Syntarsus kayentakatae</i>	0	0	0	0	1	0	0	0	0	0	0	1	0	0

<i>Zupaysaurus</i>	1	1	0	0	1	0	0	?	?	?	?	?	0	?
<i>Dilophosaurus sinensis</i> (KMV 8701)	1	1	?	0	?	1	1	0	0	?	?	?	1	?
ZLJT01	?	?	?	?	?	1	1	?	0	0	1	1	0	1
LDM-L10	1	1	?	0	?	1	1	0	0	?	?	?	?	?
<i>Dilophosaurus wetherilli</i>	?	1	0	0	1	0	0	0	0	0	0	1	?	0
<i>Cryolophosaurus</i>	1	1	0	0	1	1	1	0	0	0	0	1	0	0
<i>Ceratosaurus</i>	1	0	0	0	2	1	1	0	0	0	1	1	0	0
<i>Abelisaurus</i>	1	?	?	?	2	0	?	0	0	?	1	?	0	0
<i>Carnotaurus</i>	1	0	0	0	2	0	1	0	0	?	1	?	0	0
<i>Majungatholus</i>	?	0	?	0	2	0	1	0	0	?	1	?	0	0
<i>Masiakasaurus</i>	?	?	?	?	?	?	?	?	?	?	?	?	?	?
<i>Piatnitzkysaurus</i>	?	?	?	?	?	0	1	0	0	0	?	?	?	0
<i>Dubreuillosaurus</i>	0	0	?	?	1/2	0	1	0	0	0	?	0	?	0
<i>Afrovenator</i>	?	?	0	0	2	?	?	?	?	?	?	?	?	?
<i>Torvosaurus</i>	0	?	0	?	2	?	?	?	?	?	?	?	?	?
<i>Eustreptospondylus</i>	0	?	0	?	2	0	1	?	?	?	?	0	?	?
<i>Baryonyx</i>	0	?	0	0	0	0	1	0	0	0	?	0	0	0
<i>Suchomimus</i>	?	?	?	?	0	?	?	?	?	?	?	?	?	?
<i>Irritator</i>	1	1	?	?	0	0	1	0	0	0	0	0	0	0
<i>Monolophosaurus</i>	0	1	0	0	0	0	0	0	0	?	0	1	0	0
<i>Sinraptor</i>	0	0	0	0	1	1	1	0	0	0	1	1	1	0
<i>Carcharodontosaurus</i>	?	?	?	?	0	1	?	?	?	?	?	?	1	1
<i>Giganotosaurus</i>	0	?	0	?	0	1	1	?	0	0	0	-	1	1
<i>Acrocanthosaurus</i>	0	0	0	0	0/1	1	1	0	0	?	0	1	0	0
<i>Allosaurus</i>	0	0	0	0	1	1	1	0	0	0	0	1	0	0

<i>Neovenator</i>	?	?	?	?	?	?	?	?	?	?	?	?	?	?
<i>Dilong paradoxus</i>	-	?	1	?	0/1	0	1	?	0	?	0	?	0	0
<i>Tyrannosaurus rex</i>	1	0	1	0	0	0	1	0	0	2	0	1	0	0
<i>Compsognathus</i>	?	?	?	?	0/1	?	?	?	?	?	?	1	?	?
<i>Sinosauroptryx</i>	?	?	1	0	?	?	?	?	?	?	?	?	?	?
<i>Shenzhousaurus</i>	0	?	-	?	?	-	?	-	-	-	?	?	?	?
<i>Sinornithomimus</i>	0	0	1	?	0	0	1	0	?	?	?	?	?	?
<i>Ornitholestes</i>	0	?	0	1	1	0	1	1	1	?	0	?	?	?
<i>Deinonychus</i>	0	?	?	?	?	0	?	0	?	1	?	?	?	?
<i>Velociraptor</i>	0	-	0	1	0	0	1	0	1	1	0	1	0	0
<i>Archaeopteryx</i>	?	?	?	0	?	0	?	1	0	2	?	1	?	?
<i>Confuciusornis</i>	?	-	?	?	?	?	?	1	?	?	?	?	?	?

<b>Taxa</b>	<b>99</b>	<b>100</b>	<b>101</b>	<b>102</b>	<b>103</b>	<b>104</b>	<b>105</b>	<b>106</b>	<b>107</b>	<b>108</b>	<b>109</b>	<b>110</b>	<b>111</b>	<b>112</b>
<i>Silesaurus</i>	0	0	0	0	1	0	-	0	0	0	0	0	?	0
<i>Herrerasaurus</i>	0	0	0	0	0	0	0	0	0	0	0	?	0	0
<i>Eoraptor</i>	?	?	?	?	?	?	?	?	?	?	?	?	?	?
<i>Plateosaurus</i>	0	0	0	0	0	0	0	0	0	0	0	0	0	0
<i>Coelophysis bauri</i>	0	0	0	?	?	1	?	?	?	0	0	?	0	0
<i>Coelophysis rhodesiensis</i>	0	0	0	0	1	1	0	0	1	0	0	0	0	0
<i>Syntarsus kayentakatae</i>	0	0	0	0	1	1	0	0	1	0	0	0	0	0
<i>Zupaysaurus</i>	?	?	?	?	?	?	?	?	?	?	?	?	?	?
<i>Dilophosaurus sinensis</i> (KMV 8701)	?	?	?	?	?	?	?	?	?	?	?	?	?	?

ZLJT01	1	0	0	0	1	1	1	1	0	0	0	1	?	0
LDM-L10	?	?	?	?	?	?	?	?	?	?	?	?	?	?
<i>Dilophosaurus wetherilli</i>	0	0	0	0	0	1	0	?	1	0	0	0	0	0
<i>Cryolophosaurus</i>	0	0	0	0	?	?	?	?	?	0	0	0	?	0
<i>Ceratosaurus</i>	?	0	0	0	0	1	0	0	1	0	0	0	1	0
<i>Abelisaurus</i>	0	?	0	0	?	?	?	?	?	?	0	?	1	0
<i>Carnotaurus</i>	0	0	0	0	0	1	0	0	?	0	0	0	1	0
<i>Majungatholus</i>	0	?	0	0	?	?	0	?	1	0	0	?	1	0
<i>Masiakasaurus</i>	?	?	?	?	?	?	?	?	?	?	?	?	?	?
<i>Piatnitzkysaurus</i>	0	0	0	0	0	1	0	1	1	0	0	0	?	0
<i>Dubreuillosaurus</i>	0	0	0	0	0	1	?	1	?	0	0	0	?	0
<i>Afrovenator</i>	?	?	?	?	?	?	?	?	?	?	?	?	?	?
<i>Torvosaurus</i>	?	?	?	?	?	?	?	?	?	?	?	?	?	?
<i>Eustreptospondylus</i>	?	0	0	0	0	1	?	1	1	0	0	0	0	?
<i>Baryonyx</i>	0	0	0	0	?	1	0	?	1	0	0	1	?	0
<i>Suchomimus</i>	?	?	?	?	?	?	?	?	?	?	?	?	?	?
<i>Irritator</i>	0	0	0	0	?	1	0	?	1	0	0	1	?	0
<i>Monolophosaurus</i>	0	0	0	1	?	1	0	?	?	0	0	?	?	0
<i>Sinraptor</i>	1	1	0	1	0	1	0	0	1	0	0	0	0	0
<i>Carcharodontosaurus</i>	1	?	0	?	?	?	?	0	1	0	1	?	1	1
<i>Giganotosaurus</i>	1	?	0	?	?	?	?	0	1	0	1	0	1	1
<i>Acrocanthosaurus</i>	0	?	1	1	0	1	?	1	1	1	0	0	0	0
<i>Allosaurus</i>	0	1	1	1	0	1	0	1	1	1	0	0	0	0
<i>Neovenator</i>	?	?	?	?	?	?	?	?	?	?	?	?	?	?
<i>Dilong paradoxus</i>	0	?	0	0	0	2	1	?	1	?	?	?	0	?
<i>Tyrannosaurus rex</i>	0	0	0	0	0	2	1	1	1	1	0	0	0	0

<i>Compsognathus</i>	?	0	?	?	0	1	?	?	?	?	?	?	?	?
<i>Sinosauropteryx</i>	?	?	?	?	?	?	?	?	?	?	?	?	?	?
<i>Shenzhousaurus</i>	?	?	?	?	?	-	-	?	?	?	?	?	?	?
<i>Sinornithomimus</i>	?	?	?	?	?	?	?	?	?	?	?	?	0	?
<i>Ornitholestes</i>	?	?	?	?	?	1	?	?	?	?	?	?	?	?
<i>Deinonychus</i>	?	?	?	?	0	?	1	?	?	?	?	?	?	?
<i>Velociraptor</i>	0	0	0	1	0	1	1	?	1	0	0	0	0	0
<i>Archaeopteryx</i>	?	?	0	1	?	?	?	?	?	0	0	?	?	?
<i>Confuciusornis</i>	?	?	?	?	?	?	?	?	?	?	?	?	?	?

<b>Taxa</b>	<b>113</b>	<b>114</b>	<b>115</b>	<b>116</b>	<b>117</b>	<b>118</b>	<b>119</b>	<b>120</b>	<b>121</b>	<b>122</b>	<b>123</b>	<b>124</b>	<b>125</b>	<b>126</b>
<i>Silesaurus</i>	0	?	?	?	?	?	?	?	?	?	?	?	0	0
<i>Herrerasaurus</i>	0	0	0	0	?	?	0	1	0	0	0	0	0	0
<i>Eoraptor</i>	?	?	?	0	?	?	?	0	0	?	0	0	?	0
<i>Plateosaurus</i>	?	0	0	0	0	0	0	0	0	0	1	0	0	0
<i>Coelophysis bauri</i>	?	1	0	?	?	1	?	1	0	0	?	0	1	0
<i>Coelophysis rhodesiensis</i>	?	1	0	?	?	1	?	1	0	?	?	0	1	0
<i>Syntarsus kayentakatae</i>	?	?	0	0	?	1	?	1	0	0	1	0	1	0
<i>Zupaysaurus</i>	?	?	?	?	?	?	?	?	0	0	1	0	1	0
<i>Dilophosaurus sinensis</i> (KMV 8701)	?	?	?	?	?	?	?	1	?	?	0	0	0	0
ZLJT01	?	?	?	?	?	?	?	?	?	?	?	?	0	0
LDM-L10	?	?	?	?	?	?	?	1	0	0	0	0	0	0
<i>Dilophosaurus</i>	?	?	0	?	?	?	?	?	0	?	0	0	1	0

<i>wetherilli</i>														
<i>Cryolophosaurus</i>	?	?	?	0	0	?	?	?	?	?	?	?	?	?
<i>Ceratosaurus</i>	?	?	0	0	0	0	?	1	0	?	?	0	0	0
<i>Abelisaurus</i>	?	?	?	?	?	?	?	?	?	?	?	?	?	?
<i>Carnotaurus</i>	0	1	?	0	?	?	0	1	1	0	1	1	0	0
<i>Majungatholus</i>	?	1	0	0	?	0	0	1	1	0	1	1	0	0
<i>Masiakasaurus</i>	?	?	?	?	?	?	?	?	1	?	1	1	0	-
<i>Piatnitzkysaurus</i>	?	?	?	?	?	?	?	?	?	?	?	?	0	0
<i>Dubreuillosaurus</i>	?	?	?	?	0	2	?	?	?	?	?	0	0	0
<i>Afrovenator</i>	?	?	?	?	?	?	?	?	?	?	?	?	?	?
<i>Torvosaurus</i>	?	?	?	?	?	?	?	?	?	?	?	?	0	?
<i>Eustreptospondylus</i>	?	?	?	?	?	?	?	?	0	?	?	0	1	?
<i>Baryonyx</i>	?	?	?	?	?	?	?	?	0	1	0	0	1	0
<i>Suchomimus</i>	?	?	?	?	?	?	?	?	0	1	0	0	1	0
<i>Irritator</i>	?	?	?	?	?	?	?	?	?	?	?	0	?	?
<i>Monolophosaurus</i>	?	?	?	?	?	?	?	1	0	1	0	0	0	0
<i>Sinraptor</i>	0	1	1	0	0	2	0	1	0	0	0	0	0	0
<i>Carcharodontosaurus</i>	1	?	?	?	?	?	?	?	?	?	?	?	?	?
<i>Giganotosaurus</i>	1	?	?	?	?	1/2	?	?	?	?	?	?	2	0
<i>Acrocanthosaurus</i>	0	1	1	0	0	2	?	?	0	1	0	0	0	0
<i>Allosaurus</i>	0	1	1	0	0	2	0	1	0	1	0	0	0	0
<i>Neovenator</i>	?	?	?	?	?	?	?	?	?	?	?	?	0	?
<i>Dilong paradoxus</i>	?	?	?	?	?	?	?	?	?	1	0	0	0	0
<i>Tyrannosaurus rex</i>	0	1	1	0	?	3	1	1	0	1	0	0	0	0
<i>Compsognathus</i>	?	?	?	?	?	?	?	?	?	?	?	?	0	0
<i>Sinosauroptryx</i>	?	?	?	?	?	?	?	?	?	?	?	?	?	0
<i>Shenzhousaurus</i>	?	1	?	?	-	-	?	?	0	1	0	0	0	1

<i>Sinornithomimus</i>	?	?	?	?	?	?	?	?	0	1	0	?	0	1
<i>Ornitholestes</i>	?	?	?	?	?	2/3	?	1	0	?	0	0	?	0
<i>Deinonychus</i>	?	1	0/1	1	1	3	1	1	?	?	?	0	0	0
<i>Velociraptor</i>	0	1	?	1	1	3	1	1	?	1	0	0	0	0
<i>Archaeopteryx</i>	?	2	?	?	1	3	?	?	?	1	?	0	0	0
<i>Confuciusornis</i>	?	2	?	?	?	?	?	?	0	0	0	0	0	0

<b>Taxa</b>	<b>127</b>	<b>128</b>	<b>129</b>	<b>130</b>	<b>131</b>	<b>132</b>	<b>133</b>	<b>134</b>	<b>135</b>	<b>136</b>	<b>137</b>	<b>138</b>	<b>139</b>	<b>140</b>
<i>Silesaurus</i>	0	0	?	?	?	?	1	0	0	?	?	0	?	0
<i>Herrerasaurus</i>	0	0	0	0	0	0	1	0	0	0	0	0	0	0
<i>Eoraptor</i>	0	0	?	?	?	0	?	?	0	?	0	0	?	?
<i>Plateosaurus</i>	0/1	0	?	1	0	0	0	0	0	0	1	0	0	0
<i>Coelophysis bauri</i>	1	?	?	?	0	0	0	0	0	0	0	0	0	0
<i>Coelophysis rhodesiensis</i>	1	0	?	?	0	0	0	0	0	?	0	0	0	0
<i>Syntarsus kayentakatae</i>	1	1	0	1	?	0	1	0	0	0	0	0	0	0
<i>Zupaysaurus</i>	0	1	?	?	?	0	1	0	?	1	0	?	1	1
<i>Dilophosaurus sinensis</i> (KMV 8701)	0	0	1	?	0	1	1	0	0	1	1	1	0	0
ZLJT01	0	0	?	?	?	?	?	?	?	?	?	?	?	?
LDM-L10	0	0	1	?	0	1	1	0	0	1	?	1	0	0
<i>Dilophosaurus wetherilli</i>	0	1	?	?	0	1	1	0	1	1	0	1	?	1
<i>Cryolophosaurus</i>	?	?	?	?	?	1	1	0	1	1	0	1	1	0
<i>Ceratosaurus</i>	0	0	0	1	0	1	1	0	0	1	0	0	1	0

<i>Abelisaurus</i>	?	?	?	?	?	?	?	?	?	?	?	?	?	?
<i>Carnotaurus</i>	0	0	?	1	0	0	1	0	0	1	0	0	1	0
<i>Majungatholus</i>	0	0	?	1	0	0	1	0	0	1	0	0	1	0
<i>Masiakasaurus</i>	0	0	0	?	0	?	?	?	?	?	?	?	?	?
<i>Piatnitzkysaurus</i>	?	0	?	?	?	?	?	?	?	?	?	?	?	?
<i>Dubreuillosaurus</i>	0	0	1	1	1	?	?	?	?	?	?	?	?	?
<i>Afrovenator</i>	?	?	?	?	?	?	?	?	?	?	?	?	?	?
<i>Torvosaurus</i>	?	0	?	?	?	?	?	?	?	?	?	?	?	?
<i>Eustreptospondylus</i>	0	1	1	?	?	?	?	?	?	?	?	?	?	?
<i>Baryonyx</i>	2	1	1	1	1	1	1	?	?	?	?	?	?	?
<i>Suchomimus</i>	2	1	?	?	?	1	?	?	?	?	?	?	?	?
<i>Irritator</i>	?	?	1	?	?	1	1	0	?	?	?	?	?	?
<i>Monolophosaurus</i>	0	0	1	1	1	1	1	0	?	1	0	?	?	?
<i>Sinraptor</i>	0	0	1	1	1	0	1	0	0	1	0	1	1	0
<i>Carcharodontosaurus</i>	?	?	?	?	?	?	?	?	?	?	?	?	?	?
<i>Giganotosaurus</i>	0	0	?	?	?	?	1	?	?	?	?	1	1	1
<i>Acrocanthosaurus</i>	0	0	1	?	?	1	1	0	0	1	0	?	1	?
<i>Allosaurus</i>	0	0	1	1	1	1	1	0	0	1	0	1	1	1
<i>Neovenator</i>	0	0	?	?	?	?	?	?	?	?	?	?	?	?
<i>Dilong paradoxus</i>	0	0	1	1	?	1	1	0	?	1	?	?	1	1
<i>Tyrannosaurus rex</i>	0	0	1	1	1	1	1	0	0	1	1	?	1	1
<i>Compsognathus</i>	0	0	?	?	?	1	?	0	?	?	0	?	?	?
<i>Sinosauropteryx</i>	0	?	?	?	?	?	?	?	?	?	?	?	?	?
<i>Shenzhousaurus</i>	-	0	1	?	?	?	?	1	?	?	-	?	1	?
<i>Sinornithomimus</i>	-	?	1	?	?	?	0	1	?	1	1	1	?	?
<i>Ornitholestes</i>	0	0	1	1	?	1	0	0	0	0/1	0	?	1	1
<i>Deinonychus</i>	0	0	0	1	1	?	0	0	?	0	-	?	1	?

<i>Velociraptor</i>	0	0	0	?	1	?	0	0	0	0	0	?	1	?
<i>Archaeopteryx</i>	0	0	1	?	0	1	?	0	?	0	0	?	1	1
<i>Confuciusornis</i>	-	-	1	?	?	1	?	0	?	0	0	?	1	?

<b>Taxa</b>	<b>141</b>	<b>142</b>	<b>143</b>	<b>144</b>
<i>Silesaurus</i>	?	?	?	?
<i>Herrerasaurus</i>	0	?	?	?
<i>Eoraptor</i>	?	?	?	?
<i>Plateosaurus</i>	?	?	?	?
<i>Coelophysis bauri</i>	0	?	?	?
<i>Coelophysis rhodesiensis</i>	0	?	?	?
<i>Syntarsus kayentakatae</i>	0	?	?	?
<i>Zupaysaurus</i>	?	1	1	?
<i>Dilophosaurus sinensis</i> (KMV 8701)	0	1	1	1
ZLJT01	?	0	1	?
LDM-L10	0	?	0	1
<i>Dilophosaurus wetherilli</i>	1	?	0	1
<i>Cryolophosaurus</i>	1	1	0	1
<i>Ceratosaurus</i>	0	0	0	0
<i>Abelisaurus</i>	?	?	?	?
<i>Carnotaurus</i>	0	?	?	?
<i>Majungatholus</i>	0	?	?	?

<i>Masiakasaurus</i>	?	?	?	?
<i>Piatnitzkysaurus</i>	?	?	?	?
<i>Dubreuillosaurus</i>	?	?	?	?
<i>Afrovenator</i>	?	1	?	?
<i>Torvosaurus</i>	?	?	?	?
<i>Eustreptospondylus</i>	?	?	?	?
<i>Baryonyx</i>	?	0	?	?
<i>Suchomimus</i>	?	?	?	?
<i>Irritator</i>	?	?	?	?
<i>Monolophosaurus</i>	?	1	1	0
<i>Sinraptor</i>	0	1	?	?
<i>Carcharodontosaurus</i>	?	1	?	?
<i>Giganotosaurus</i>	0	?	?	?
<i>Acrocanthosaurus</i>	1	0	?	?
<i>Allosaurus</i>	0	1	?	?
<i>Neovenator</i>	?	?	?	?
<i>Dilong paradoxus</i>	?	1	?	?
<i>Tyrannosaurus rex</i>	0	1	?	?
<i>Compsognathus</i>	?	?	?	?
<i>Sinosauropteryx</i>	?	?	?	?
<i>Shenzhousaurus</i>	?	?	?	?
<i>Sinornithomimus</i>	0	?	?	?
<i>Ornitholestes</i>	?	0	?	?
<i>Deinonychus</i>	?	0	?	?
<i>Velociraptor</i>	0	0	?	?
<i>Archaeopteryx</i>	?	?	?	?
<i>Confuciusornis</i>	?	?	?	?